Improvements in the Relaxation Theory of Spectral Line Broadening in Plasmas

By

JOSEPH EDWARD WHALEN

A DISSERTATION PRESENTED TO THE GRADUATE COUNCIL OF THE UNIVERSITY OF FLORIDA IN PARTIAL FULFILLMENT OF THE REQUIREMENTS FOR THE DEGREE OF DOCTOR OF PHILOSOPHY

UNIVERSITY OF FLORIDA

1972

ACKNOWLEDGMENTS

The author wishes to thank Dr. Charles F. Hooper, Jr. for his guidance during this effort. He also wishes to thank Dr. Larry Roszman, Dr. John O'Brien, Dr. Tony Barker, and Dr. James Dufty for the help they have given him through many discussions and conversations. Also, he wishes to thank Judith Lipofsky for her programming assistance and Sally Kirk who typed the final manuscript.

TABLE OF CONTENTS

LIST OF FIGURES

Abstract of Dissertation Presented to the
Graduate Council of the University of Florida in Partial Fulfillment
of the Requirements for the Degree of Doctor of Philosophy

IMPROVEMENTS IN THE RELAXATION THEORY OF SPECTRAL LINE BROADENING IN PLASMAS

By

Joseph Edward Whalen

June, 1972

Chairman: Dr. Charles F. Hooper, Jr.
Major Department: Physics and Astronomy

Several improvements in previous treatments of the relaxation theory of spectral line broadening in a plasma are presented in this dissertation:

1. To second order in the coupling constant, the theory is extended to include ion-field effects in the atomic Boltzmann factors and the electron collision operators.

2. The theory is extended to include full Coulomb interaction between the radiating atoms and the perturbing electrons.

3. The effect of using a strong collision cut-off on the theoretical computations is examined.

4. The effects of electron symmetry are introduced through an effective Boltzmann distribution.

5. A static wing formula is developed.

Computations are presented for the Lyman-alpha transition

in hydrogen and ionized helium. For frequency separations from the line center greater than 10 times the ion plasma frequency, the calculated profiles for the Lyman-alpha line agree quite well with the experimental data. However, there are noticeable differences in the theoretical results in the line center; these discrepancies are examined.

From the behavior of the Lyman-alpha profile, when the full Coulomb interaction is used, it is concluded that higher order terms in the coupling constant are required to properly describe the intensity in the line center. An explicit expression is derived for a typical higher order term in the perturbation expansion and an upper bound is obtained for this term. It is shown that the perturbation expansion does indeed break down for small frequency separations corresponding to the line center.

The calculated results using the static wing formula are compared with the experimental data for frequency separations greater than the electron plasma frequency. This theory provides an inexpensive means for computing wing profiles which may be useful to experimentalists and astrophysicists.

CHAPTER I

CAUSES OF SPECTRAL LINE BROADENING IN PLASMAS

(I.1) INTRODUCTION

The discrete spectrum of radiation emitted from isolated atoms and molecules is broadened considerably when the radiators are placed in a plasma. The resulting intensity distribution as a function of frequency is called a line shape.[1] The major causes of line broadening are discussed in Chapter I. The detailed behavior of the line shape under different approximations is investigated in subsequent chapters.

The broadening mechanisms can be grouped into three major categories: the effects of charged-particle fields on the radiation, collisions between the radiator and various neutral constituents in the plasma, and Doppler effects. In this chapter, the Lyman-alpha line of hydrogen will be considered in order to illustrate the region of the line shape where the different broadening effects are important; unless otherwise stated, all numerical results pertain to a hydrogen plasma at a temperature of 20,400 degrees Kelvin and an electron density of $3.6 \times 10^{17}/cm^3$. However, most of the analysis will hold for temperatures and densities which may vary by factors as large as 4 for the temperatures and 10 for the density; exceptions will be noted.

(I.2) TIME OF INTEREST

To examine the effects of the various broadening mechanisms on the line shape, it is useful to define a time of interest.[2] The line shape can be expressed as a Fourier transform of an auto-correlation function, $\Phi(t)$,[3,4,5]

$$I(\omega) = \int \exp(i\Delta\omega t)\, \Phi(t)\, dt$$

where $\Phi(t) = \mathrm{Tr}\langle \vec{d} \cdot \vec{d}(t) \rangle$ and $\Delta\omega$ is the frequency separation from the line center. For times such that $\Delta\omega\tau > 1$, contributions to the integral are small due to oscillations of the exponential function. Also, for cases investigated in this dissertation, $\Phi(\tau)$ can be shown to be small for large times.[5] Thus, contributions to the integral are significant only for times less than $1/\Delta\omega$. Thus, $\tau = 1/\Delta\omega$ defines the time of interest.

Experimental profiles for the Lyman-alpha line for wavelengths less than the half width, $\Delta\lambda_{HW} = .15$ Å, are not well defined.[6,7] Using this value of $\Delta\lambda_{HW}$ the corresponding time of interest can be calculated,

$$t_{HW} \approx 0.5 \times 10^{-12}\ s.$$

Changes in physical quantities such as the ion-field, which are appreciable only for times greater than t_{HW}, have small influence on the profile for $\Delta\lambda > \Delta\lambda_{HW}$. Hence, they will

be neglected in this dissertation; for example, the static ion approximation will be employed.

(I.3) DOPPLER BROADENING

Doppler broadening is caused by motion of the radiator during the time of interest.[1] Neglecting the effects of collisions and the ion-field on the motion of the radiator, the Doppler profile can be written as,

$$I_D(\Delta\lambda) = \left(\frac{Mc^2}{2\pi k_B T \lambda_D^2}\right) exp\left(-\frac{Mc^2\Delta\lambda^2}{2k_B T \lambda_D^2}\right), \qquad (1.1)$$

where M is the mass of the radiator, c the velocity of light, k_B the Boltzmann constant, and λ_D the Debye length. For cases considered in this dissertation, the Doppler broadening will be assumed statistically independent from other broadening effects. Under this assumption the line profile can be represented as a convolution[8] of the Doppler profile and the profile resulting from all other broadening mechanisms,

$$I_{TOTAL}(\Delta\lambda) = \int_{-\infty}^{\infty} I(\Delta\lambda') I_D(\Delta\lambda - \Delta\lambda') d(\Delta\lambda'), \qquad (1.2)$$

where $I(\Delta\lambda)$ is the profile arising from all other effects.

For long times of interest, which correspond to the line center, the motional effects of the radiator will become more pronounced. Thus in most cases, Doppler effects are significant only in the line center. This fact is illustrated in reference 9.

The Doppler profile given in equation (1.1) also neglects the effects of electron collisions on the motion of the radiator.[10,11] This is a valid approximation since the momentum transferred to the radiator during an electron collision is small due to the large difference in the electron and atom masses.

In this dissertation, attention will be focused on theoretical treatments of $I(\Delta\lambda)$.

(I.4) PERTURBING IONS AND ELECTRONS

Almost all treatments of line broadening to date use the static ion approximation.[1,12,13] In this approximation the broadening effects of ion motion or ion dynamics are neglected. In reference 9 it is shown that the relative motion of the ions is small for times corresponding to wavelengths greater than the plasma frequency for the ions. For the cases investigated in this dissertation, the plasma frequency for the ions is smaller than the half width. Hence, the effects of ion dynamics can be neglected for wavelengths greater than $\Delta\lambda_{HW}$.

The criterion used in determining the region of the line shape in which electron motion is important is the same as that used when ion dynamics are considered. The wavelength corresponding to the electron plasma frequency is 2 Å. Thus electron dynamics will have relatively less importance for wavelengths greater than 2 Å. As will be shown in Chapters IV and V, a complete static treatment for both the electrons and ions yields a theoretical profile that is in substantial agreement with the experimental data in the line wings.

The effects of electron shielding on the ion microfield distribution function must also be considered. A comparison of the relative motion of the electrons to that of the ions during the time of interest yields

$$\frac{(\delta\nu_{sw}/\nu_{sw})_{ELECTRON}}{(\delta\nu_{sw}/\nu_{sw})_{ION}} = \sqrt{\frac{M_i}{M_e}} \approx 42.$$

Since electron motion during the time of interest is large, the electrons may be considered to effectively shield the ion-ion interaction. Thus the appropriate ion microfield is the low-frequency microfield.[14]

The same argument can not be applied to a treatment of the electron microfield. Because of the low mobility of the ions, the electron-electron interaction is not fully shielded. To explore the effects of shielding in the electron microfield, the static wing profile calculated using a low-frequency electron microfield is compared to that obtained using the high-frequency electron microfield.[15] These two cases should provide bounds for the effect of ion shielding on the electron microfield.

In the line center, 0.0 - 5.0 Å, for the temperature and density under investigation, the interaction between the radiating atom and the perturbing electrons is treated as a collision process (i.e., no static electron field broadening is included). One approximation often used in describing these collisions is to assume that the electrons travel in a classical path.[13,16] In many of these treatments logarithmic divergences are encountered when the dipole approximation is used, and only terms to second order in the coupling

constant are retained.[17,18] These divergences are removed by using minimum and maximum impact parameters.[19,20,21,22]

The maximum impact parameter is assumed to be the Debye length or a constant close to unity times the Debye length. Several different criteria are used to determine the minimum impact parameter cut-off or strong collision cut-off. For the Lyman-alpha transition, the minimum impact parameter is often in the region in which the dipole approximation for the interaction between the radiator and perturbing electrons is inadequate. By using the quantum mechanical treatment developed in the relaxation theory, employing either the dipole approximation or the full Coulomb interaction, there is no mathematical need for a strong collision cut-off in the second order term for frequencies greater than the half width. However, in order to obtain realistic results a strong collision cut-off is required.[23]

(I.5) INTERACTIONS BETWEEN THE RADIATORS

Collisions between the neutral radiators are neglected in most plasma line broadening treatments. To examine the validity of this approximation, the nature of the radiator-radiator interaction must be examined. One can compute the average density of neutral atoms from a knowledge of the percent ionization. The percent ionization can be determined from recent computations by Barker.[24] For an electron density of $1.0 \times 10^{18}/cm^3$ and a temperature of 20,000 degrees Kelvin, the percent ionization is approximately 75 percent corresponding to an average distance between radiators of approximately 1.0×10^{-6} cm. During the time of interest the ratio of the average motion of the radiator to the average separation is less than 1. Also, since the radiator-radiator interaction potential is short range, typically a $1/r^6$ dependency, the effective mean free path will be much larger than the distance between radiators.[25] Thus, during the time of interest there will be few radiator-radiator collisions. The broadening due to these collisions will be neglected compared to the effect of the electron-radiator collisions which interact through long range potentials.

(I.6) THE NO-QUENCHING APPROXIMATION

In the context of line broadening theories the no-quenching approximation neglects radiationless transitions between the initial atomic states and all other atomic states having a different principal quantum number. This is a good approximation between states which are well separated in energy such as the lower transitions in the first few series in hydrogen and helium. However, quenching can become appreciable for higher members in a series for which the transition probability to states of different principal quantum numbers is large. Including quenching effects in the lower member transitions is computationally feasible; unfortunately, this is not the case for higher transitions because integrations over the inverse of large matrices are required. Quenching has been examined for the Lyman-alpha transition by using a matrix perturbation expansion approach. It is shown that the effect is small (see Chapter V). The approach used could be extended to the higher series members. However, at this time it is felt that such an extension would be premature since other approximations have a more significant effect on the line profile and should be removed first.

CHAPTER II

THE RELAXATION THEORY

(II.1) INTRODUCTION

The relaxation theory[9,12] of spectral line broadening in plasmas is reformulated in this chapter to include the following: (1) the full Coulomb interaction between radiating atoms and perturbing electrons, (2) ion-field splitting of initial atomic levels, both in the Boltzmann factors and in the electron collision operators.

In the relaxation theory the profile, $I(\omega)$, of a broadened spectral line is given by the Fourier transform of[9,12,26]

$$\Phi(t) = Tr\left(\vec{d}\cdot T(t)^{\dagger}\rho\vec{d}\,T(t)\right). \tag{2.1a}$$

Hence,

$$I(\omega) = Im\int exp(i\omega t)\,\Phi(t)dt, \tag{2.1b}$$

where Tr represents a trace over all states of the plasma system which consists of radiators, electrons, and ions. T(t) is the time development operator and ρ is the density matrix of the system. This dissertation is concerned with atomic dipole radiation from partially ionized plasmas; hence, $\vec{d}$ is restricted to be the atomic dipole operator of the radiator.

Under the conditions outlined in Chapter I, the radiators can be assumed isolated from one another. Also all the radiators will have the same spectrum of states and are independent of one another as shown in Section (I.5). Hence, to obtain a useful line profile expression, it is sufficient to consider the ensemble average over all states accessible to a single radiator. The corresponding Hamiltonian for a radiator immersed in a gas of charged particles is

$$H = H_o + H_e + K_i + V_{ii} + V_{ei} + V_{ae} \qquad (2.2)$$

where subscripts a, e, i represent atoms, electrons, and ions, respectively. V represents the total potential energy operator, and K the total kinetic energy operator. H_e is the Hamiltonian for the electrons defined by

$$H_e = K_e + V_{ee} .$$

Previous treatments[9,12] of the relaxation theory used an unperturbed atomic Hamiltonian of the form $K_a + V_a$. In this dissertation, the effect of the ion-field on the atomic states is included and, hence, the unperturbed atomic Hamiltonian in the following derivation is taken to be

$$H_o = K_a + V_a + e\vec{R}\cdot\vec{\mathcal{E}}_i$$

where e is the electron charge, $\vec{R}$ the position operator for the atomic electron, and $\vec{\mathcal{E}}_i$ is the static ion-field.

To at least qualitatively account for electron shielding (see Chapter I, Section I.4) the operator, $V_{ii} + V_{ei}$, is

replaced by an effective potential, V_{eff}, which depends only on ion coordinates. Debye Hückel theory[27] for ions in a neutralizing electron background is used to obtain V_{eff}.

(II.2) THE DENSITY MATRIX

The canonical density matrix for a system whose Hamiltonian is given by equation (2.2), with $V_{ii} + V_{ei}$ replaced by V_{eff}, is[28]

$$\rho = c \exp(-(H_o + V_{ae} + H_e + K_i + V_{eff})/k_B T) \tag{2.3}$$

where k_B is Boltzmann's constant, T is the temperature and c is a normalization constant obtained by requiring that

$$T_n(\rho) = 1.$$

Making the static ion approximation is equivalent to assuming that the following commutator is negligibly small

$$[K_i + V_{eff}, H] = 0. \tag{2.4}$$

Since $K_i + V_{eff}$ commutes with itself and commutator relations are distributive, equation (2.4) implies that

$$[H_o + H_e + V_{ae}, K_i + V_{eff}] = 0. \tag{2.5}$$

Using equation (2.5), we may write the density matrix in the following convenient form

$$\rho = c \exp(-(H_o + H_e + V_{ae})/k_B T) \exp(-(K_i + V_{eff})/k_B T). \tag{2.6}$$

The operators V_{ae} and H_o will not in general commute because V_{ae} contains the atomic electron position operator and H_o contains the atomic electron momentum operator. However, the exponential factor containing V_{ae} may be expressed as

$$\exp(-(H_o+H_e+V_{ae})/k_BT) = \exp(-(H_o+H_e+(V_{ae}-\overline{V}_{ae})+\overline{V}_{ae})/k_BT) \quad (2.7)$$

where $\overline{V}_{ae}$ is an effective potential which is defined to depend only on the electron coordinates: an average over atomic electron coordinates is performed to obtain $\overline{V}_{ae}$. It is assumed that the term $(V_{ae} - \overline{V}_{ae})$ is small compared to both V_{ae} and k_BT. Hence, we neglect it in a first approximation allowing equation (2.7) to be factored,

$$\exp(-(H_o+H_e+V_{ae})/k_BT) = \exp(-H_o/k_BT) \times \exp(-(H_e+\overline{V}_{ae})/k_BT). \quad (2.8)$$

The entire density matrix can now be written as a product of the density matrices for the three subsystems ... atoms, electrons, and ions

$$\rho = C\,\rho_a\,\rho_e\,\rho_i$$

where

$$\rho_a = \exp(-H_o/k_BT), \quad (2.9a)$$

$$\rho_e = \exp(-(H_e+\overline{V}_{ae})/k_BT), \quad (2.9b)$$

$$\rho_i = \exp(-(K_i+V_{eff})/k_BT), \quad (2.9c)$$

C = normalization constant.

We next consider further approximations to ρ_e . It is often stated or assumed that weak electron collisions account for the major contribution to the electron broadening. However, it is not usually pointed out that a primary reason why a perturbing electron is relatively unlikely to get close enough to a radiator to cause a strong collision is due to electron symmetry effects. For the purpose of estimating symmetry effects between the atomic electron and perturbing electrons, an atomic model is adopted in which the atomic electron is superimposed on the nucleus. With this rough approximation, $\overline{V}_{ae}$ can be written as a sum of the classical Coulomb interaction, V_{cl}, plus a term V_s arising from symmetry effects. Since the classical potential produced by the above model is zero, $\overline{V}_{ae}$ reduces to V_s. The expression for the density matrix ρ_e is factored yielding

$$\rho_e = \exp(-H_e/k_BT)\exp(-V_s/k_BT) \qquad (2.10)$$

where the commutators between H_e and V_s are neglected. Again, in the spirit of the previous approximations, it is assumed that this commutator will be small compared to k_BT. For temperatures under consideration in this dissertation, the form for ρ_e given in equation (2.10) should be adequate when estimating the qualitative effects of electron symmetry.

The potential, V_s, is determined from the radial distribution functions for electron-proton and an electron-electron system, as computed by Barker.[24,29] The details for

deriving the radial distribution functions and the corresponding effective potentials are discussed in Appendix A.

A plot of $\exp(-V_s/k_B T)$ versus the distance between the perturbing electron and radiator is given in Figure 1. The rapid decrease in magnitude for small distances implies a decreased probability for strong collisions. The resulting effect on the line profile can be represented by an effective strong collision cut-off. The value of the cut-off obtained in this manner is indicated in Figure 1. It is larger than cut-offs used in other treatments of line broadening. Thus, for this model electron symmetry effects tend to decrease the broadening caused by the electron collisions.

Figure 1. Effective probability function for an electron a distance x from the nucleus of the hydrogen atom.

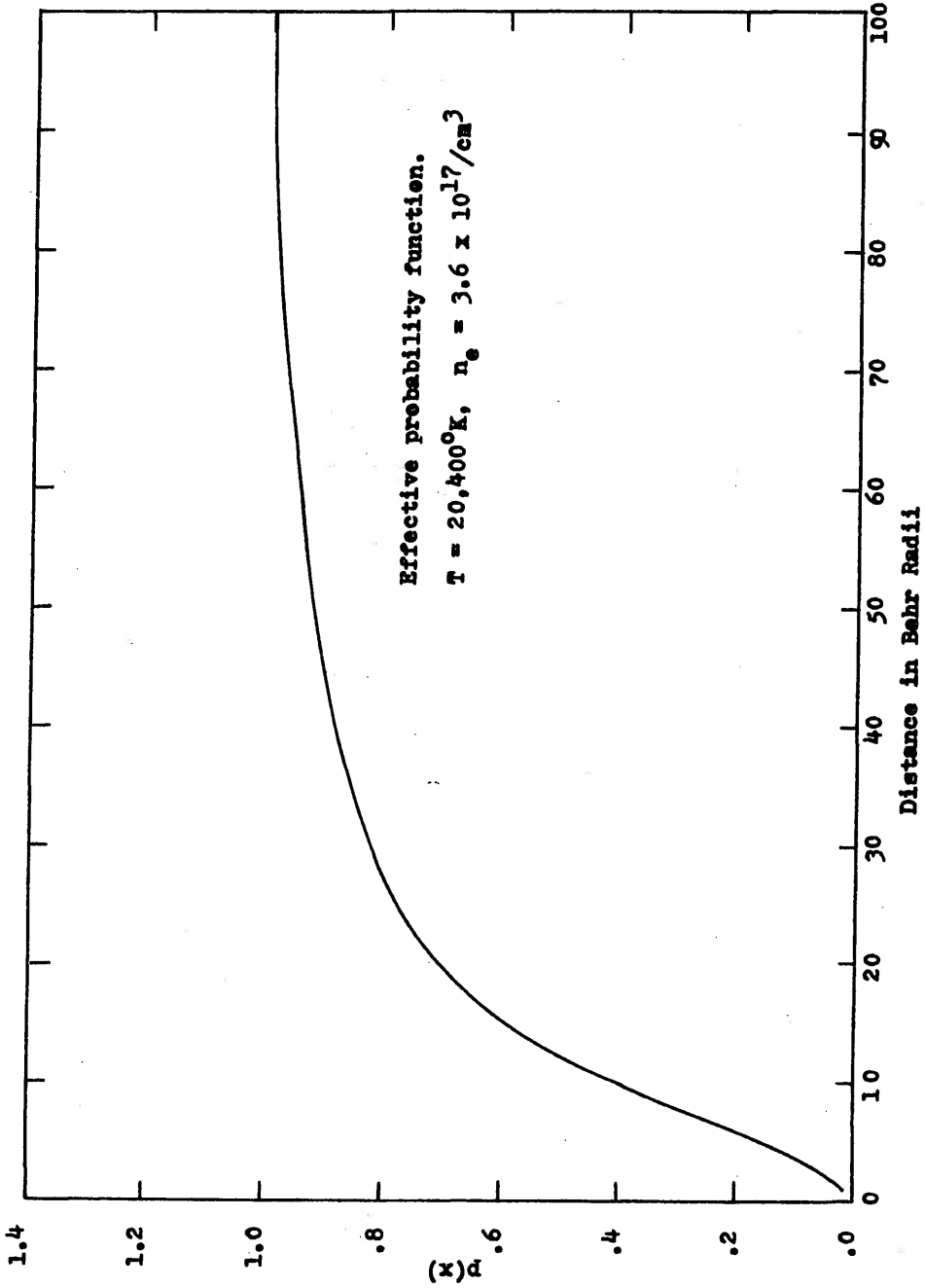
Effective probability function.
T = 20,400°K, n_e = 3.6 x 10^{17}/cm^3
P(x)
1.4
1.2
1.0
.8
.6
.4
.2
.0
0
10
20
30
40
50
60
70
80
90
100
Distance in Bohr Radii

(II.3) THE TIME DEVELOPMENT OPERATOR, T(t)

The time development operator appearing in $\Phi(t)$ is defined in terms of the Hamiltonian given in equation (2.2) with $V_{ei} + V_{ii}$ replaced by V_{eff}.

$$T(t) = \exp(iHt/\hbar)$$

$$= \exp(i(H_o + H_e + V_{ee})t/\hbar)\exp(i(K_i + V_{eff})t/\hbar) \tag{2.11}$$

where the commutator relation given in equation (2.5) has been used. Using the commutator relations given in equations (2.4) and (2.5) one can show that

$$T^{+}(t)\rho\vec{d}\,T(t) = \rho_i \exp(-iH't/\hbar)\rho_a\rho_e\vec{d}\exp(iH't/\hbar) \tag{2.12}$$

where

$$H' = H_o + H_e + V_{ee}\,. \tag{2.13}$$

$T^{+}(t)\,\rho_a\,\rho_e\,\vec{d}\,T(t)$ is evaluated in Section (II.5) using the Zwanzig projection operator technique.[4]

(II.4) THE AVERAGE OVER THE ION MICROFIELD

Using the properties of the Dirac delta function, we can write $\Phi(x)$ as[30]

$$\Phi(x) = Tr\left[\rho_i \int \vec{d}\cdot \exp(-iH'x/\hbar)\,\rho_a\rho_e \exp(iH'x/\hbar) \times \vec{d}\,\delta(\vec{\mathcal{E}}-\vec{\mathcal{E}}_i)\,d^3\mathcal{E}\right]$$

$$= \int Q(\mathcal{E})\, Tr_{ae}\left(\vec{d}\cdot\exp(-iH'x/\hbar)\,\rho_a\rho_e\exp(iH'x/\hbar)\vec{d}\right) d^3\mathcal{E} \qquad (2.14)$$

where $Q(\mathcal{E}) = Tr_i\left(\rho_i\,\delta(\vec{\mathcal{E}}-\vec{\mathcal{E}}_i)\right)$ is the ion microfield distribution function.[31] Using the above form for $\Phi(x)$ in the expression for the line profile given in equation (2.1b), one can show that[9,12]

$$I(\omega) = \pi^{-1}\,Real\int Q(\mathcal{E})\,\rho_e \int_0^\infty \exp(i\omega x)\, Tr_{ae}\left(\vec{d}\cdot\exp(-iH'x/\hbar) \times \vec{d}\exp(iH'x/\hbar)\right) dx\, d^3\mathcal{E}$$

$$\equiv \int Q(\mathcal{E})\, J(\omega,\mathcal{E})\, d^3\mathcal{E}\,. \qquad (2.15)$$

It should be emphasized that here, unlike previous treatments of the relaxation theory, the ion-field is retained in H'. Including the ion-field introduces field shifted frequencies in the effective Liouville operator occurring in $J(\omega,\mathcal{E})$.

(II.5) APPLICATION OF THE ZWANZIG PROJECTION OPERATOR TECHNIQUE

We must now reduce the line profile expression to a tractable form. A useful technique to effect this reduction employs the projection operator procedure develcped by Zwanzig;[4] this procedure involves defining a projection operator, P, that projects out the relevant part of an operator, $\vec{D}(\tau)$, that satisfies an equation of the form

$$i\hbar \frac{\partial \vec{D}(\tau)}{\partial \tau} = L \vec{D}(\tau) \tag{2.16}$$

where L is the Liouville operator. The projection operator allows one to remove the irrelevant part of $\vec{D}(\tau)$ at an early stage in the derivation, thus often simplifying the analysis. For example, if $\vec{D}_1$ is the relevant part of $\vec{D}$ and $\vec{D}_2$ is the irrelevant part, one has

$$\vec{D}_1(\tau) = P \vec{D}(\tau), \tag{2.17}$$

$$\vec{D}_2(\tau) = (1-P)\vec{D}(\tau). \tag{2.18}$$

Applying the projection operator procedure results in an integro-differential equation for $\vec{D}_1(\tau)$.

It is often unclear exactly what part of an operator is relevant particularly during the earlier steps of a derivation. A simple example of a relevant part of an operator might be the diagonal elements of a matrix operator. A

projection operator which selects only the diagonal elements of a matrix operator would be appropriate when the non-diagonal matrix elements are negligibly small or when the non-diagonal elements in no way affect the final result. An example of the latter situation is when an average of an operator, A, is taken in the following manner:

$$\langle A \rangle = Tr(\rho A).$$

The non-diagonal elements of (ρA) in no way effect the average value of the operator A.

In the case of line broadening, one is concerned with the behavior of the radiator, either an ion or an atom in the cases considered in this dissertation. Hence, the atomic subsystem can be considered the relevant subsystem. One performs an average over the broadening effects of the ions and electrons. The ion broadening effects are taken into account via the microfield average. A suitable procedure for simplifying the electron average involves a projection operator of the following form[9]

$$P = \rho_e Tr_e \tag{2.19}$$

where ρ_e is defined in equation (2.10). It should be noted that P is indempotent, i.e., $P^2 = P$.

The projection operator technique is now applied to the expression appearing in equation (2.12). We define as $D(t)$

$$\vec{D}(t) = T^{+}(t)\, \rho \vec{d}\, T(t) \tag{2.20}$$

which is the Heisenberg representation for $\rho \vec{d}^{32}$.

The procedure for finding an expression for $\vec{D}_1(t)$ is to apply the operator P and (1-P) to equation (2.16) and then eliminate the operator $\vec{D}_2(t)$ from the resulting equations. In this manner one obtains an integro-differential equation

$$i\hbar \frac{\partial \vec{D}_1}{\partial t} = PL\left[\vec{D}_1(t) + \exp(-it(1-P)L/\hbar)\vec{D}_2(0) - i/\hbar \int_0^{\infty} \exp(-is(1-P)L/\hbar)(1-P)L\vec{D}_1(t-s)\,ds\right]. \tag{2.21}$$

For most problems of interest the operator $\vec{D}_2(0)$ occurring in equation (2.21) is zero. This is shown for the projection operator P defined in equation (2.19)[9]

$$\begin{aligned}\vec{D}_2(0) &= (1-P)\vec{D}(0) = (1-P)\rho_e\rho_a\vec{d} \\ &= \rho_e\rho_a\vec{d} - \rho_e \mathrm{Tr}_a\rho_e\rho_a\vec{d} \\ &= \rho_e\rho_a\vec{d} - \rho_e\rho_a\vec{d} \\ &= 0.\end{aligned} \tag{2.22}$$

Thus equation (2.21) becomes

$$i\hbar \frac{\partial \vec{D}_1}{\partial t} = PL\left[\vec{D}_1(t) - i/\hbar \int_0^{\infty} \exp(-is(1-P)L/\hbar) \times (1-P)L\vec{D}_1(t-s)\,ds\right]. \tag{2.23}$$

The following integral must be determined to evaluate the line shape expression:

$$\int_0^\infty \exp(i\omega s)\, Tr_{ae}\,(\vec{d}\cdot\vec{D}_1(s))\,ds$$

$$= Tr_{ae}\Big(\vec{d}\cdot\int_0^\infty \exp(i\omega s)\,\vec{D}_1(s)\,ds$$

$$= Tr_a\Big(\vec{d}\cdot\int_0^\infty \exp(i\omega s)\,Tr_g\,\vec{D}_1(s)\Big)ds$$

$$= Tr_a\big(\vec{d}\cdot\vec{\mathcal{D}}_1(\omega)\big) \qquad (2.24)$$

where

$$\vec{\mathcal{D}}_1(\omega) = \int_0^\infty \exp(i\omega s)\,\vec{D}_1(s).$$

An equation for $\vec{\mathcal{D}}_1(\omega)$ can be obtained by taking the Fourier transform of equation (2.23). Using the procedure outlined in reference 9 one can show that

$$\int_0^\infty \exp(i\omega s)\, Tr_a\,(\vec{d}\cdot\vec{\mathcal{D}}_1(\omega))\,ds$$

$$= -i\, Tr_a\big(\vec{d}\cdot(\omega - \langle T(\omega)\rangle)^{-1}\rho_a\,\vec{d}\big). \qquad (2.25)$$

$\langle \cdots\cdots \rangle$ is defined by $\langle A\rangle = Tr_e(A\,\rho_e)$ where A is an arbitrary operator. $T(\omega)$ satisfies the Lippmann-Schwinger equation[33]

$$\hbar T(\omega) = L + L\big[\hbar\omega - (1-P)L\big]^{-1}(1-P)L, \qquad (2.26)$$

Substituting the above result into the expression for the line profile given in equation (2.15) yields

$$I(\omega) = \pi^{-1} I_m \int Q(\mathcal{E})\, T_{n_a}(\vec{d} \cdot K(\omega)\, \rho_a(\mathcal{E})\, \vec{d}\,)\, d^3\mathcal{E} \tag{2.27}$$

where the resolvent operator $K(\omega)$ has been introduced:

$$K(\omega) = (\omega - \langle T(\omega) \rangle)^{-1}. \tag{2.28}$$

The Liouville operator, L, encountered in the above derivation is defined in terms of the Hamiltonian, H', specified in equation (2.13) and the identity operator I:

$$L = H' \otimes I - I \otimes H'^{*}. \tag{2.29}$$

$\otimes$ stands for a direct product. L can be rewritten as a sum of two operators L_0 and L_1 defined by,

$$L_0 = (H_a + V_{ai} + H_e) \otimes I - I \otimes (H_a + V_{ai} + H_e)^{*} \tag{2.30}$$

$$L_1 = V_{ao} \otimes I - I \otimes V_{ai}^{*}. \tag{2.31}$$

Unlike the derivation in reference 9, the ion-field dependence is retained in L_0. If equation (2.26) for $T(\omega)$ and the above definitions for L_1 and L_0 are used, $\langle T(\omega) \rangle$ can be reduced to

$$\hbar \langle T(\omega) \rangle = \langle L_0 \rangle + \langle L_1 \rangle + \langle L [\hbar\omega - (1-P)L]^{-1} (1-P) L \rangle. \tag{2.32}$$

The operator L_0 can be written in terms of the Hamiltonian for the atom and electron subsystems,

$$L_0 = L_0^{a} + L_0^{e}, \tag{2.33}$$

where

$$L_o^a = (H_a + V_{ai}) \otimes I - I \otimes (H_a + V_{ai})^* \tag{2.34}$$

and

$$L_o^e = H_e \otimes I - I \otimes H_e^* . \tag{2.35}$$

With the assumption that the density matrix, ρ_e, is diagonal in the electron states, it follows from symmetry that $\langle L_1 \rangle$ and $\langle L_0 \rangle$ are zero.[9] Hence, equation (2.32) becomes

$$\hbar \langle T(\omega) \rangle = \langle L_o^a \rangle + \hbar \mathcal{H}(\omega) \tag{2.36}$$

where

$$\hbar \mathcal{H}(\omega) \equiv \langle L [\hbar\omega - (1-P)L]^{-1} (1-P) L \rangle .$$

The matrix elements of $\langle L_0^a \rangle$ are specified in Section (II.6).

Five identities derived in Appendix B that are required to further reduce $\mathcal{H}(\omega)$ are given below:

$$\langle PA \rangle = \langle A \rangle \tag{2.37}$$

$$[L_o, P] = 0 \tag{2.38}$$

$$\langle A(1-P)L \rangle = \langle A(1-P)L_1 \rangle \tag{2.39}$$

$$\langle L(1-P)A \rangle = \langle L_1 (1-P) A \rangle \tag{2.40}$$

$$[\hbar\omega - (1-P)L_0]^{-1} = [\hbar\omega - L_0]^{-1}(1-P) \tag{2.41a}$$

$$[\hbar\omega - (1-P)L_0]^{-1} = (1-P)[\hbar\omega - L_0]^{-1} \tag{2.41b}$$

where A is an arbitrary operator.

Using the above identities, $\mathcal{H}(\omega)$ can be reduced to an expansion in powers of the operator L_1,[9,12]

$$\hbar\mathcal{H}(\omega) = \left\langle L_1 \sum_{n=1}^{\infty} \left(\frac{(1-P)}{\hbar\omega - L_0} L_1 \right)^n \right\rangle. \tag{2.42}$$

Introducing the unperturbed resolvent operator, $K_0(\omega)$, defined by

$$K_0(\omega) \equiv (\hbar\omega - L_0)^{-1}$$

equation (2.42) becomes

$$\hbar\mathcal{H}(\omega) = \left\langle L_1 \sum_{n=1}^{\infty} \left(K_0(\omega)(1-P)L_1/\hbar \right)^n \right\rangle. \tag{2.43}$$

The first term in the above expansion becomes

$$\begin{aligned} \hbar^2\mathcal{H}(\omega) &= \langle L_1 \, K_0(\omega)(1-P)L_1 \rangle \\ &= \langle L_1 K_0(\omega) L_1 \rangle - \langle L_1 K_0(\omega) \rangle \langle L_1 \rangle \\ &= \langle L_1 K_0(\omega) L_1 \rangle. \end{aligned} \tag{2.44}$$

In this dissertation the above term is the highest order term used in the numerical results presented. However, the order of magnitude and the qualitative behavior of higher

order terms are examined in Section (II.7). It is shown that the higher order terms may become important in the line center.

(II.6) MATRIX ELEMENTS OF THE OPERATOR $\langle T(\omega) \rangle$

To obtain matrix elements of the tetradic $\langle T(\omega) \rangle$, the matrix elements of L_0^a and $\mathcal{H}(\omega)$ are required. Let the indices μ, μ' represent atomic states and α, β represent electron states. The matrix elements of $\langle L_0^a \rangle$ given in equation (2.45) are obtained by performing an electron average of equation (B.9)

$$L^{a}_{0\,\mu\alpha\nu\beta,\,\mu'\alpha'\nu'\beta'} = (\hbar\omega_{\mu\nu}\,\delta_{\mu\mu'}\,\delta_{\nu\nu'} + e\vec{\mathcal{E}}_i \cdot (\vec{R}_{\mu\mu'}\,\delta_{\nu\nu'} - \vec{R}^{*}_{\nu\nu'}\,\delta_{\mu\mu'}))\,\delta_{\alpha\alpha'}\,\delta_{\beta\beta'} \equiv \hbar\,\overline{\omega}_{\mu\nu} \qquad \text{(B.9)}$$

$$\langle L_0^a \rangle_{\mu\nu,\mu'\nu'} = \sum_{\alpha\beta} L^{a}_{0\,\mu\alpha\nu\beta,\,\mu'\alpha'\nu'\beta}\, f_{\alpha\beta}\,. \qquad (2.45)$$

The Boltzmann factor $f_{\alpha\beta}$, defined in equation (B.4) is assumed to be diagonal and is normalized to 1. Hence, equation (2.45) becomes

$$\langle L_0^a \rangle_{\mu\nu,\mu'\nu'} = \hbar\omega_{\mu\nu}\,\delta_{\mu\mu'}\,\delta_{\nu\nu'} + e\vec{\mathcal{E}}_i \cdot (\vec{R}_{\mu\mu'}\,\delta_{\nu\nu'} - \vec{R}^{*}_{\nu\nu'}\,\delta_{\mu\mu'}). \qquad (2.46)$$

The matrix elements of $\langle \mathcal{H}(\omega) \rangle$ can be written as

$$\hbar^2 \langle \mathcal{H}(\omega) \rangle_{\mu\nu,\mu'\nu'} = \langle L_1 | K_0(\omega) L_1 \rangle$$

$$= \sum_{\substack{\alpha\beta \\ \mu''\nu''\beta'' \\ \mu'''\alpha'''\nu'''\beta'''}} L_{1\,\mu\alpha\nu\beta,\,\mu''\alpha''\nu''\beta''} K_0(\omega)_{\mu''\alpha''\nu''\beta'',\,\mu'''\alpha'''\nu'''\beta'''}$$

$$\times L_{1\,\mu'''\alpha'''\nu'''\beta''',\,\mu'\beta\nu'\beta} f_{\beta\beta}. \qquad (2.47)$$

Matrix elements of the operator $K_0(\omega)$ appear in equation (2.47). The operator $K_0(\omega)$ contains L_0; hence, to derive an expression for the matrix elements of $K_0(\omega)$ appearing in equation (2.47), the matrix elements of L_0 are required. Combining equations (2.46) and (B.10) one has

$$L_{0\,\mu\alpha\nu\beta,\,\mu'\alpha'\nu'\beta'} = (\hbar\omega_{\mu\nu}\delta_{\mu\mu'}\delta_{\nu\nu'} + \hbar\omega_{\alpha\beta}\delta_{\mu\mu'}\delta_{\nu\nu'}$$

$$+ e\vec{\mathcal{E}}_i \cdot (\vec{R}_{\mu\mu'}\delta_{\nu\nu'} - \vec{R}^{*}_{\nu\nu'}\delta_{\mu\mu'}))\delta_{\alpha\alpha'}\delta_{\beta\beta'}$$

$$\equiv L_{0\,\mu\alpha\nu\beta,\,\mu'\alpha'\nu'\beta'}\delta_{\alpha\alpha'}\delta_{\beta\beta'}. \qquad (2.48)$$

To simplify the matrix elements of $K_0(\omega)$, $K_0(\omega)$ is expanded in powers of L_0/ω and then matrix elements are taken of the individual terms in the expansion. In order to carry out this procedure, the matrix elements of L_0^n are required. One obtains,

$$(L_0/\omega)^m_{\mu\alpha\nu\beta,\,\mu'\alpha'\nu'\beta'} = \sum_{\mu^1\alpha^1\nu^1\beta^1} \cdots\cdots \sum_{\mu^{m-1}\alpha^{m-1}\nu^{m-1}\beta^{m-1}} L_{0\,\mu\alpha\nu\beta,\,\mu^1\alpha^1\nu^1\beta^1}$$

$$\times L_{0\,\mu^1\alpha^1\nu^1\beta^1,\,\mu^2\alpha^2\nu^2\beta^2} \cdots\cdots\cdots L_{0\,\mu^{m-1}\alpha^{m-1}\nu^{m-1}\beta^{m-1},\,\mu'\alpha'\nu'\beta'}$$

$$\times \delta_{\alpha\alpha^1}\,\delta_{\alpha^1\alpha^2}\cdots\delta_{\alpha^{m-1}\alpha'}\;\delta_{\beta\beta^1}\,\delta_{\beta^1\beta^2}\cdots\delta_{\beta^{m-1}\beta'},$$

where the results given in equation (2.48) have been used. Resumming the above results leads to

$$K_0(\omega)_{\mu\alpha\nu\beta,\,\mu'\alpha'\nu'\beta'} = k^m_{0\,\mu\alpha\nu\beta,\,\mu'\alpha'\nu'\beta'}\,\delta_{\alpha\alpha'}\,\delta_{\beta\beta'} \qquad (2.49)$$

where the superscript m signifies that transitions between initial and final states due to the ion-field are included in k^m_0. The above results are inserted into the expression for $\hbar^2\mathcal{P}(\omega)$ given in equation (2.47). Using the properties of the delta functions, we can perform two of the summations. The results are,

$$\hbar^2\langle\mathcal{P}(\omega)\rangle_{\mu\nu,\,\mu'\nu'} = \sum_{\substack{\alpha\beta\\ \mu''\alpha''\nu''\beta''\\ \mu'''\nu'''}} L_{1\,\mu\alpha\nu\beta,\,\mu''\alpha''\nu''\beta''}\,k_{0\,\mu''\alpha''\nu''\beta'',\,\mu'''\alpha'''\nu'''\beta'''}$$

$$\times L_{1\,\mu''\alpha'''\nu'''\beta'',\,\mu'\beta\nu'\beta}\,F_{\beta\beta}$$

$$= \sum_{\substack{\alpha\beta\\ \mu''\alpha''\nu''\beta''\\ \mu'''\nu'''}} \left(\langle\mu\alpha|V_{ae}|\mu''\alpha''\rangle\,\delta_{\nu\nu'}\,\delta_{\alpha\beta''} - \langle\nu\alpha|V^*_{ae}|\nu''\beta''\rangle\,\delta_{\mu\mu''}\,\delta_{\alpha\alpha''}\right)$$

$$\times k^m_{0\,\mu''\alpha''\nu''\beta'',\,\mu'''\alpha'''\nu'''\beta'''}\left(\langle\mu'''\alpha'''|V_{ae}|\mu'\beta\rangle\,\delta_{\nu''\nu'}\,\delta_{\beta''\beta}\right.$$

$$\left. - \langle\nu'''\beta''|V^*_{ae}|\nu'\beta\rangle\,\delta_{\mu'''\mu'}\,\delta_{\alpha''\beta}\right)F_{\beta\beta}. \qquad (2.50)$$

When the above expression is multiplied out, four terms are obtained. Many of the summations occurring in these terms can be performed using the properties of the Delta function. The final result after carrying out these summations is

$$\hbar^2 \langle \mathcal{H}(\omega) \rangle_{\mu\nu,\mu'\nu'} = \sum_{\substack{\alpha \\ \mu''\alpha'' \\ \mu'''}} F_{\alpha\alpha} \langle \mu\alpha | V_{ae} | \mu''\alpha'' \rangle k^{\mu'''}_{\mu''\alpha'',\nu\alpha,\mu'''\alpha''\nu'\alpha} \langle \mu'''\alpha'' | V_{ae} | \mu'\alpha \rangle$$

$$- \sum_{\substack{\gamma\beta \\ \mu''\nu'''}} F_{\beta\beta} \langle \mu\alpha | V_{ae} | \mu''\beta \rangle k^{\mu'''}_{\mu''\beta\nu\alpha,\mu'\beta\nu'''\alpha} \langle \nu'''\alpha | V^*_{ae} | \nu'\beta \rangle$$

$$- \sum_{\substack{\alpha\beta \\ \nu''\mu'''}} F_{\beta\beta} \langle \nu\alpha | V^*_{ae} | \nu''\beta \rangle k^{\mu'''}_{\mu\nu''\beta,\mu'''\alpha\nu'\beta} \langle \mu'''\alpha | V_{ae} | \mu'\beta \rangle$$

$$+ \sum_{\substack{\alpha \\ \nu''\beta'' \\ \nu'''}} F_{\alpha\alpha} \langle \nu\alpha | V^*_{ae} | \nu''\beta'' \rangle k^{\mu'''}_{\mu\nu''\beta'',\mu'\alpha\nu'''\beta''} \langle \nu'''\beta'' | V^*_{ae} | \nu'\alpha \rangle .$$

(2.51)

If the transitions between initial and final atomic states due to the ion-field are neglected and the no-quenching approximation made for electrons, additional summations in equation (2.51) can be performed. Under the no-quenching approximation (see Section I.4), $V_{ae\,\mu\mu'}$, is zero unless μ and μ' have the same principal quantum number. The effect of neglecting these terms is small for initial and final states that are well separated in energy; this is the case for the Lyman-alpha line. However, since the line profile is given in terms of an integral over all

ion fields, one always encounters fields large enough to cause transitions between initial and final states. However, the behavior of $\langle L_0^a(\mathcal{E}) \rangle$ occurring in $T(\omega)$ is such that the integrand is small for such large fields and, except for the far wings of the line, can be neglected: i.e., for $|\Delta\lambda| > 15\text{Å}$. For the line profile computations presented in this dissertation, the transitions between initial and final states arising from the ion fields will be neglected.

It simplifies the derivation of $\mathcal{H}(\omega)$ if the parabolic representation for the atomic states is used. In the parabolic representation the z component of the atomic matrix element $\vec{R}$ is diagonal with respect to the principal quantum number. Using this representation and choosing a coordinate system for the ion-field integration such that $\mathcal{E}_{iz}$ lies in the $\vec{R}$ direction, the operator L_0 reduces to

$$L_{0\,\mu\nu\beta,\mu'\nu'\beta'} = (\hbar\omega_{\mu\nu} + \hbar\omega_{\nu\beta} + e\mathcal{E}_i(z_{\mu\mu'} - z_{\nu\nu'}))\delta_{\mu\mu'}\delta_{\beta\beta'}\delta_{\mu\mu'}\delta_{\nu\nu'}. \tag{2.52}$$

When this expression is used in the expansion for $K_0(\omega)$ one can show that

$$K_0(\omega)_{\mu\nu\beta,\mu'\nu'\beta'} = k^{mm}_{\mu\nu\beta}\,\delta_{\mu\mu'}\delta_{\nu\nu'}\delta_{\nu\nu'}\delta_{\beta\beta'}. \tag{2.53}$$

When the above form for $K_0(\omega)$ is used in the equation for $\hbar^2\mathcal{H}(\omega)$, the matrix elements reduce to an expression similar to those in equation (3.119) in reference 9:

$$\hbar^2 \langle \mathcal{H}(\omega) \rangle_{\mu\nu,\mu'\nu'} = \delta_{\nu\nu'} \sum_{\substack{\alpha \\ \mu''\alpha''}} F_{\alpha\alpha} \langle \mu\alpha | V_{ae} | \mu''\alpha'' \rangle k_0^{nm}{}_{\mu''\alpha'',\nu\alpha} \langle \mu''\alpha'' | V_{ae} | \mu'\alpha \rangle$$

$$- \sum_{\alpha\beta} F_{\beta\beta} \langle \mu\alpha | V_{ae} | \mu'\beta \rangle k_0^{nm}{}_{\mu'\beta,\nu\alpha} \langle \nu\alpha | V_{ae}^* | \nu'\beta \rangle$$

$$- \sum_{\alpha\beta} F_{\beta\beta} \langle \nu\alpha | V_{ae}^* | \nu'\beta \rangle k_0^{nm}{}_{\mu\alpha,\nu'\beta} \langle \mu\alpha | V_{ae} | \mu'\beta \rangle$$

$$+ \delta_{\mu\mu'} \sum_{\substack{\alpha \\ \nu''\beta''}} F_{\alpha\alpha} \langle \nu\alpha | V_{ae}^* | \nu''\beta'' \rangle k_0^{nm}{}_{\mu\alpha,\nu''\beta''} \langle \nu''\beta'' | V_{ae}^* | \nu'\alpha \rangle, \qquad (2.54)$$

where the nm superscript indicates that the transitions between initial and final states due to the ion-field are not included. Note that k_0^{nm} contains the ion-field, whereas the corresponding expression in reference 9 does not contain the ion-field.

Computational forms for equation (2.54) are derived in Appendix C. If V_{ae} is taken to be the full Coulomb interaction and if symmetry effects in $F_{\alpha\alpha}$ are neglected, one obtains

$$\mathcal{H}(\omega) \propto \sum_{\mu''} \int_0^\infty dq \left[\sqrt{\frac{\pi}{4}} \exp(\alpha/2) \exp\left(-\alpha^2 m k_B T/2q^2 - q^2/8mk_B T\right) \right.$$

$$\left. + iD\left(\alpha \left(\frac{2mk_B T}{4q^2}\right)^{1/2} - \left(\frac{q^2}{2mk_B T}\right)^{1/2}\right) \right] G_{\mu\mu''} G_{\mu''\mu'}$$

$$\times \left(1 - \frac{1}{1 + (\lambda_D q/\hbar)^2}\right) \frac{1}{q^3} \qquad (2.55)$$

where $a = \frac{\hbar\Delta\omega}{k_B T}$, $G_{\mu\mu'}$ is defined in Appendix D, and λ_D is the Debye length. The above expression is the result of evaluating the first term in equation (2.54). If lower state interactions are neglected, the other terms do not enter into the computations. In the dipole approximation the lower state interaction is identically zero for the Lyman-alpha transition. However, when the full Coulomb interaction is used, the lower state interaction is not zero. Computations for the Coulomb case were performed in which the lower state interaction was included; the results show that these lower state interactions produce less than a 5 percent effect on the line profile in the temperature density cases examined. However, these interactions may have a larger effect for the higher series transitions.[34]

From the above analytic form it appears that when the integration variable approaches zero, convergence problems arise in the line center. This would in fact be the case if electron correlations were neglected in the electron distribution function. However, the second term in brackets contains electron correlations and provides convergence in the line center. When electron correlations are neglected, the resulting divergence in $\mathcal{H}(\omega)$ produces a dip in the center of the computed profile.[9,35]

(II.7) HIGHER ORDER TERMS IN $\mathcal{H}(\omega)$

Most of the interactions between the radiator and perturbing electrons are weak because the probability is small that electrons get close enough to the radiator to cause a strong collision (see Section II.2). Since $\mathcal{H}(\omega)$ is expanded in terms of the coupling constant, it is expected that the perturbation expansion for $\mathcal{H}(\omega)$ will converge rapidly for weak interactions or weak coupling. However, in what follows, it is shown that higher order terms may become appreciable for small frequencies: the perturbation expansion breaks down as $\Delta\omega \rightarrow 0$ $(t \rightarrow \infty)$.

The computation of higher order terms is not tractable. Hence, only an approximate analysis of the behavior of a higher order term in the expansion for $\mathcal{H}(\omega)$ is considered. The procedure followed is a generalization of the method used in obtaining an expression for the first term (see Appendix C).

The $n = 2$ terms in the expansion vanish because of the symmetry of the electron distribution function and the radiator-electron interaction.[9] Thus, the next contributing term is the $n = 3$ term. There are $(n + 1)^2 = 16$ such terms. A typical term has the form

$$\sum_{\substack{\alpha''\mu'' \\ \alpha'''\mu''' \\ \alpha^{iv}\mu^{iv}}} \delta_{\nu\nu'} \langle\alpha|V_{\alpha\alpha}|_{\mu\mu''}|\alpha''\rangle k_{0\,\mu''\alpha'',\nu'\alpha'''} \langle\alpha''|V_{\alpha\alpha}|_{\mu''\mu'''}|\alpha'''\rangle$$

$$\times k_{0\,\mu'''\alpha''',\nu'\alpha^{iv}} \langle\alpha'''|V_{\alpha\alpha}|_{\mu'''\mu^{iv}}|\alpha^{iv}\rangle k_{0\,\mu^{iv}\alpha^{iv},\nu'\alpha}$$

$$\times \langle\alpha^{iv}|V_{\alpha\alpha}|_{\mu^{iv}\mu'}|\alpha\rangle F_{\alpha\alpha}. \qquad (2.56)$$

The other fifteen terms are obtained by permutations of the indices in the above term.

For the purpose of estimating the magnitude of the above expression the no-quenching approximation is made and the ion-field splitting of the atomic levels is neglected. Under these conditions the operator k_0 can be written as

$$k_{0\,\mu\alpha,\nu\beta} = -i\int_0^\infty \exp\left(i\tau(\omega-\omega_{\mu\nu}-\omega_{\alpha\beta})\right)d\tau. \qquad (2.57)$$

Inserting these results into equation (2.56) yields

$$i\sum_{\substack{\alpha''\mu'' \\ \alpha'''\mu''' \\ \alpha^{iv}\mu^{iv}}} \delta_{\nu\nu'} \langle\alpha|V_{\alpha\alpha}|_{\mu\mu''}|\alpha''\rangle\int\exp\left(i\tau(\omega-\omega_{\mu''\nu'}-\omega_{\alpha''\alpha'''})\right)d\tau$$

$$\times \langle\alpha''|V_{\alpha\alpha}|_{\mu''\mu'''}|\alpha'''\rangle\int\exp\left(i\tau'(\omega-\omega_{\mu'''\nu'}-\omega_{\alpha'''\alpha^{iv}})\right)d\tau'$$

$$\times \langle\alpha'''|V_{\alpha\alpha}|_{\mu'''\mu^{iv}}|\alpha^{iv}\rangle\int\exp\left(i\tau''(\omega-\omega_{\mu^{iv}\nu'}-\omega_{\alpha^{iv}\alpha})\right)d\tau''$$

$$\times \langle\alpha^{iv}|V_{\alpha\alpha}|_{\mu^{iv}\mu'}|\alpha\rangle F_{\alpha\alpha}. \qquad (2.58)$$

The terms $\omega_{\alpha\alpha'}$ are the change in energy of the perturbing electron during a collision. At the line center $\omega_{\alpha\alpha'}$ is small because changes in the energy of the atomic electron are small and there are no other significant mechanisms in this theoretical treatment which could cause a large change in the perturbing electrons' energy. Also, the terms $\omega - \omega_{\mu\nu}$ are small in the line center. Thus, at the line center the exponentials do not oscillate rapidly as they do in the wings of the line. Hence, it is expected that higher order terms may become large in the line center but not in the line wings since the oscillating nature of the exponentials assures that the above term is small in the line wings.

If the procedure used in Appendix C is generalized, an integral expression for the n = 3 term in $\mathcal{H}(\omega)$ can be obtained. The following multi-dimensional integral is encountered;

$$\sum_{\mu''\mu'''\mu^{IV}} \iiiint d\vec{x}\, d\vec{y}\, d\vec{z}\, d\vec{w} \iiiint d\vec{p}\, d\vec{p}'\, d\vec{p}''\, d\vec{p}''' \iiint d\omega\, d\omega'\, d\omega''$$

$$\times \exp\left(i(\omega + p^2/2mk_BT - p'^2/2mk_BT)\omega\right) \exp\left(i(\omega + p'^2/2mk_BT - p''^2/2mk_BT)\omega'\right)$$

$$\times \exp\left(i(\omega + p''^2/2mk_BT - p'''^2/2mk_BT)\omega''\right) \exp\left(-p^2/2mk_BT\right)$$

$$\times V_{\alpha\alpha}(x)\rho^2(x)\; V_{\alpha\alpha}(y)\; V_{\alpha\alpha}(z)\; V_{\alpha\alpha}(w)\; \langle x|p\rangle\langle p|y\rangle$$

$$\times \langle y|p'\rangle\langle p'|z\rangle\langle z|p''\rangle\langle p''|w\rangle\langle w|p'''\rangle\langle p'''|x\rangle$$

where the meaning of the various terms in this equation and

in subsequent equations in this section are explained in Appendix C. After transforming to relative coordinates and performing all possible integrals analytically, one obtains

$$\sum_{\mu''\mu'''\mu'''\nu} \iiint d\vec{z}\, d\vec{z}'\, d\vec{z}''\, \delta(\vec{z})\,\delta(\vec{z}')\,\delta(\vec{z}'')\left(1 - \frac{1}{1+(\lambda_D z/\hbar)^2}\right)$$

$$\times G_{\mu\mu''}(z)\, G_{\mu''\mu'''}(|\vec{z}'-\vec{z}|)\, G_{\mu'''\mu^{IV}}(|\vec{z}''-\vec{z}'|)\, G_{\mu^{IV}\mu'}(z'')$$

$$\div \left(z^2 z''^2 |\vec{z}'-\vec{z}|^2 |\vec{z}''-\vec{z}'|^2\right).$$

(2.59)

The electron correlations provide a convergence factor for the q integration as they do in the first term, n = 1, of the expansion (see Section II.6). However, the q' and q" integrations do not have suitable convergence factors for small frequency separations. The results of performing the q" integration will be similar to the results obtained in the n = 1 term for i = j (see equation C.23, Appendix C). This factor diverges in the line center. Thus, the q' and q" integrations yield results which diverge in the line center. Hence, the higher order terms are appreciable in the line center.

The above arguments hold whether the full Coulomb interaction or the dipole approximation is used. However, there are differences between the two treatments which are considered next.

In the Lyman-alpha transition, four matrix elements

appearing in the first order term (n = 1) for $\mathcal{H}(\omega)$ are found to account for most of the broadening. When these elements are calculated using the full Coulomb interaction they are larger than the corresponding terms in the dipole approximation. The ratio of the dipole approximation to the full Coulomb interaction treatment for one of the most significant matrix elements is shown in Figure 2. The ratio is always greater than one for the various strong collision cut-offs considered. Therefore, the perturbation expansion for $\mathcal{H}(\omega)$ using the full Coulomb interaction will break down somewhat sooner as $\Delta\omega$ approaches zero than it will when the dipole approximation is employed. This behavior may partially explain the differences between the two treatments in the line center.

Figure 2. Ratio of the matrix element W_{33} computed using the full Coulomb interaction to the same term using the dipole approximation.

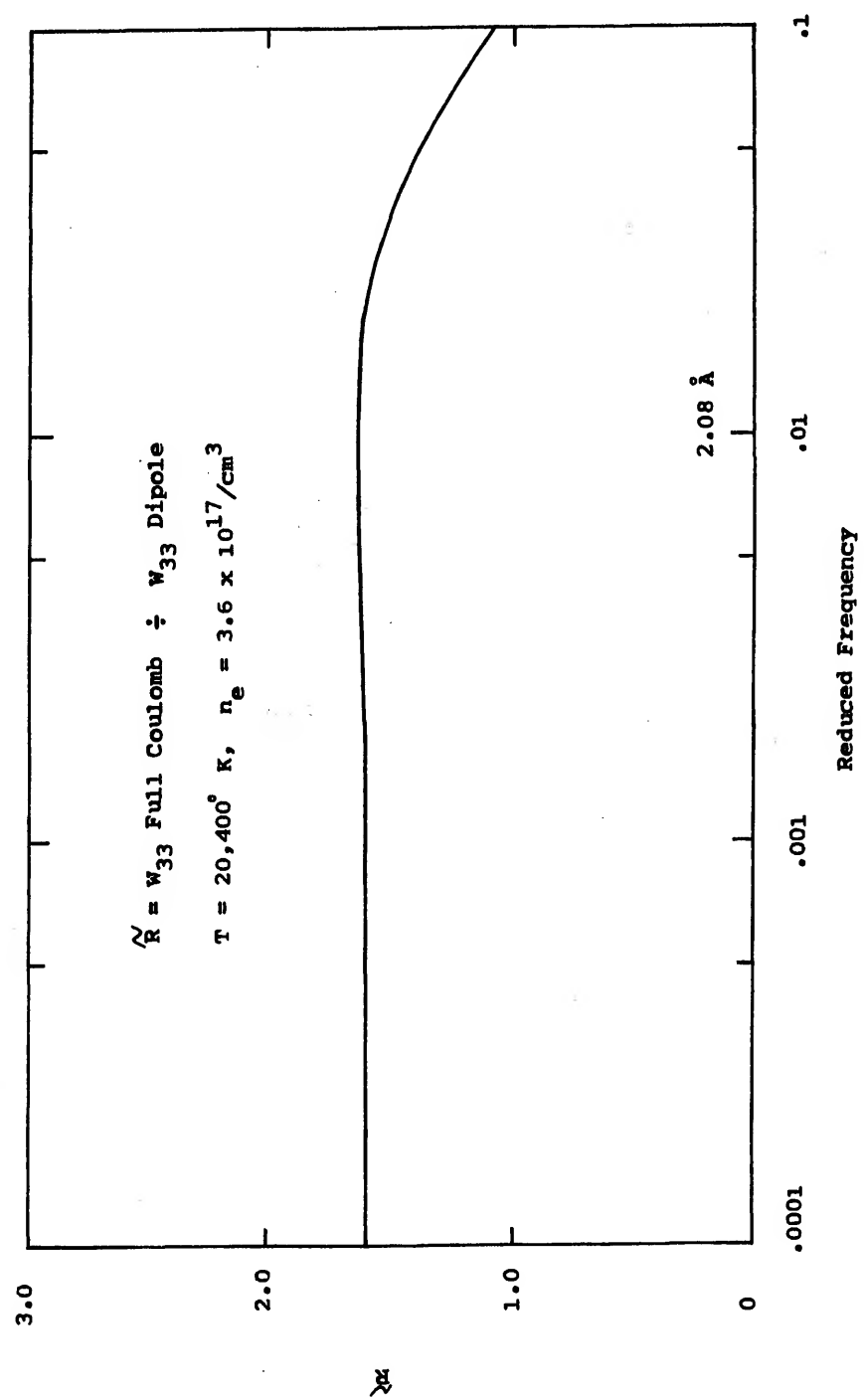
$\tilde{R} = W_{33}$ Full Coulomb ÷ W_{33} Dipole
T = 20,400° K, $n_e = 3.6 \times 10^{17}/cm^3$
2.08 Å
$\tilde{R}$
3.0
2.0
1.0
0
.0001
.001
.01
.1
Reduced Frequency

CHAPTER III

QUALITATIVE ANALYSIS OF THE LINE SHAPE EXPRESSION

(III.1) INTRODUCTION

The mathematical aspects of the line shape problem necessary to interpret the theoretical results are analyzed in this chapter. Expressions for the line shape are derived in which the effects of various approximations can be easily related to the computed profiles. In certain cases, functional aspects of the mathematical expressions are examined rather than the complete expressions used in the computations.

(III.2) THE OPERATOR $\omega - \langle T(\omega)\rangle$

To compute a line profile the expression

$$Tr_a\left(\vec{d}\cdot(\omega - \langle T(\omega)\rangle)^{-1}\rho_a\,\vec{d}\right)$$

must be evaluated. This implies that the matrix elements of the operator $\omega - \langle T(\omega)\rangle$ must be calculated. Due to the Liouville operators occurring in $\langle T(\omega)\rangle$, these matrix elements will be high order tensors requiring, in general, four or more indices. The matrix elements of the Liouville operator, L_0, and of the effective interaction operator, $\mathcal{H}(\omega)$, are given in equations (2.48) and (2.55) respectively. When these are used in the expression for $(\omega - \langle T(\omega)\rangle)$, one obtains the following:

$$\begin{aligned}
\left(\omega - \langle T(\omega)\rangle\right)_{\mu\nu,\mu'\nu'} &= \left[(\omega - \omega_{\mu\nu})\,\delta_{\mu\mu'}\,\delta_{\nu\nu'}\right] \\
&\quad - \left[\frac{e\vec{E}\cdot}{\hbar}\left(\vec{R}_{\mu\mu'}\,\delta_{\nu\nu'} - \vec{R}^{*}_{\nu\nu'}\,\delta_{\mu\mu'}\right)\right] \\
&\quad - \left[c_1 \sum_{\mu''} \int_0^\infty dq\, V(q)\, G_{\mu\mu''}\, G^{*}_{\mu''\mu'}\left(1 - \frac{1}{1+(\lambda_D q/\hbar)^2}\right)\frac{\delta_{\nu\nu'}}{q^3}\right] \\
&\quad - \left[c_2 \int_0^\infty dq\, V(q)\, G_{\mu\mu'} \cdot G_{\nu\nu'}\left(1 - \frac{1}{1+(\lambda_D q/\hbar)^2}\right)/q^3\right]
\end{aligned} \tag{3.1}$$

where C_1 and C_2 are constants. As indicated in Appendix C, the function $\psi(\beta)$ depends on the ion-field shifted frequency.

The first bracketed term in the above expression represents the frequency separation from the line center. Mathematically it can be interpreted as the independent variable.

The second term contains the broadening effects of the static ions. $\vec{R}^{*}_{vv'}$ is restricted to lower states and $\vec{R}_{uu'}$ is restricted to the upper states. Hence, lower state interactions with the ion-fields are included. The lower state ion-field broadening is identically zero for the Lyman-alpha line in hydrogen. However, it may become important in the Balmer beta transition having as much as a 10 percent effect in certain cases.[31]

The last two terms in equation (3.1) represent the effects of electron broadening. In the relaxation theory these terms are not symmetric in $\omega - \omega_{uv}$ and are solely responsible for a red asymmetry in the line center that changes to blue in the far wings of the line. The red to blue cross over is quite apparent for the Lyman-alpha transition in ionized helium.[36,37] It also appears in the Lyman-alpha profile for hydrogen but only in the far wings of the line, $\Delta\lambda > 8\text{Å}$.

As discussed in Section (II.6), lower state perturbations due to electron interactions are contained in the last term in brackets in equation (3.1).

In reference 9 it is shown that for the Lyman-alpha transition only the $v = v' = 1$ terms contribute to the line

profile. In the no-quenching approximation the states $\mu\mu'$ are restricted to initial states. Thus, for the Lyman-alpha transition only two indices are required to specify the elements in the tetradic $\omega - \langle T(\omega) \rangle$. That is $(\omega - \langle T(\omega) \rangle)$ has a convenient matrix representation. Furthermore, since a hydrogenic state having principal quantum number n, has n^2 degenerate levels, the matrix representation will be $n^2 \times n^2$; it will also have a block diagonal form as will be shown in the next section.

(III.3) THE PARABOLIC REPRESENTATION

The Schroedinger equation without an external field is separable in the parabolic coordinate system. The resulting wave functions are given by[38]

$$\Psi_{n_\mu s_\mu m_\mu}(\mu,\lambda,\phi) = \left[\frac{\quad}{\quad}\right]^{1/2} \exp(i m_\mu \phi)\,(\sqrt{\lambda\mu}/n_\mu a_0)^{|m_\mu|}$$

$$\times \exp(-(\lambda+\mu)/2n_\mu a_0)\, L^{|m_\mu|}_{s_\mu}(\lambda/n_\mu a_0)\, L^{|m_\mu|}_{n_\mu - s_\mu - |m_\mu| - 1}(\mu/n_\mu a_0) \tag{3.2}$$

where $n_\mu s_\mu m_\mu$ are the parabolic quantum numbers associated with the atomic state, $|\mu\rangle$. The other symbols are defined in Appendix D. It should be emphasized that the parabolic wave functions given above are not "Stark" wave functions since they are not solutions to the Schroedinger equation for a system consisting of a hydrogen atom in an external field.

The parabolic representation is used for mathematical convenience. For a given principal quantum number, the z component of the dipole matrix element is diagonal in this representation. Hence, the atomic density matrix occurring in the line profile expression is diagonal; the second term in brackets in equation (3.1) is also diagonal, and many of the other matrices reduce to a block diagonal form. These

simplifications are particularly convenient for computational purposes.

In the full Coulomb interaction case, the term $G_{\mu\mu''} G^{*}_{\mu''\mu'}$ occurring in $\omega - \langle T(\omega) \rangle$ contains a delta function factor of the form

$$\delta_{m_\mu m_{\mu''}} \delta_{m_{\mu''} m_{\mu'}} = \delta_{m_\mu m_{\mu'}}$$

where m_μ is the magnetic quantum number. Thus, $G_{\mu\mu''} G^{*}_{\mu''\mu'}$ is diagonal in m when the full Coulomb interaction is used.

In the dipole approximation the third term in the expression for $\omega - \langle T(\omega) \rangle$, given in equation (3.1), becomes

$$-C_1 \sum_{\mu''} \vec{R}_{\mu\mu''} \cdot \vec{R}_{\mu''\mu'} \int_0^\infty J(q) \left(1 - \frac{1}{1 + (\lambda_0 q/\hbar)^2}\right) \frac{\delta_{\nu\nu'}}{q^3} \, dq .$$

With the results of Appendix F, the dot product $\vec{R}_{\mu\mu''} \cdot \vec{R}_{\mu''\mu'}$ is found to contain delta function products of the form

$$\delta_{m_\mu m_{\mu''}} \delta_{m_{\mu''} m_{\mu'}} = \delta_{m_\mu m_{\mu'}}$$

$$\delta_{m_{\mu''}, m_\mu - 1} \delta_{m_{\mu''} m_{\mu'} - 1} = \delta_{m_\mu m_{\mu'}}$$

$$\delta_{m_{\mu''}, m_\mu + 1} \delta_{m_{\mu''} m_{\mu'} + 1} = \delta_{m_\mu m_{\mu'}} .$$

Thus in both the dipole interaction and the full Coulomb interaction, the matrix $(\omega - \langle T(\omega) \rangle)$ has the form

$(\omega - \langle T(\omega) \rangle) \longrightarrow$

$\mu \backslash \mu'$	1	2	3	4	5
1	1 1	0	0	0	0
2	0	2 2	0	0	0
3	0	0	3 3	3 4	0
4	0	0	4 3	4 4	0
5	0	0	0	0	5 5

where the parabolic states are labeled as follows:

$|1\rangle \equiv |100\rangle$
$|2\rangle \equiv |20\text{-}1\rangle$
$|3\rangle \equiv |200\rangle$
$|4\rangle \equiv |210\rangle$
$|5\rangle \equiv |201\rangle$.

Blocks which arise from the same magnitude of m but different signs are mathematically equivalent and can be shown to give identical contributions to the line profile: thus, the 22 block contributes the same as the 55 block. This follows from the form of the wave function given in equation (3.2): the wave function depends on the sign of m only through the term $\exp(im\phi)$ which does not affect the magnitude or sign of any of the matrix elements (see Appendices D and F).

Following a similar procedure for the Balmer beta transition, it is found that the orders of the matrices enoountered range from 1 to 4.

(III.4) THE LYMAN-ALPHA TRANSITION

From the previous section, it is clear that the symmetry of the atomic states in the parabolic representation greatly simplifies the computational effort. However, there still remains the problem of reducing the line shape expression given in equation (2.25) to quadratures. This section outlines the procedure for reducing the Lyman-alpha line shape expression to a convenient calculable form.

The matrix elements of the operator $(\omega - \langle T(\omega)\rangle)$ are

$$(\omega - \langle T(\omega)\rangle)_{\mu\mu'} = \frac{\hbar \Delta\omega_{\mu 1}}{k_B T}\delta_{\mu\mu'} - \frac{e\mathcal{E}_0 \epsilon}{k_B T}\left(R^{z}_{\mu\mu'}\delta_{\nu\nu'} - R^{z}_{\nu\nu'}\delta_{\mu\mu'}\right) + i\,\frac{2e^4 n_e}{3\hbar k_B T}\left(\frac{8\pi m}{k_B T}\right)^{1/2} a_0^2\, W_{\mu\mu'} \tag{3.3}$$

where

$\mathcal{E}_0 = 2.61\, e\, n_e^{2/3}$

$\mathcal{E}$ = ion microfield

$W_{\mu\mu'}$ = electron collision term.

In the dipole approximation $W_{\mu\mu'}$ is given by

$$W_{\mu\mu'} = a_0^{-2} \sum_{\mu''=2}^{5}{}' \vec{R}_{\mu\mu''} \cdot \vec{R}_{\mu''\mu'}\, q(\overline{\Delta\omega}_{\mu''1}) \tag{3.4}$$

where $\overline{\Delta\omega}_{\mu''1}$ contains the ion-field. Using the results derived in Appendix F we find that the non zero matrix

elements of $W_{\mu\mu'}$ are

$$W_{22} = 4.5\left(g(\overline{\Delta\omega_{21}}) + g(\overline{\Delta\omega_{41}})\right)$$

$$W_{33} = 9\left(g(\Delta\omega_0) + g(\overline{\Delta\omega_{31}})\right)$$

$$W_{34} = 9\, g(\Delta\omega_0)$$

$$W_{44} = 9\left(g(\Delta\omega_0) + g(\overline{\Delta\omega_{41}})\right)$$

$$W_{43} = W_{34}$$

(3.5)

where $\Delta\omega_0 \equiv \overline{\Delta\omega_{21}} = \overline{\Delta\omega_{51}}$ is the unshifted frequency separation. The corresponding elements of $(\omega - \langle T(\omega)\rangle)$ are

$$\left(\omega - \langle T(\omega)\rangle\right)_{22} = \frac{\hbar\Delta\omega_0}{k_B T} + iC_W W_{22}$$

$$\left(\omega - \langle T(\omega)\rangle\right)_{33} = \frac{\hbar\Delta\omega_0}{k_B T} - Z_{33}\frac{e\mathcal{E}_\phi \mathcal{E}}{k_B T} + iC_W W_{33}$$

$$\left(\omega - \langle T(\omega)\rangle\right)_{34} = iC_W W_{34}$$

$$\left(\omega - \langle T(\omega)\rangle\right)_{44} = \frac{\hbar\Delta\omega_0}{k_B T} - Z_{44}\frac{e\mathcal{E}_\phi \mathcal{E}}{k_B T} + iC_W W_{44}$$

$$\left(\omega - \langle T(\omega)\rangle\right)_{55} = \left(\omega - \langle T(\omega)\rangle\right)_{22}$$

$$\left(\omega - \langle T(\omega)\rangle\right)_{43} = \left(\omega - \langle T(\omega)\rangle\right)_{34}$$

(3.6)

where $Z_{33} = 3a_0$, $Z_{44} = -3a_0$, and the definition of c_w follows from equation (3.3),

$$c_w = \frac{2\pi^4 n_e}{3\hbar k_B T}\left(\frac{8\pi m}{k_B T}\right)^{1/2} a_0^2$$

All other matrix elements are zero or do not enter into the computations because of the restriction that $\vec{d}$ have matrix elements only between the initial and final states.

The resolvent operator, $K(\omega)$, appearing in the line shape expression is the inverse of $\omega - \langle T(\omega)\rangle$. For block diagonal matrices one has

$$\begin{pmatrix} (22) & & \\ & \begin{pmatrix} 33 & 34 \\ 43 & 44 \end{pmatrix} & \\ & & (55) \end{pmatrix}^{-1} = \begin{pmatrix} (22)^{-1} & & \\ & \begin{pmatrix} 33 & 34 \\ 43 & 44 \end{pmatrix}^{-1} & \\ & & (55)^{-1} \end{pmatrix} = \begin{pmatrix} (22)^{-1} & & \\ & \frac{1}{D}\begin{pmatrix} 44 & -34 \\ -43 & 33 \end{pmatrix} & \\ & & (55)^{-1} \end{pmatrix}$$

where D is the determinant of the 2 x 2 matrix.

The determinant of the 2 x 2 block reduces to

$$\left(\frac{\hbar\Delta\omega_0}{k_B T}\right)^2 - \left(\frac{3a_0 e\mathcal{E}_0 \mathcal{E}}{k_B T}\right)^2 + ic_w \frac{3a_0 e\mathcal{E}_0}{k_B T}(W_{33} - W_{44})\mathcal{E}$$
$$+ c_w^2 (W_{34}^2 - W_{33} W_{44}) + ic_w \frac{\hbar\Delta\omega_0}{k_B T}(W_{33} + W_{44})$$

which can be rewritten in the following convenient form:

$$\left(\frac{\hbar\Delta\omega_0}{k_B T}\right)^2 - \left(\frac{3a_0 e\mathcal{E}_0 \mathcal{E}}{k_B T}\right)^2 + A\mathcal{E} + B \qquad (3.7)$$

where A and B are complex coefficients that depend on the matrix elements of W. A and B are small compared to $\hbar \Delta\omega_0 / R_B^T$ except in the line center (see Chapter V for actual numerical comparisons). Hence, the determinant provides a resonant denominator which has a minimum at ion-fields given by

$$\mathcal{E} \simeq \frac{\hbar \Delta\omega_0}{3 q_0 e \mathcal{E}} \,. \tag{3.8}$$

The function $J(\omega, \mathcal{E})$ used to compute the line profile (see equation 2.15) will be peaked at values of the field given in the above equation. $J(\omega, \mathcal{E})$ can be interpreted as a line profile from a radiating atom that is placed in a constant ion-field and perturbed by the electrons. This interpretation is useful since considerable physical insight into the effects of electron broadening can be gained by studying the function $J(\omega, \mathcal{E})$ rather than the full line profile.

For transitions more complicated than the Lyman-alpha profile, there will be additional resonant denominators corresponding to the various Stark shifted levels. For example, in the Balmer beta line there are three different z matrix elements resulting in three distinct resonant denominators.

To compute a line shape, the imaginary part of the following trace is required

$$Tr_a \left(\vec{d} \cdot K(\omega) \rho_a \vec{d} \right).$$

The matrix $\vec{d}$ occurring in the above expression is restricted to have elements only between initial and final states. The matrix elements of the x, y, and z components are computed in Appendix F.

In the no-quenching approximation, the atomic density matrix ρ_a can be written as,

$$\rho_a \rightarrow \begin{pmatrix} 1 & & & \\ & 1 & & \\ & & \rho_{33} & \\ & & & \rho_{44} \end{pmatrix}$$

where $\rho_{\mu\mu} = \exp\left(-R^{E}_{\mu\mu}\left(\frac{e\mathcal{E}_0\mathcal{E}}{kT}\right)\right)$.

Using the above results the trace over atomic states can be performed. The results are:

$$T_{r_a}\left(\vec{d}\cdot K(\omega)\rho\vec{d}\right) \rightarrow \text{CONSTANT}\left[4K_{22} + \rho_{33}\left(K_{33}-K_{34}\right) + \rho_{44}\left(K_{44}-K_{34}\right)\right].$$

(3.9)

The leading term in brackets does not have a strong ion-field dependence in the dipole approximation and is field independent in the full Coulomb interaction treatment. In the dipole approximation, this term can be interpreted as representing the effects of electron broadening on the initial levels, $|3\rangle$ and $|4\rangle$. In the dipole approximation the K_{22} term depends on the dipole matrix elements having different magnetic (m) quantum number as can be seen by examining the W_{22} matrix element given in equation (3.4).

However, the full Coulomb interaction does not mix states having different m values; as a consequence, the leading term is field independent.

In both the dipole approximation and the full Coulomb interaction case, the K_{22} contribution is significant only in the line center. For a temperature of 20,000° K and an electron density of $3 \times 10^{17}/cm^3$ the K_{22} contribution for the dipole approximation is significant from 0 - 1 Å from the line center. Whereas, for the full Coulomb interaction treatment the range of importance is from 0 - .8 Å. The net effect of this slightly different behavior is to produce a shoulder in the line shape when the full Coulomb interaction is used. It is interesting to note that a similar behavior is encountered in the dipole approximation at higher temperatures in hydrogen and in the Lyman-alpha transitions in ionized helium.

By taking the $W \to 0$ limit in equation (2.54) a static wing formula can be obtained. This is the subject of the next chapter.

CHAPTER IV

ASYMPTOTIC WING FORMULA

(IV.1) INTRODUCTION

The purpose of the present chapter is to derive an expression that accurately describes the wings of the profile. In Section (IV.2) a heuristic derivation of a static wing formula is presented. The resulting formula is shown to be the leading term in a rigorous perturbation expansion presented in Section (IV.3). Higher order terms in this expansion are shown to include the effects of electron dynamics.

(IV.2) HEURISTIC DERIVATION OF A STATIC WING FORMULA

In the derivation considered in this section, it is assumed that the only broadening mechanisms are static fields. Under this assumption a wing formula can be obtained from the line profile expression (equation 3.9) presented in Chapter III by the following procedure: 1. Replace all static ion-fields, $\mathcal{E}_i$, by the total static field, $\mathcal{E}_T$ ($\mathcal{E}_T = \mathcal{E}_i + \mathcal{E}_e$). 2. Take the limit as the electron dynamic terms go to zero. In this limit the line profile becomes

$$I_{(\omega)}_{STATIC} = P_{33}(\mathcal{E}_T) P_T(\mathcal{E}_T) \Big|_{\mathcal{E}_T = \frac{\hbar \Delta\omega}{3 a_0 e \mathcal{E}_\phi}} + P_{44}(\mathcal{E}_T) P_T(\mathcal{E}_T) \Big|_{\mathcal{E}_T = -\frac{\hbar \Delta\omega}{3 a_0 e \mathcal{E}_\phi}} + 4 K_{22} \tag{4.1}$$

where $P_T(\mathcal{E}_T)$ is the microfield probability function for the combined electron- and ion-fields, defined as $\mathcal{E}_T^2 Q(\mathcal{E}_T)$. Since $P_{33}(\mathcal{E}) = P_{44}(-\mathcal{E})$ (see Section III.4) and $P_T(\mathcal{E}_T)$ is symmetric[14] in $\mathcal{E}_T$, the above expression is equivalent to

$$I_{(\omega)}_{STATIC} = 2 P_{33}(\mathcal{E}_T) P_T(\mathcal{E}_T) \Big|_{\mathcal{E}_T = \frac{\hbar \Delta\omega}{3 a_0 e \mathcal{E}_\phi}} + 4 K_{22} \,. \tag{4.2}$$

The atomic density matrix element ρ_{33} evaluated at $\mathcal{E}_T = \frac{\hbar \Delta\omega}{3 a_0 e \mathcal{E}_p}$ is equal to 1/e where e is the natural logarithm base. Thus

$$I_{STATIC}(\omega) = 2 P_T \left(\mathcal{E}_T = \frac{\hbar \Delta\omega}{3 a_0 e \mathcal{E}_p} \right) / e \quad + 4 K_{22} . \tag{4.3}$$

Determining the microfield distribution function for the total field from first principals is non trivial. As a first approximation a convolution of the electron microfield with an ion microfield is used. The procedure for obtaining the total microfield in terms of a convolution follows.

The microfield is defined as

$$Q(\mathcal{E}_T) = T_{n_{ei}} \left(\rho_{ei} \, \delta(\vec{\mathcal{E}}_T - \vec{\mathcal{E}}_i - \vec{\mathcal{E}}_e) \right) . \tag{4.4}$$

By writing the density matrix in factored form, one can show that the above reduces to [39]

$$\begin{aligned} Q(\mathcal{E}_T) &= T_{n_{ei}} \left(\rho_e \rho_i \, \delta(\vec{\mathcal{E}}_T - \vec{\mathcal{E}}_i - \vec{\mathcal{E}}_e) \right) \\ &= \int d^3\mathcal{E}' T_{n_i} (\rho_i \, \delta(\vec{\mathcal{E}}' - \vec{\mathcal{E}}_i)) T_{n_e} (\rho_e \, \delta(\vec{\mathcal{E}}_T - \vec{\mathcal{E}}' - \vec{\mathcal{E}}_e)) \\ &= \int d^3\mathcal{E}' \, Q(\mathcal{E}') Q(\mathcal{E}' - \mathcal{E}_T) \end{aligned} \tag{4.5}$$

where the properties of the Dirac delta distribution have been used to obtain the last expression which is a convolution of microfields.

It should be emphasized that the above expression for the total microfield is an approximation: in order to obtain the factored form for the density matrix, the electron-ion interaction was taken into account by an effective potential which depends only on the ion coordinates (see Section II.1 and Section I.4). Hence, the electron-ion interaction is contained only in the ion microfield. It is expected that this treatment of the electron-ion interaction should be good since the mobility of the electrons is much larger than the ion mobility resulting in a shielding of the ion-ion interaction. To examine the effects of shielding on the electron-electron interaction, line profiles obtained from convolutions of various combinations of low- and high-frequency microfields are compared in Chapter V.

(IV.3) THEORETICAL DERIVATION OF A WING FORMULA

In the line wings the time of interest is small; hence, a perturbation expansion in which the time is an expansion parameter may prove to be useful in the line wings. Such an expansion is derived in this section and carried to second order. The procedure for generating higher order terms follows from a straightforward extension of the method used to calculate the second order term.

The Hamiltonian appearing in the function, $\Phi(x)$, can be written as

$$H = H_1 + H_2$$

where

$$H_1 = H_a + V_{ii} + V_{aa} \tag{4.6a}$$

$$H_2 = H_e + H_i + V_{ei}. \tag{4.6b}$$

Using the above definitions the time development operator $T(x)$ appearing in $\Phi(x)$ can be written as

$$\exp(-ixH/\hbar) = \exp(-ix(H_1+H_2)/\hbar) \approx$$
$$\exp(-ixH_1/\hbar)\exp(-ixH_2/\hbar)\exp(-x^2[H_1,H_2]/(2\hbar^2)) \tag{4.7}$$

where exponents containing third and higher order terms have

been neglected: i.e.,

$$\exp(-x^n [H_1,\cdots[H_1, H_2]\cdots]) \approx 1, \text{ for } n > 2.$$

Similarly

$$\exp(ixH/\hbar) \approx \exp(x^2[H_1,H_2]/\hbar^2)\exp(ixH_2/\hbar) \times \exp(ixH_1/\hbar).$$

Substituting the above results in to $\Phi(x)$ yields

$$\Phi(x) = T_n\left(\vec{d}\cdot \exp(x^2[H_1,H_2]/2\hbar^2 \exp(ixH_2/\hbar) \times \left(\exp(ixH_1/\hbar)\rho\vec{d}\exp(-ixH_1/\hbar)\right) \times \exp(-ixH_2/\hbar)\exp(-x^2[H_1,H_2]/2\hbar^2)\right).$$

(4.8)

It is convenient to regroup the above equation into the following form:

$$\Phi(x) = T_n\left(\vec{d}\cdot \exp(x^2[H_1,H_2]/2\hbar^2 + ixH_2/\hbar)\exp(ixH_1/\hbar) \times \rho\vec{d}\exp(-ixH_1/\hbar)\exp(-x^2[H_1,H_2]/2\hbar^2 - ixH_2/\hbar)\right)$$

(4.9)

where again terms such as $\exp(\mathcal{O}x^3)$ have been set equal to one.

The following operator expansion[40] is used to further reduce $\Phi(x)$:

$$\exp(A)\,B\exp(-A) = B + [A,B] + \frac{1}{2!}[A,[A,B]] + \cdots \tag{4.10}$$

where A and B are operators defined as

$$B \equiv \exp(ixH_1/\hbar)\,\rho\,\vec{d}\,\exp(-ixH_1/\hbar)$$

$$A \equiv -x^2[H_1,H_2]/2\hbar^2 - ixH_2/\hbar \tag{4.11}$$

and then applying the above to equation (4.9) for $\Phi(x)$ yields

$$\begin{aligned}\Phi(x) \simeq\ & T_n\left(\vec{d}\cdot\exp(ixH_1/\hbar)\,\rho\,\vec{d}\,\exp(-ixH_1/\hbar)\right)\\ &+\frac{ix}{\hbar}T_n\left(\vec{d}\cdot[H_2,\exp(ixH_1/\hbar)\,\rho\,\vec{d}\,\exp(-ixH_1/\hbar)]\right)\\ &+\frac{x^2}{2\hbar^2}T_n\left(\vec{d}\cdot\left[\tfrac{1}{\hbar}[H_1,H_2],\exp(ixH_1/\hbar)\,\rho\,\vec{d}\,\exp(-ixH_1/\hbar)\right]\right.\\ &\left.-[H_2,[H_2,\exp(ixH_1/\hbar)\,\rho\,\vec{d}\,\exp(-ixH_1/\hbar)]]\right)\\ &+O(x^3).\end{aligned} \tag{4.12}$$

Clearly the above expression will break down for large times. Hence, as smaller frequency separations are approached, higher order terms will become increasingly important. It is expected that electron dynamics will certainly be

significant for frequencies less than the electron plasma frequency; thus, for the region of the profile corresponding to $\Delta\omega < \Delta\omega_p$ terms linear in τ and perhaps even higher order terms will be required to adequately represent the intensity. Based on comparisons with experimental data presented in Chapter V, this behavior indeed appears to be verified.

CHAPTER V

ANALYSIS OF THE THEORETICAL RESULTS

(V.1) INTRODUCTION

An analysis of the theoretical computations is presented in this chapter. The theoretical results are compared with the experimental data and with other theoretical computations.

(V.2) THE FUNCTION $J(\omega, \mathcal{E})$

The line profile involves an integration over $\mathcal{E}$ of the product of $P(\mathcal{E})$ times $J(\omega, \mathcal{E})$. The region of the profile in which various field dependent effects are important can be determined by an analysis of $J(\omega, \mathcal{E})$.

$J(\omega, \mathcal{E})$ consists of a field independent term plus a field dependent term:

$$J(\omega, \mathcal{E}) = j(\omega) + \mathcal{J}(\omega, \mathcal{E}). \qquad (5.1)$$

In the case of Lyman-alpha radiation, a graph of $\mathcal{J}(\omega, \mathcal{E})$ vs. $\mathcal{E}$ will have one sharp peak due to the resonance denominator discussed in Section III.4 (see Figure 3).

A slightly more complicated result is found when $\mathcal{J}(\omega, \mathcal{E})$ vs. $\mathcal{E}$ is plotted for the Lyman-beta transition in hydrogen. In this case, the ion-field removes the degeneracy in the upper level, splitting it into three distinct levels, two of which are shifted. Hence, the graph of the field dependent part of $J(\omega, \mathcal{E})$ will have two peaks. $\mathcal{J}(\omega, \mathcal{E})$ for the Lyman-beta transition is plotted in Figure 4. For $\mathcal{E} = 0$ both peaks coincide and occur at $\mathcal{E} = 0$. As the frequency increases two peaks appear.

A few general characteristics of $\mathcal{J}(\omega, \mathcal{E})$ and some of the resulting implications are listed below.

Figure 3. Field dependent part of the function $J(\omega, \xi)$ for the Lyman-alpha profile.

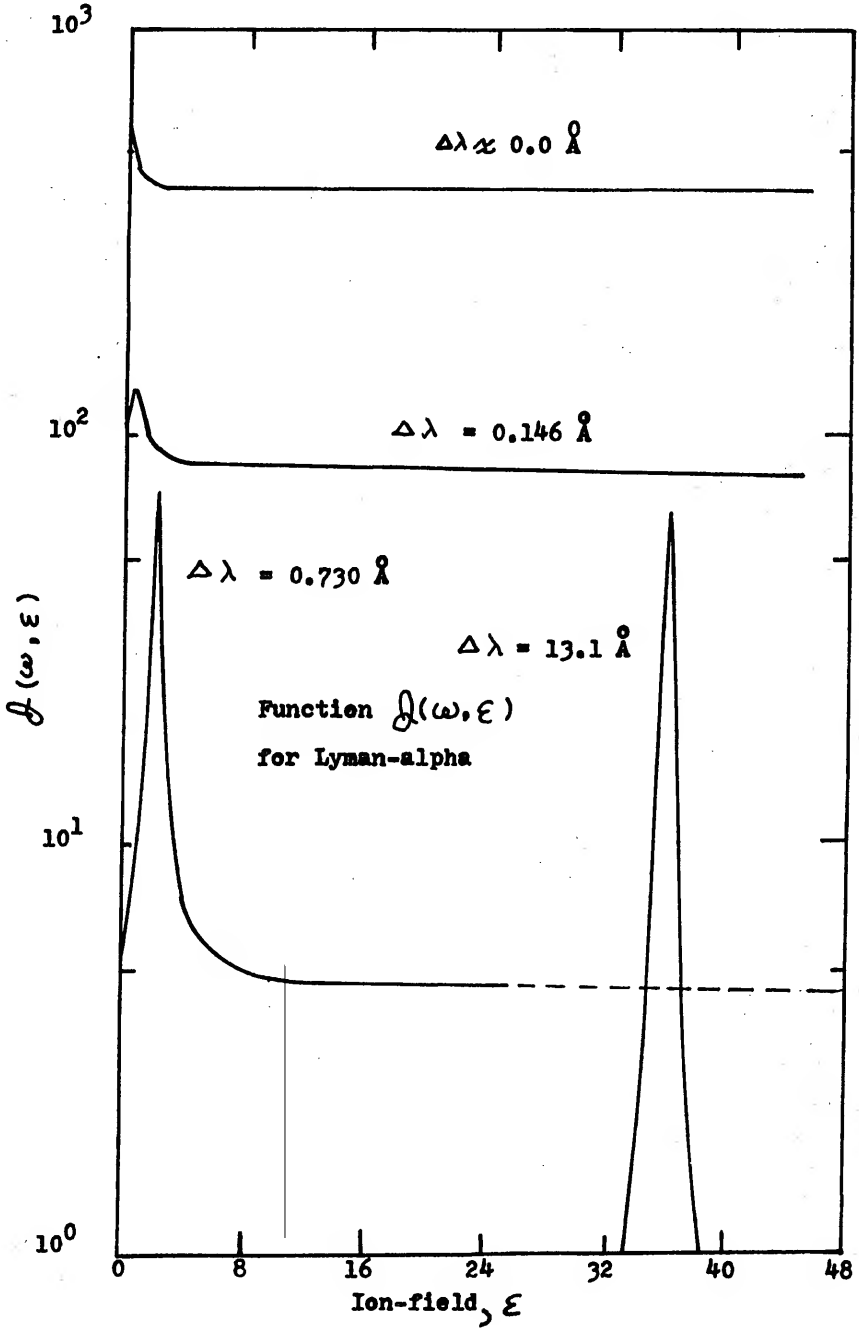
10^3
10^2
10^1
10^0
$\Delta\lambda \approx 0.0$ Å
$\Delta\lambda$ = 0.146 Å
$\Delta\lambda$ = 0.730 Å
$\Delta\lambda$ = 13.1 Å
Function $\beta(\omega, \varepsilon)$
for Lyman-alpha
$\beta(\omega, \varepsilon)$
0
8
16
24
32
40
48
Ion-field, ε

Figure 4. Field dependent part of the function $J(\omega, \xi)$ for the Lyman-beta profile.

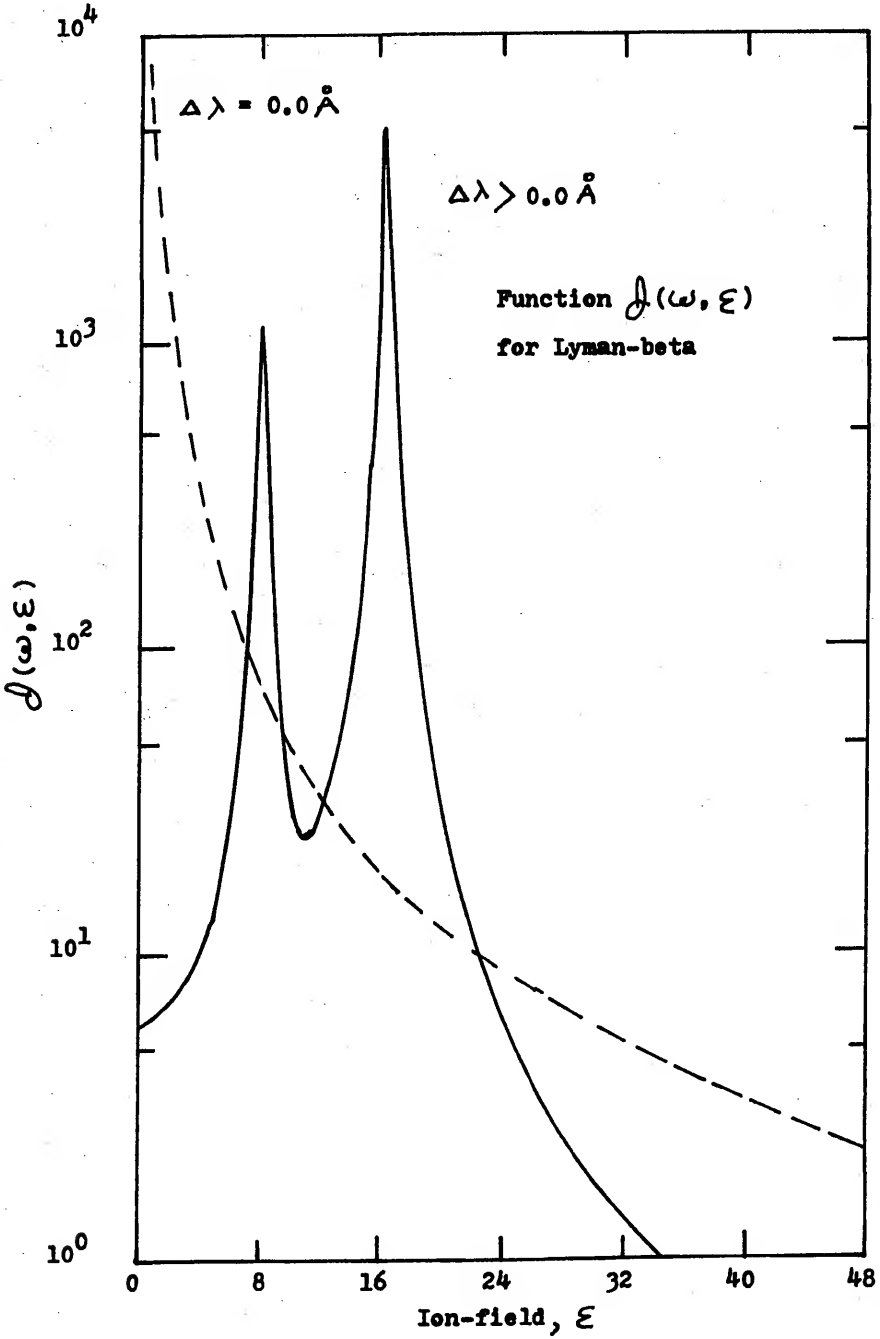
10^4
10^3
10^2
10^1
10^0
$\beta(\omega, \varepsilon)$
$\Delta\lambda = 0.0$ Å
$\Delta\lambda > 0.0$ Å
Function $\beta(\omega, \varepsilon)$
for Lyman-beta
0
8
16
24
32
40
48
Ion-field, ε

1) For large frequency separations from the line center, most of the contribution to the field integration appearing in the line shape expression arises from large values of the field.

2) The relative maximum of $\mathcal{J}(\omega, \mathcal{E})$ increases as the frequency increases while the half-width decreases. This suggests that replacing the peaks in the function $\mathcal{J}(\omega, \mathcal{E})$ by delta function distributions should be accurate in the line wings. This limiting behavior was used in the heuristic derivation of the static wing formula discussed in Section (V.2).

3) The maximum value of $\mathcal{J}(\omega, \mathcal{E})$ decreases rapidly as the frequency increases, but the rate of decrease diminishes for larger values of the frequency.

4) For every value of $\Delta\omega$, $\mathcal{J}(\omega, \mathcal{E})$ will approach a fairly constant value for field values greater than those for which $\mathcal{J}(\omega, \mathcal{E})$ peaks.

From the behavior of $\mathcal{J}(\omega, \mathcal{E})$ it is easy to determine the range in frequency for which various field dependent effects are important. For example, a field dependent effect that is directly proportional to the strength of the field will be most important in the line wings. One such effect which exhibits this dependency arises from the field dependence in the atomic Boltzmann factors. This is the subject of the next section.

(V.3) THE ION-FIELD DEPENDENT ATOMIC DENSITY MATRIX

The Stark shift in energy levels caused by the ion-field is frequently neglected in the atomic density matrix occurring in the line shape expression. Neglecting the field assumes that the density of states is equal for all atomic levels corresponding to a given principal quantum number. The ion-field removes the degeneracy of the excited states via the Stark effect yielding $2n - 1$ distinct energy levels or Stark levels where n is the principal quantum number.[32] The field dependent atomic density matrix weights Stark states that are lower in energy more heavily than states of higher energy. Since transitions from lower energy initial states give rise to the red wing of the line profile, inclusion of the ion-field in the atomic density matrix will cause a net red asymmetry. To determine whether this effect is uniform over the entire profile one can analyze the function $\mathcal{J}(\omega, \mathcal{E})$. In the previous section, curves that demonstrate the behavior of $\mathcal{J}(\omega, \mathcal{E})$ were presented. For the Lyman-alpha transition the peak in $\mathcal{J}(\omega, \mathcal{E})$ occurs at a field value given approximately by

$$\mathcal{E} \approx \hbar \Delta\omega / (3 a_0 e \mathcal{E}_0) \qquad (5.2)$$

Thus, for large frequency separations, $\mathcal{J}(\omega, \mathcal{E})$ peaks at large values of the ion microfield. The exponent appearing

in the Boltzmann factors in the atomic density matrix is directly proportional to the ion-field and hence, the larger the field, the greater the effect in the density matrix. Thus, the effect of including the field in the atomic density matrix is relatively more important in the wings of the line than it is in the line center. Profiles calculated with and without an ion-field dependent atomic density matrix are given in Figures 5 and 6 respectively. From these curves it is demonstrated that including the ion-field can produce a noticeable effect for wavelengths greater than 4 Å.

The dependence of the atomic density matrix on temperature and on the magnitude of the dipole matrix element should also be considered. The ion-field dependent factor appearing in the exponent of the atomic density matrix is proportional to $\mathcal{E} R^z / k_B T$ where T is the temperature and R^z is the z component of the atomic dipole operator. Thus, at low temperatures, the importance of the Boltzmann factor increases. Also, for higher series transitions R^z is larger and the effect may become large. Since radiation from higher series transitions will be of longer wavelength, the corresponding frequency separations will be smaller. For small values of the frequency separation the field integration over $\beta(\omega, \mathcal{E})$ contributes significantly only for small values of the field. Thus, for higher series transitions, the product $\mathcal{E} R^z$ is not as large as one might otherwise expect.

For the Lyman-alpha transition in ionized helium, the z component of the atomic dipole matrix element is smaller by a

Figure 5. Lyman-alpha profile using a field dependent atomic density matrix.

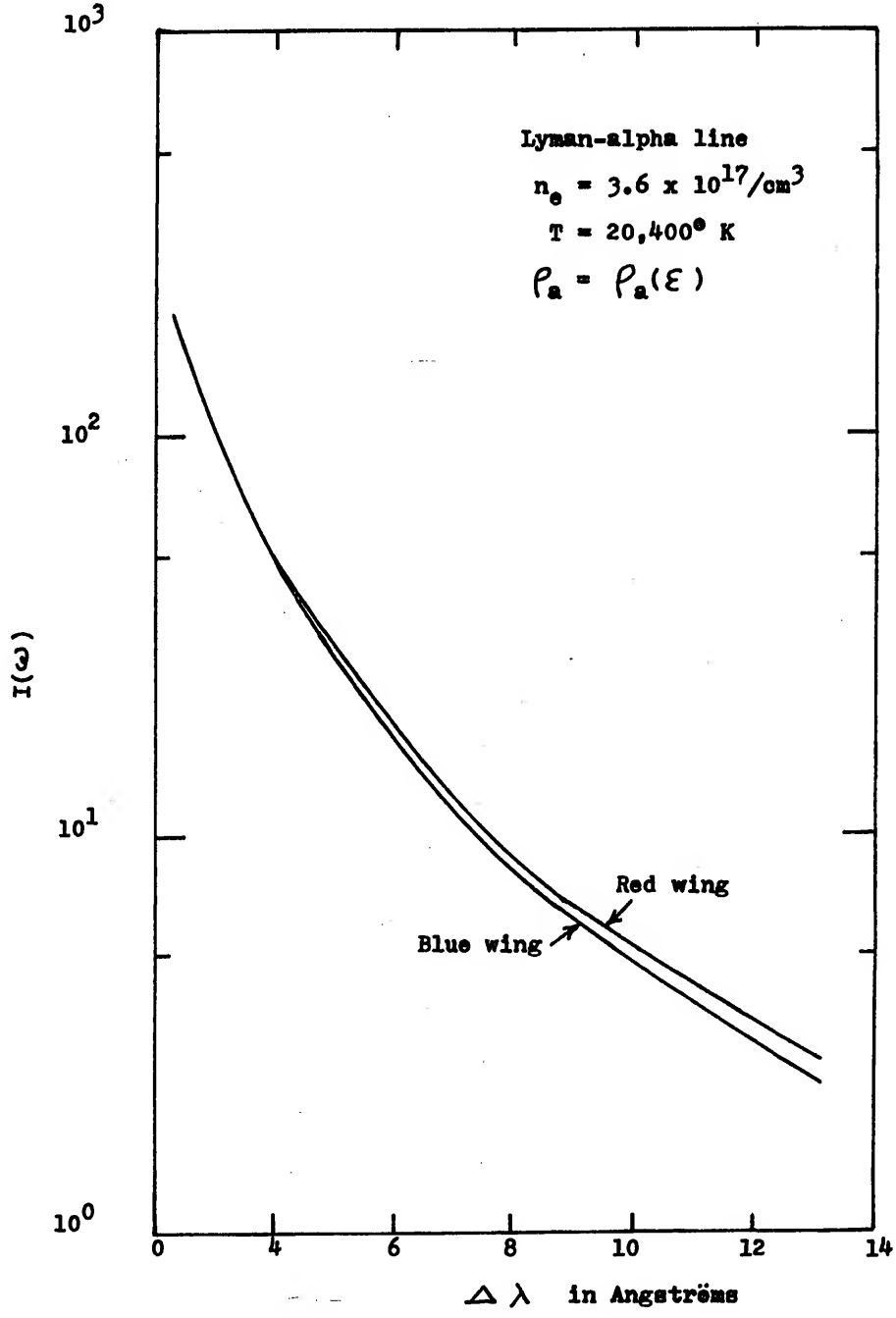
Lyman-alpha line
$n_e = 3.6 \times 10^{17}/cm^3$
T = 20,400° K
$\rho_a = \rho_a(\varepsilon)$
10^3
10^2
10^1
10^0
I(ω)
Red wing
Blue wing
0
4
6
8
10
12
14
Δ λ in Angströms

Figure 6. Lyman-alpha profile neglecting the field dependence in the atomic density matrix.

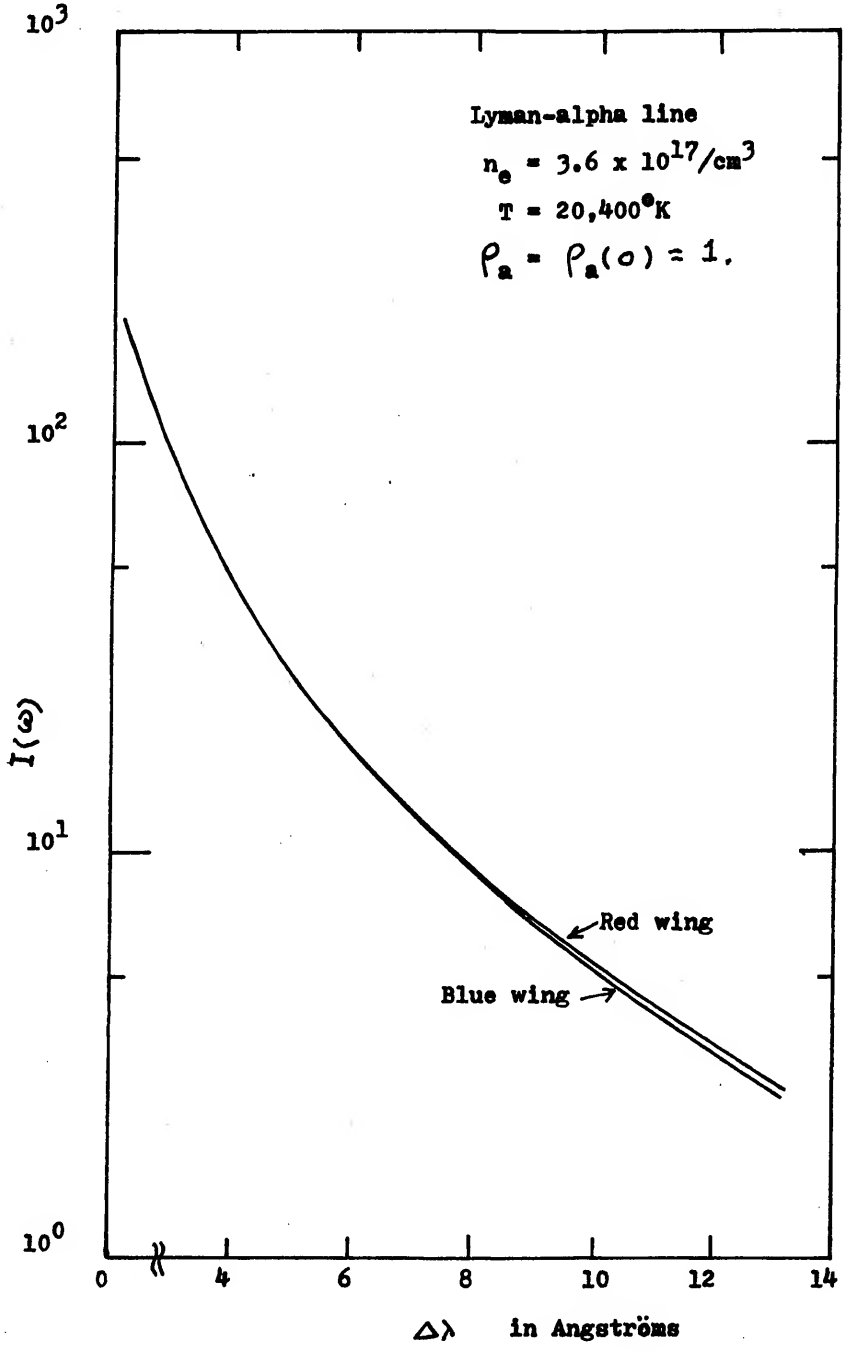
Lyman-alpha line
$n_e = 3.6 \times 10^{17}/cm^3$
$T = 20{,}400^{\circ}K$
$\rho_a = \rho_a(o) \simeq 1.$
10^3
10^2
10^1
10^0
$I(\omega)$
Red wing
Blue wing
0
4
6
8
10
12
14
$\Delta\lambda$ in Angströms

factor of two compared to the matrix elements in hydrogen. Also, the helium profiles presented in this dissertation correspond to temperatures that are about twice as large as those considered in the hydrogen line calculations. Thus, the exponent appearing in the atomic density matrix is decreased by a factor of approximately 4, and the effect of the ion-field in the density matrix can be neglected.

(V.4) THE FULL COULOMB INTERACTION

One of the approximations used in most treatments of the line broadening problem is the assumption that the interaction between the perturbing electrons and the radiating atoms is a dipole interaction. Such an approximation provides an accurate description of the interaction for large distances between the atom and perturbing electron. To achieve 10 percent agreement between the exact interaction and the dipole approximation for all orientations of an electron-proton dipole, the distance between the dipole and the point at which the potential is measured must be greater than 10 times the length of the dipole. For excited states resulting in Lyman-alpha radiation, the average distance between the nucleus and atomic electron is 4 Bohr radii. Hence, to achieve at least 10 percent agreement between the dipole approximation and exact interaction, the distance between the perturbing electron and radiating atom should be greater than 40 Bohr radii. The strong collision cut-offs used in various theories[1,2,9,16,21] for the Lyman-alpha transition are less than 15 Bohr radii which is in a region where the dipole approximation is not highly accurate. These conditions provided the motivation for developing a line broadening theory which uses the full Coulomb potential to describe the atom-perturbing electron interaction.

However, it should be emphasized that even in the full Coulomb treatment, a strong collision cut-off should be used to approximate symmetry effects usually neglected in the electron density matrix (see Section II.2).

One effect of including the full Coulomb interaction in this second order theory is to produce a shoulder at about 0.5 Å in the Lyman-alpha profile. A shoulder is also obtained in the dipole approximation. Although, it is not as pronounced as in the full Coulomb treatment. In the parabolic representation the dipole matrix elements for the initial states have non zero x and y components between states having different magnetic quantum numbers (see Appendix F). However, matrix elements of the full Coulomb interaction are diagonal with respect to magnetic quantum number (see Appendix D). Also, the magnitude of the matrix elements of W are different for the two approximations. The matrix elements which appear in the function $j(\omega)$ in the full Coulomb interaction treatment are smaller than the corresponding elements in the dipole approximation and are primarily responsible for the more pronounced shoulder. The numerical values for the W matrix for the two cases are compared in Figure 7 for various strong collision cut-offs. The computed line shape results for the full Coulomb treatment are presented in Figure 8.

With either the full Coulomb interaction or dipole approximation, the line profile can be written as

$$I(\omega) = j(\omega) + \int P(\varepsilon) \, \mathcal{J}(\omega, \varepsilon) \, d\varepsilon . \qquad (5.3)$$

Figure 7. A comparison of the matrix element W_{33} for various approximations. $T = 20{,}400^{\circ}K$, $n_e = 3.6 \times 10^{17}/cm^3$

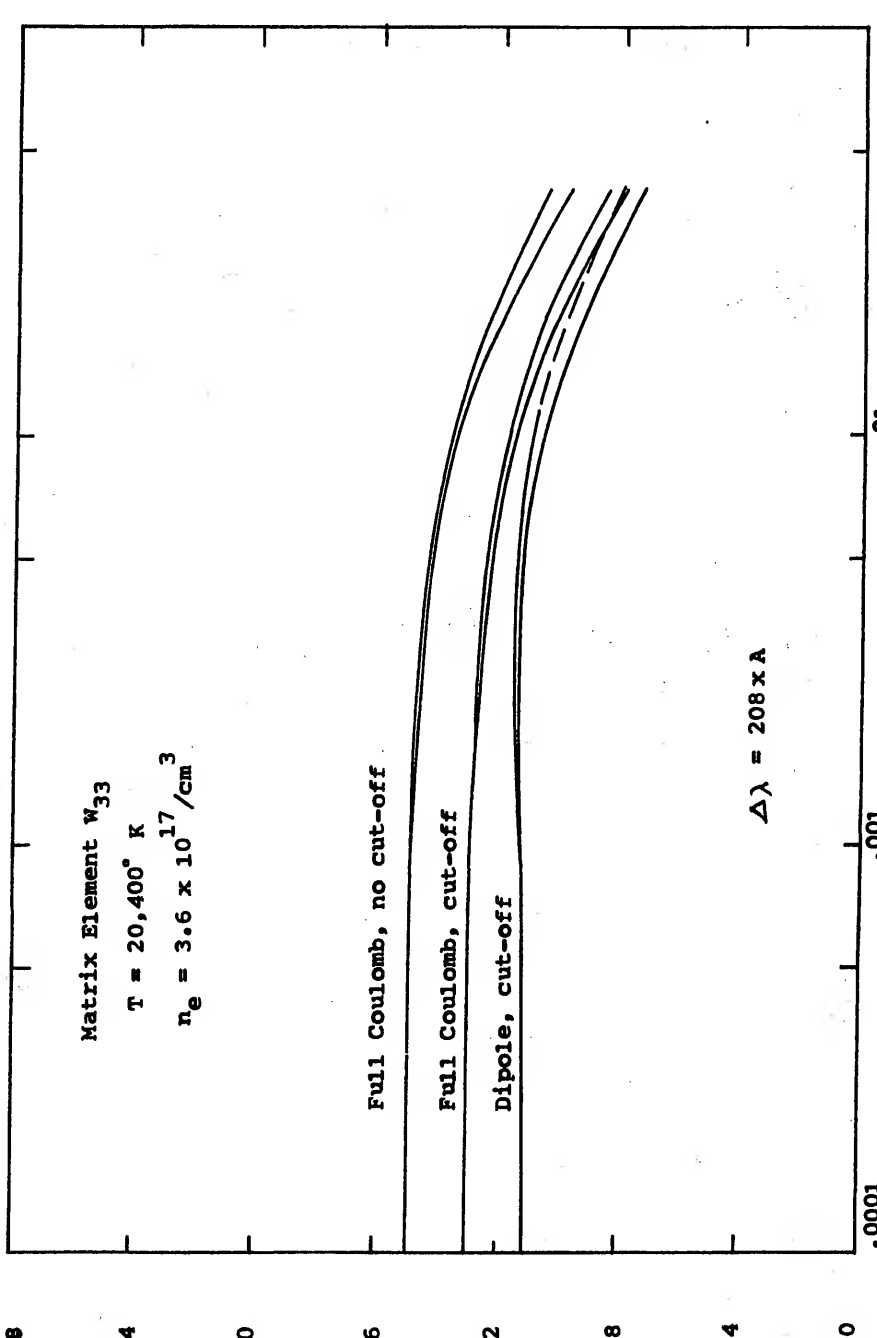
Matrix Element W_{33}
T = 20,400° K
n_e = 3.6 x 10^{17}/cm^3
Full Coulomb, no cut-off
Full Coulomb, cut-off
Dipole, cut-off
$\Delta\lambda$ = 208 x A
$A = \hbar\Delta\omega/k_B T$
W_{33}
2.8
2.4
2.0
1.6
1.2
.8
.4
0.0
.0001
.001
.01
.1

Figure 8. Lyman-alpha profile using the full Coulomb interaction. Solid line does not use a strong collision cut-off. Dashed line uses a strong collision cut-off.

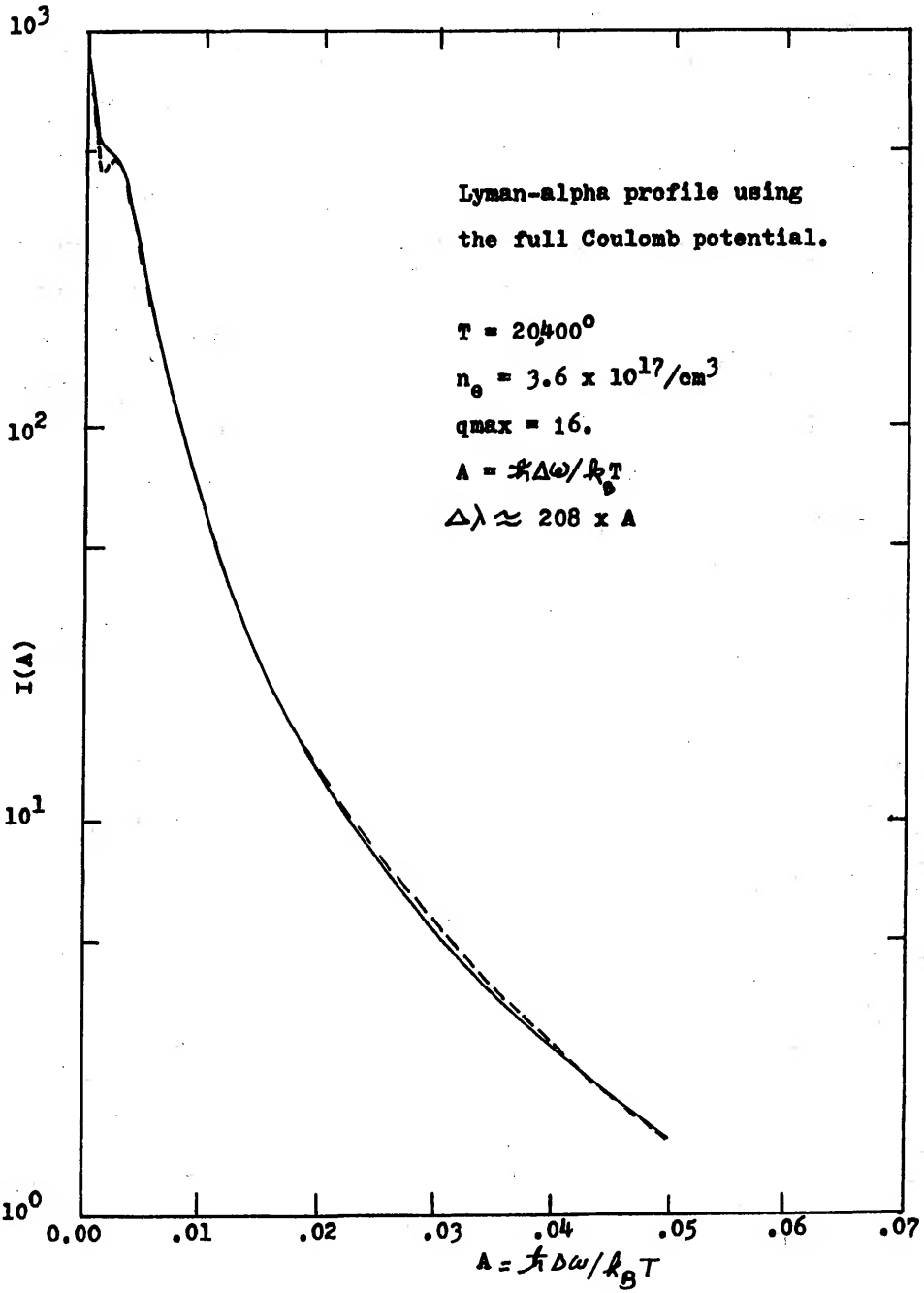
Lyman-alpha profile using
the full Coulomb potential.
T = 20400°
n_e = 3.6 x $10^{17}/cm^3$
qmax = 16.
A = $\hbar\Delta\omega/k_BT$
$\Delta\lambda \approx$ 208 x A
10^3
10^2
10^1
10^0
I(A)
0.00
.01
.02
.03
.04
.05
.06
.07
A = $\hbar\Delta\omega/k_BT$

It is of interest to analyze and compare the term containing the field integration and $j(\omega)$ separately. Curves for $I(\omega)$, $j(\omega)$, and $\int P(\mathcal{E}) \mathcal{J}(\omega,\mathcal{E}) d\mathcal{E}$ are given in Figure 9 for the full Coulomb interaction and in Figure 10 for the dipole approximation. As is demonstrated in these figures, the term $j(\omega)$, which is equal to four times the K_{22} matrix element, is important only in the line center. Its region of importance is slightly greater in the dipole approximation than in the full Coulomb interaction case. This difference is primarily responsible for the shoulder obtained from the full Coulomb computations and illustrated in Figure 8.

A treatment of the line shape problem that uses a full multi-pole expansion for the electron-atom interaction to all orders in the coupling constant has been carried out by M. E. Bacon, K. Y. Shen, and J. Cooper,[41,42] In the case of the Lyman-alpha transition, all multi-poles higher than quadrupolar terms vanish due to the orthonormality of the atomic states.

The major features of the calculation by Bacon et al. can be summarized as follows:

1. The S matrix is summed to all orders in the coupling constant.

2. Time ordering is included in the S matrix.

3. The perturbing electron trajectories are represented by classical paths.

4. Minimum and maximum impact parameter cut-offs are used to account for strong collisions and electron correlations

Figure 9. Functions $I(\omega)$, $j(\omega)$, $\mathcal{J}(\omega, \varepsilon)$ for the full Coulomb interaction case.

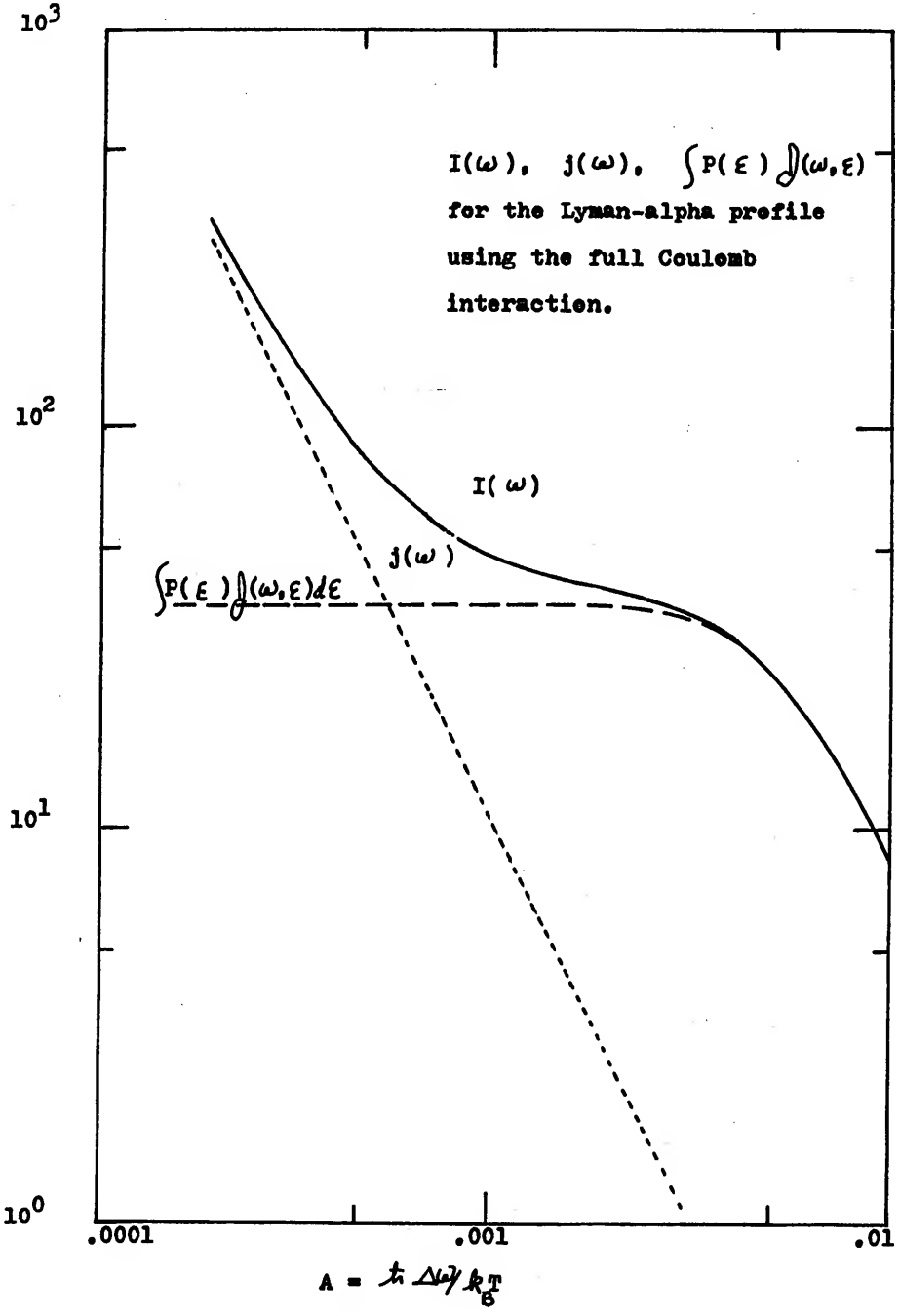
10^3
10^2
10^1
10^0
I(ω), j(ω), ∫P(ε) J(ω,ε)
for the Lyman-alpha profile
using the full Coulomb
interaction.
I(ω)
j(ω)
∫P(ε) J(ω,ε)dε
.0001
.001
.01
A = ħΔω/kT

Figure 10. Functions $I(\omega)$, $j(\omega)$, $\mathcal{J}(\omega, \epsilon)$ for the dipole approximation.

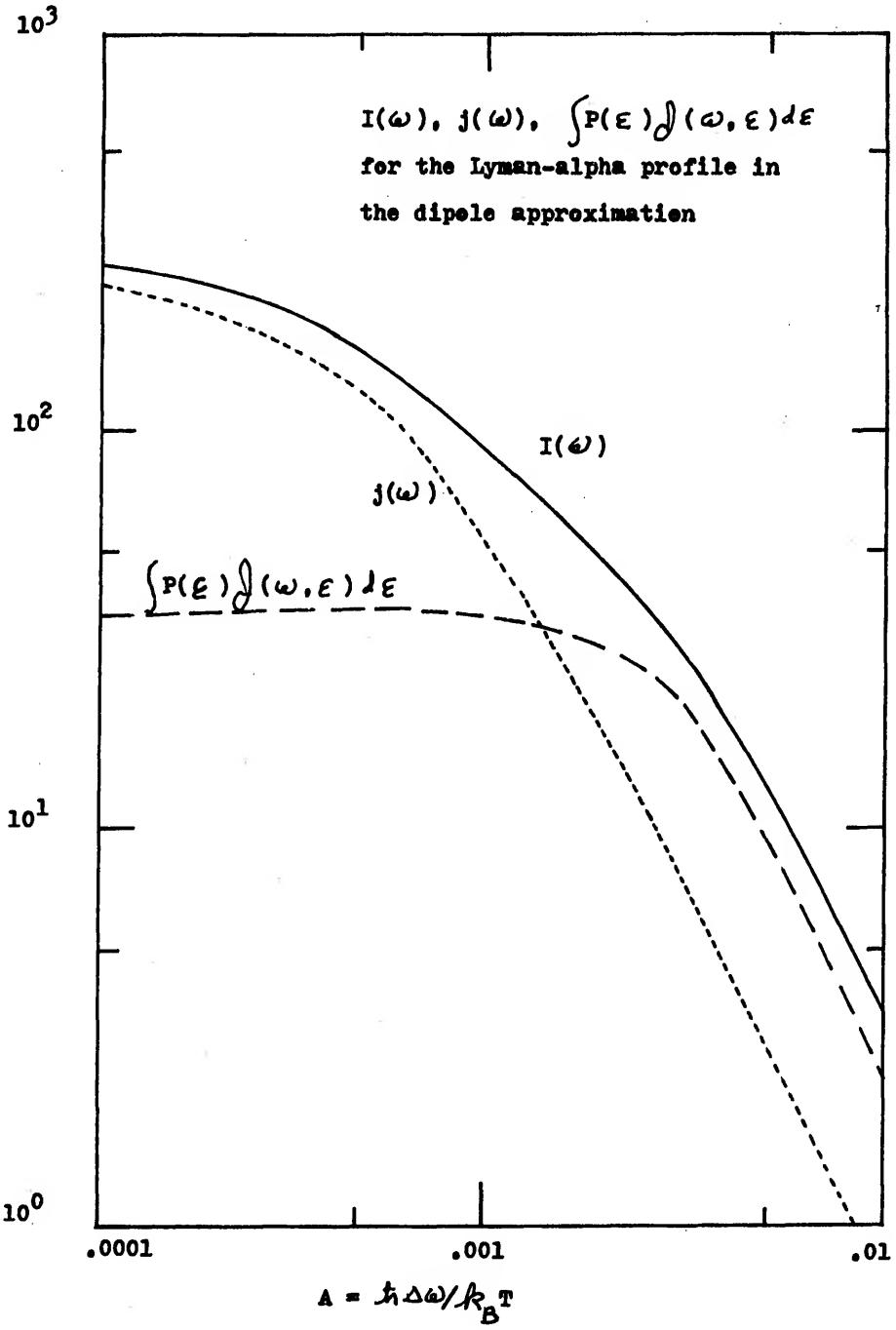
$I(\omega)$, $j(\omega)$, $\int P(\varepsilon)\mathcal{J}(\omega,\varepsilon)d\varepsilon$
for the Lyman-alpha profile in
the dipole approximation
10^3
10^2
10^1
10^0
$I(\omega)$
$j(\omega)$
$\int P(\varepsilon)\mathcal{J}(\omega,\varepsilon)d\varepsilon$
.0001
.001
.01
$A = \hbar\Delta\omega/k_BT$

respectively.

5. A minimum velocity cut-off is employed.

A comparison of the present theoretical results with those of Bacon et al. are presented in Figure 11 for a temperature of 20,000° K and an electron density of 1.0 x $10^{17}/cm^3$. Only the center and near wing of the profile are plotted. The agreement is fairly good for wavelengths greater than 0.4 Å. However, the profiles differ considerably for $\Delta\lambda < 0.4$ Å.

The full Coulomb treatment presented in this dissertation uses a strong collision cut-off. However, reasonable variations in the value of the strong collision cut-off does not improve the agreement between the two theories near the line center. Also, if electron correlations are accounted for by a cut-off rather than by the use of the electron pair distribution function, the agreement is not improved.

In the quantum mechanical treatment presented here, the atom-perturbing electron potential is transformed into a momentum representation in which convergence at zero momentum is assured by other momentum dependent factors in the integrand for $\Delta\omega$ not equal to zero. For zero frequency separation the manner in which electron correlations are treated assures convergence in the line center (see Sections II.6 and II.7 for further discussion). The major convergence factor, $\mathcal{J}(q)$, appears explicitly in the derivation after the time integration appearing in $\mathcal{H}(\omega)$ is performed. In second order theories of spectral line broadening in plasmas time

Figure 11. A comparison of the Lyman-alpha profile using the full Coulomb interaction to computations performed by Bacon et al.[41,42]

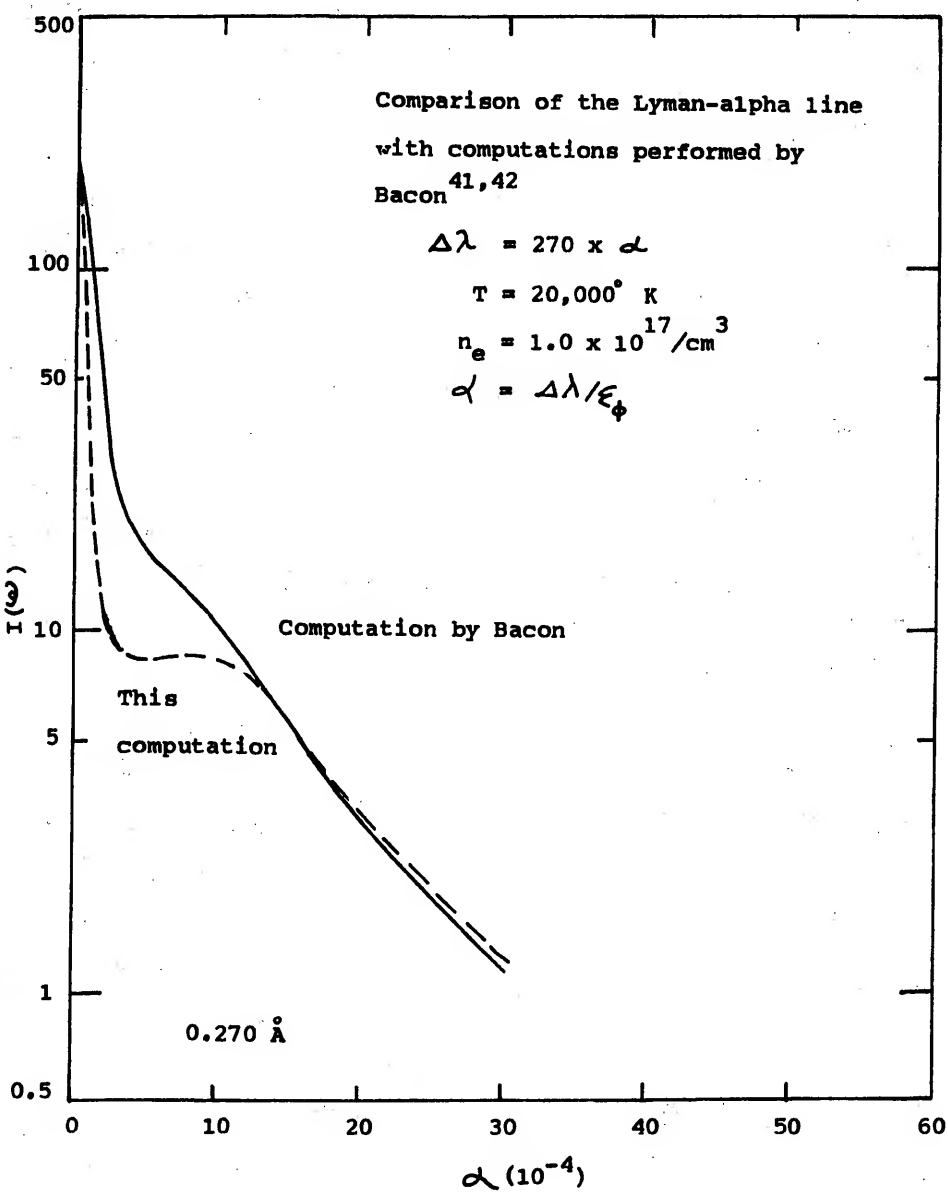
Comparison of the Lyman-alpha line with computations performed by Bacon[41,42]
Δλ = 270 x α
T = 20,000° K
n_e = 1.0 x 10^17/cm^3
α = Δλ/ε_φ
Computation by Bacon
This computation
0.270 Å
H(α)
α (10^-4)
500
100
50
10
5
1
0.5
0
10
20
30
40
50
60

ordering can be significant.[43] This may mean that the time ordered integrations in higher order terms do not provide convergence factors of the same form as $J(q)$. At the present time, the effects of time ordering in higher order terms are not fully understood.

One other point regarding higher order terms should be mentioned. In the present treatment the W_{22} matrix element appearing in $\mathcal{H}(\omega)$ is approximately 1 percent as large as the W_{33} term. In the full Coulomb treatment, the states $|2\rangle$ and $|3\rangle$, defined in Chapter III, are not mixed. However, they will be mixed if higher order terms in the perturbation expansion are retained. Thus, although a higher order term that would constitute a relatively small effect on the second order W_{33} term, may through mixing of states in higher orders, have a relatively large effect on the much smaller second order W_{22} term.

Another effect of using the full Coulomb interaction is to reduce the asymmetry in the line profile near the line center as is illustrated in Figure 12 (compare curves 1 and 3). This behavior is a consequence of the differences in magnitude of the unshifted components in the two treatments. The unshifted components in this second order theory are broadened only by the perturbing electrons. It can be shown that the electrons are mainly responsible for the asymmetry encountered in this version of the relaxation theory: a profile computation in which $\mathcal{H}(\omega)$ is symmetric results in a symmetric line shape. In the region of the profile

Figure 12. A comparison of red to blue ratios for various approximations.

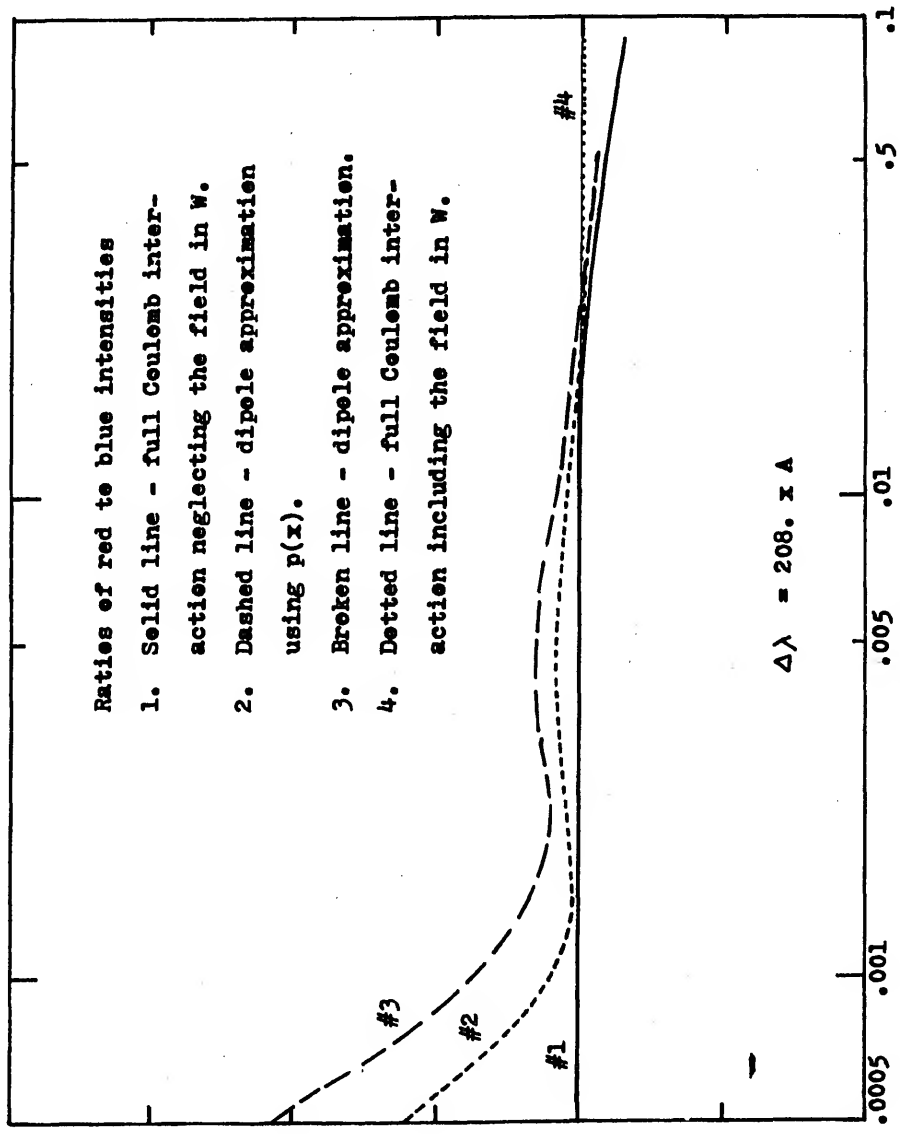
Ratios of red to blue intensities
1. Solid line - full Coulomb interaction neglecting the field in W.
2. Dashed line - dipole approximation using p(x).
3. Broken line - dipole approximation.
4. Dotted line - full Coulomb interaction including the field in W.
#1
#2
#3
#4
Ratio
2
1
0
.0005
.001
.005
.01
.5
.1
Δλ = 208. x A
A = λΔω/kT

where the asymmetry is large, $\hbar\Delta\omega/k_B T < .002$ or $\Delta\lambda < .4$ Å, the major contribution to the intensity in the dipole approximation arises from the function $j(\omega)$ given in equation (5.3). However, in the full Coulomb treatment the percent contribution from the function $j(\omega)$ to the intensity is not as large in this region. Hence, asymmetries in the function $J(\omega,\xi)$ tend to be amplified in the dipole approximation compared to the full Coulomb treatment, thus resulting in a larger asymmetry.

A comparison of a line profile calculated using the full Coulomb interaction with the experimental data and with other theories appears in Figures 13 and 14. The agreement between the profiles appears to be quite good over the region for which the experimental data is accurate: for a wavelength separation greater than approximately 0.8 Å. The accuracy of the experimental data is limited for wavelength separations less than 0.8 Å due to self absorption effects. In reference 6 it is estimated that in the experimental data presented here, the uncertainty resulting from self absorption corrections can be as large as 10-15 percent at 0.5 Å and even greater at smaller wavelengths. Hence, a more accurate procedure for performing self absorption corrections would be necessary in order to determine whether the shoulder encountered in the computations presented here is physically meaningful or whether it is a weakness in the theoretical treatment. If the latter proves to be the case, a more extensive analysis including higher order terms in the

Figure 13. A comparison of the present computation using the full Coulomb interaction with the complete multi-pole treatment by Bacon.[41]

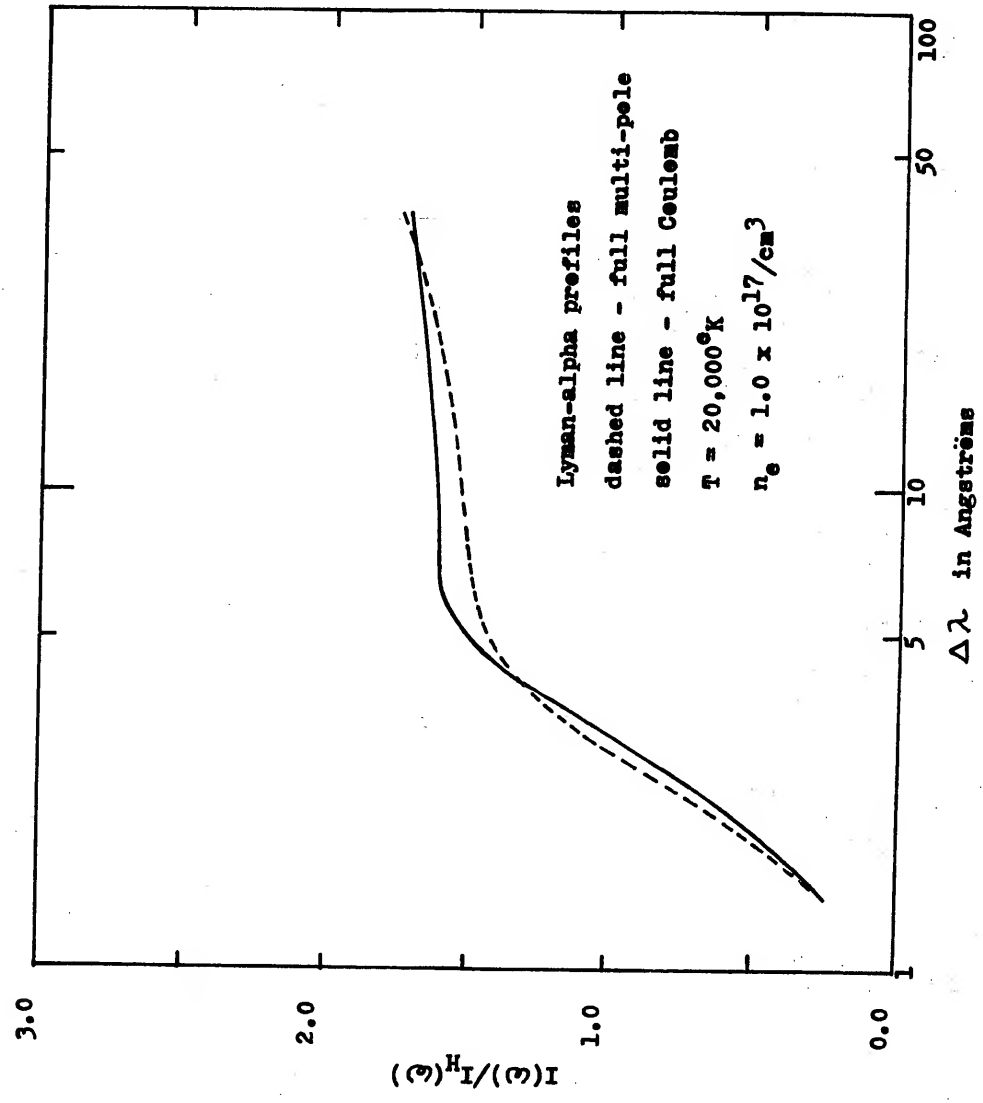
Lyman-alpha profiles
dashed line - full multi-pole
solid line - full Coulomb
T = 20,000°K
n_e = 1.0 x 10^{17}/cm^3
$I(\Delta\lambda)/I_H(\Delta\lambda)$
$\Delta\lambda$ in Angströms
0.0
1.0
2.0
3.0
1
5
10
50
100

Figure 14. A comparison of the present computation with the unified theory results and with the experimental data.

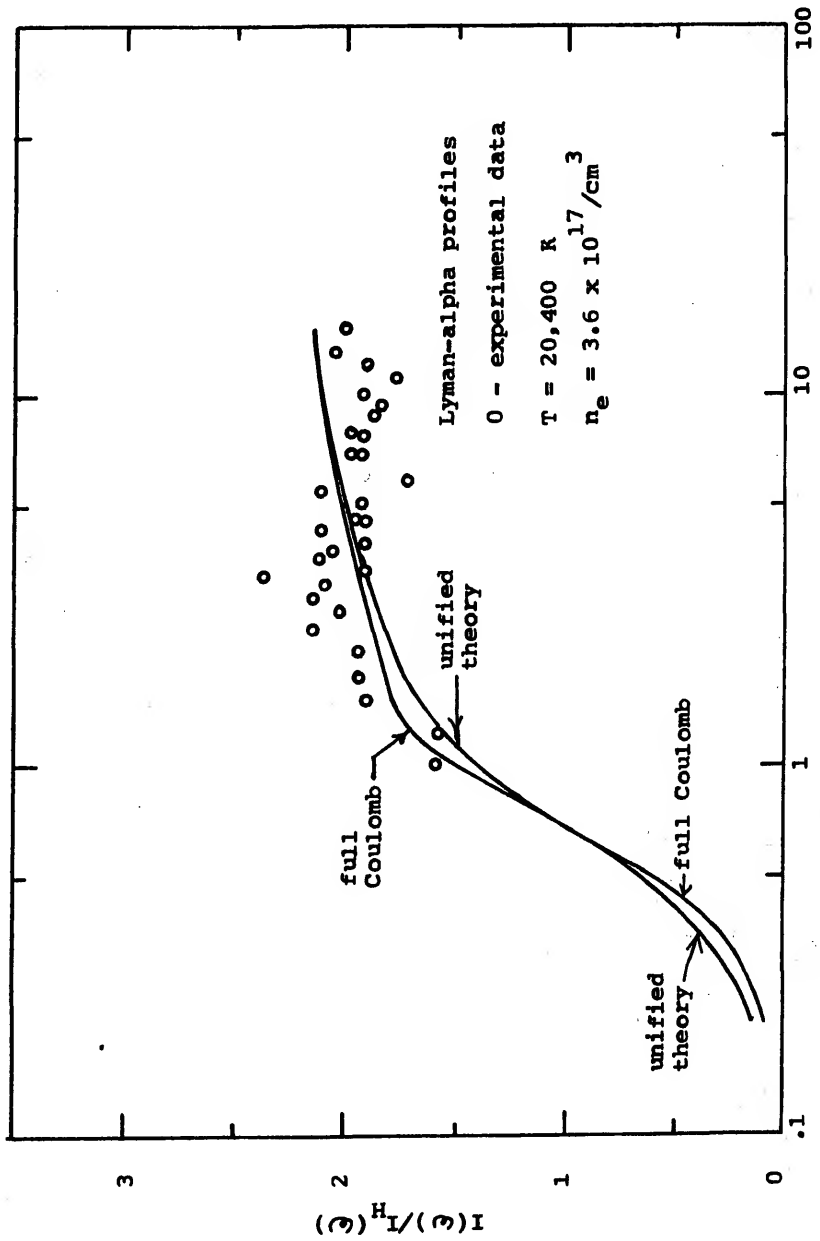
Lyman-alpha profiles
0 - experimental data
T = 20,400 K
$n_e = 3.6 \times 10^{17}/cm^3$
unified theory
full Coulomb
full Coulomb
unified theory
$I(\varepsilon)/I_H(\varepsilon)$
$\Delta\lambda$ in Angströms
0
1
2
3
.1
1
10
100

perturbation series in both the ion and electron interaction terms may be necessary.

(V.5) ION-FIELD EFFECTS IN THE ELECTRON COLLISION OPERATOR

The Stark splitting of the energy levels is directly proportional to the ion-field strength; hence, by the analysis presented in Section V.2, its effect should be most important in the line wings. This proves to be the case as can be seen in Figure 12, which contains plots of the red to blue intensity ratios. When the ion-field is included in the electron collision operator, $\mathcal{H}(\omega)$, the asymmetry is decreased (compare curves 1 and 4 in Figure 12). Analytically the asymmetry can be understood from an analysis of the operator, $\mathcal{H}(\omega)$. In the wings of the line the major cause of the asymmetry in the profile arises from the factor $\exp(\hbar\Delta\omega/k_B T - R^{\mathcal{E}}_{uu'}(\mu\xi_\phi \mathcal{E}/k_B T))$ appearing in Appendix C. For any given frequency, larger values of $\mathcal{E}$ will reduce the relative effects of asymmetry in this factor. Hence, the asymmetry in the line profile is also reduced.

Physically the asymmetry in $\mathcal{H}(\omega)$ can be related to the nature of the perturbing electron-atom interaction. The following heuristic explanation is proposed. The energy difference between a lower energy Stark shifted level of an excited state and the ground state energy is less than the energy difference between the unshifted Stark level and the ground state. Hence, mixing of the lower Stark state with the ground state is increased, thus increasing the probability

of a transition. On the other hand, the higher energy Stark level has a larger spatial extension than the unshifted level, thus increasing the strength of the perturbing electron-atom interaction and therefore also increasing the transition probability. These two effects tend to counterbalance one another, but are not expected to be of the same magnitude for all frequency separations.

(V.6) EFFECTS OF LOWER STATE INTERACTIONS

In the dipole approximation the effect of electron perturbationson the lower or final state is identically zero since the matrix element of the atomic dipole operator is zero for the final state. However, in the full Coulomb interaction treatment, the lower state matrix element of the perturbing electron-atom interaction is not zero. The effect of including lower state interactions is illustrated in Figure 15. In this particular curve no strong collision cut-off is employed. When a cut-off is employed the magnitude of this effect is only slightly reduced. Inclusion of the lower state interactions leads to a narrowing of the line profile. This indicates that perturbations that decrease (increase) the energy of the initial level also decrease (increase) the energy of the final level, thus narrowing the spread in energy differences between initial and final states resulting in a narrowing of the line profile.

Figure 15. A comparison of Lyman-alpha profiles with and without lower state interactions.

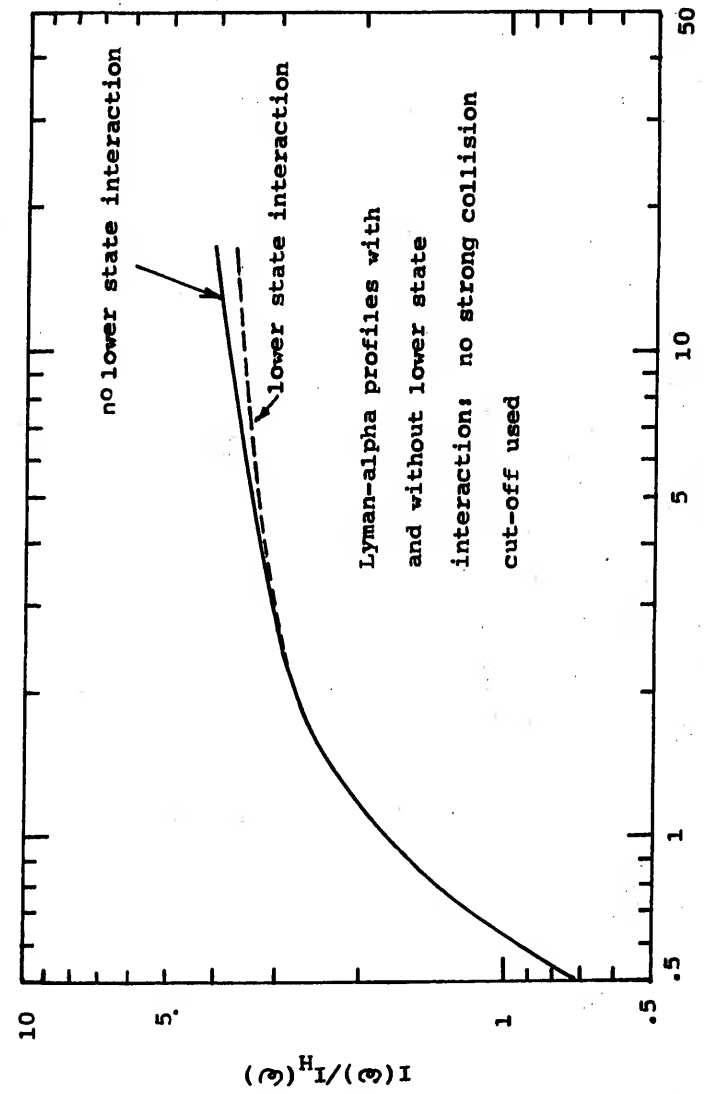
no lower state interaction
lower state interaction
Lyman-alpha profiles with
and without lower state
interaction: no strong collision
cut-off used
10
5
1
.5
.5
1
5
10
50
Δλ in Angströms
I(ε)/I_H(ε)

(V.7) THE EFFECTIVE DISTRIBUTION FUNCTION RESULTS

The effect of electron symmetry on the Lyman-alpha profile was included through the use of an effective distribution function, p(x), for the perturbing electrons (see Section II.2). The computations were restricted to the dipole approximation for computational convenience.

The contribution to the profile from matrix elements W_{33} and W_{44} appearing in $\mathcal{H}(\omega)$ is dominant for $\Delta\lambda > 1.0$ Å. Since these two elements are of the same form, we discuss the effects of electron symmetry only for the W_{33} matrix element. A comparison of this term, calculated using an effective distribution function, with the same term calculated using various strong collision cut-offs is given in Figure 7. By plotting W_{33}, at several frequencies, as a function of strong collision cut-off and comparing these results with those obtained using p(x), an effective strong collision cut-off was obtained. The resulting effective cut-off lies between 14 and 20 Bohr radii, which is larger than cut-offs currently being used.[1,2,22] Computations using this effective cut-off agree with those using p(x).

The present calculations using p(x) increase the intensity in the line center and decrease the intensity in the line wings. The amount of change is approximately a 9 percent decrease at 0.6 Å and an 8 percent increase at 3 Å.

A comparison with other treatments is best accomplished by plotting the ratio, R:

$$R = I(\omega)/I_H(\omega)$$

where $I_H(\omega)$ is the Holtsmark profile. Such comparisons appear in Figure 16. For wavelengths greater than 1.5 Å, the ratio obtained using p(x) does not increase as rapidly as in other treatments, thus resulting in better qualitative agreement with the experimental data for 1.5 Å than achieved by other treatments. It is expected that the agreement may improve if higher order terms in the perturbation expansion for $\mathcal{F}(\omega)$ are retained.

The red to blue wing ratio exhibits a small decrease in magnitude as is illustrated in Figure 18. A decrease in the ratio is expected since the asymmetric electron collision term is smaller in magnitude when the effective distribution function is used; hence, the relative effects of asymmetries in this term are correspondingly reduced.

Figure 16. A comparison of a Lyman-alpha profile computed using the effective distribution function to the unified theory and the experimental data.

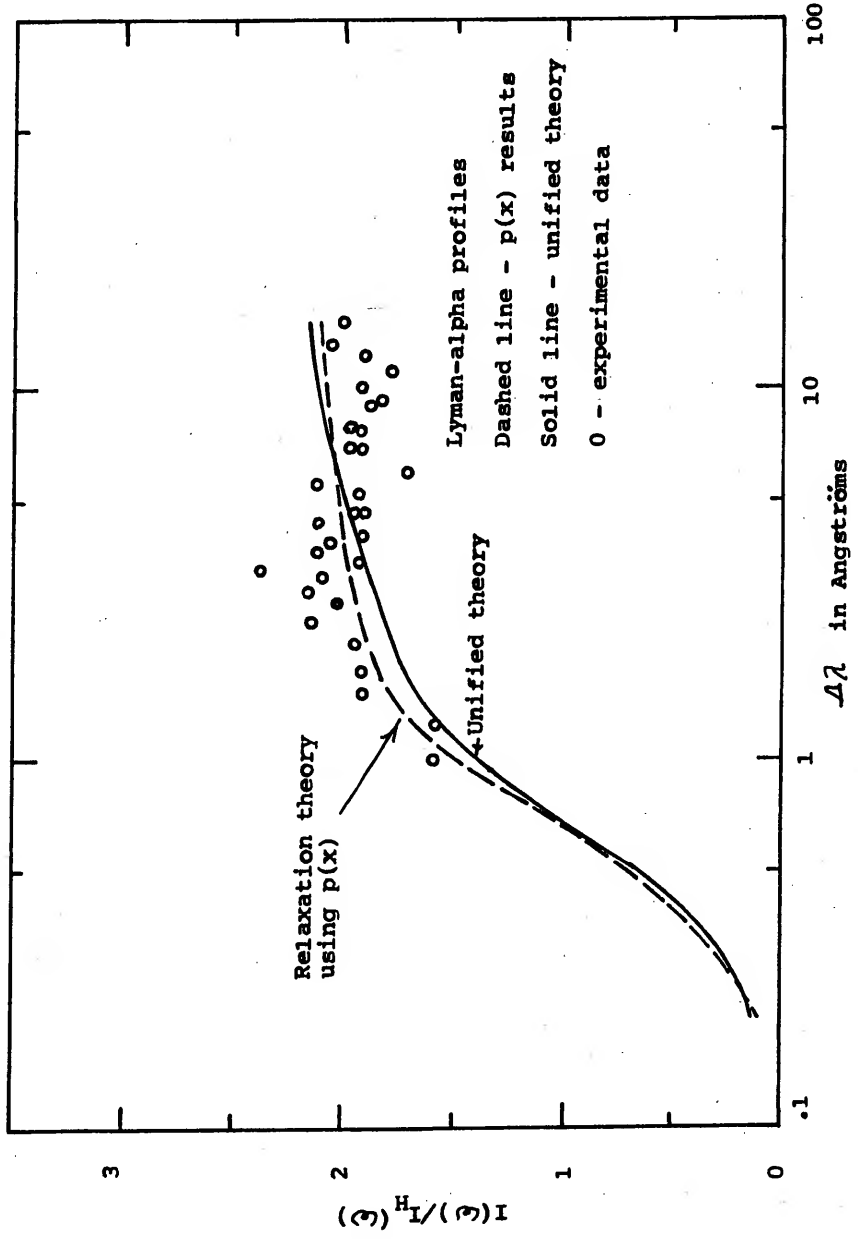
Lyman-alpha profiles
Dashed line - p(x) results
Solid line - unified theory
0 - experimental data
Relaxation theory
using p(x)
Unified theory
$I(\Delta\lambda)/I_H(\Delta\lambda)$
$\Delta\lambda$ in Angströms
0
1
2
3
.1
1
10
100

(V.8) STATIC WING RESULTS

In the derivation of the Holtsmark microfield, $P_h(\beta)$, ion-ion interactions and the effects of electron screening are neglected. For large values of the microfield, which are important in the line wings, $P_h(\beta)$ provides an adequate description of the microfield function. To support this claim, reference is made to more exact treatments of the microfield by Baranger and Mozer,[44] and Hooper.[14,15] For large values of the field, their results reduce to the Holtsmark distribution. Thus, one would expect the ratio of the more exact theoretical profiles to the profile computed in the static limit using the Holtsmark distribution should approach a constant for large frequency separations. For the static wing formula developed in Chapter IV the asymptotic value of the ratio, R defined in Section (V.7), is chosen to be two. If the dynamic electron terms do not have the proper static limit, the asymptotic limit of R for large frequency will not in general approach this value. Such behavior is encountered in relaxation theory computations.

The theoretical results for the static wings are compared in Figure 17. If one assumes that the experimental data is valid, the full unified theory and the relaxation theory in the dipole approximation appear to underestimate

Figure 17. Static wing results for the Lyman-alpha profile compared with the experimental data.

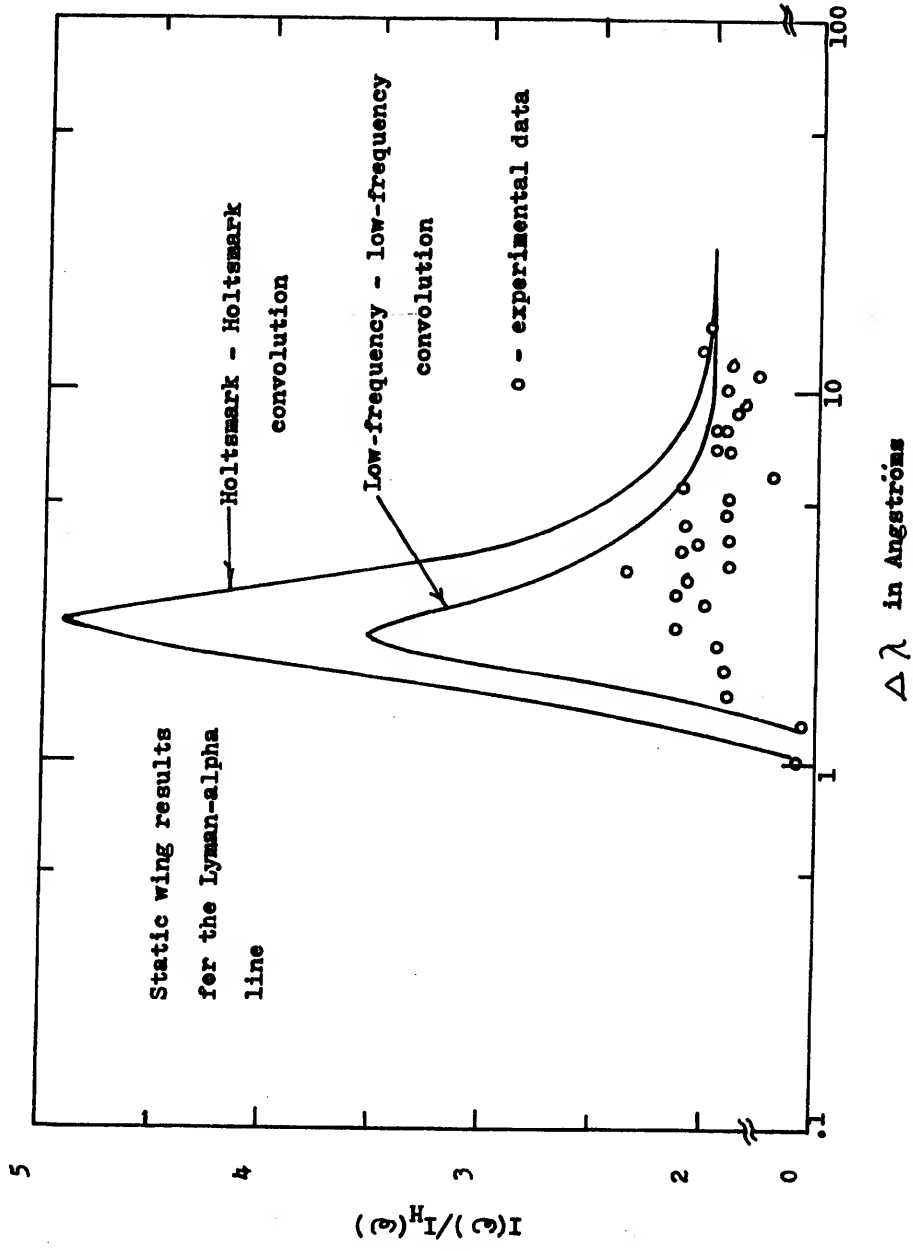
Static wing results
for the Lyman-alpha
line
Holtsmark - Holtsmark
convolution
Low-frequency - low-frequency
convolution
o - experimental data
$I(\Delta\lambda)/I_H(\Delta\lambda)$
$\Delta\lambda$ in Angströms
0
2
3
4
5
.1
1
10
100

Figure 18. The Lyman-alpha profile in ionized helium. The full Coulomb results are compared with the dipole treatment.

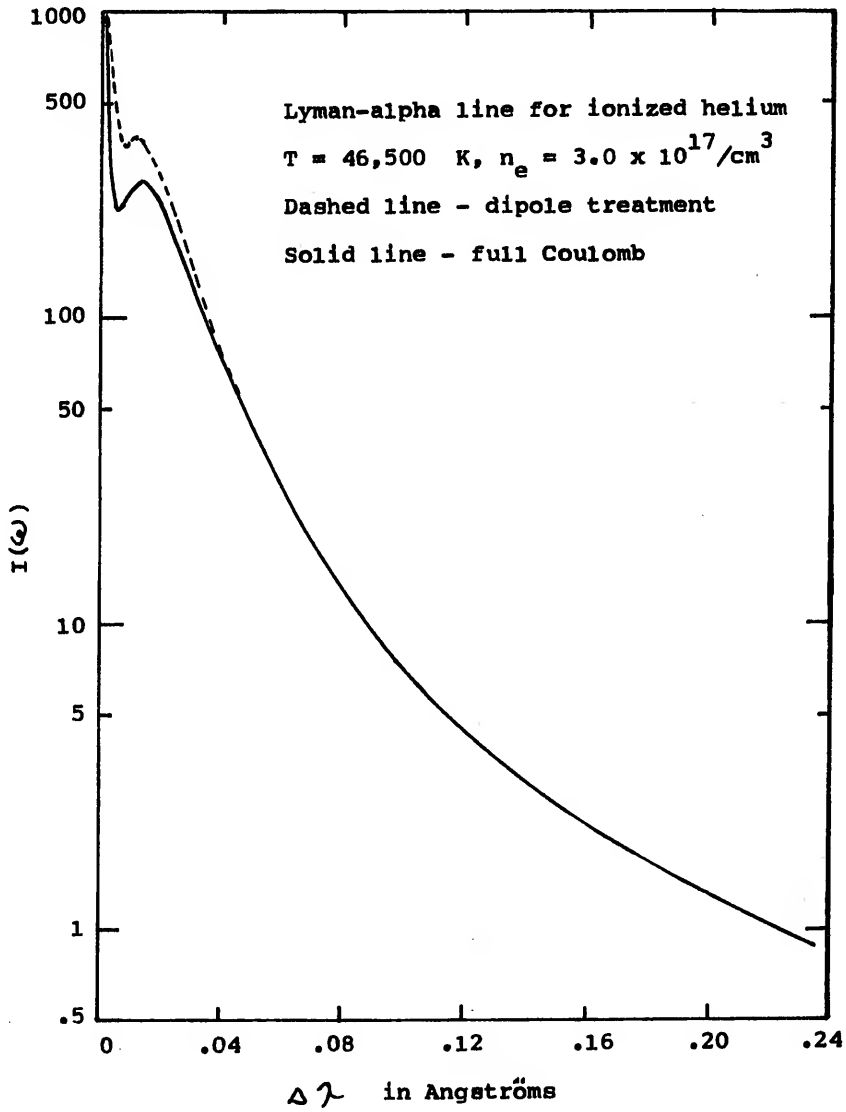
Lyman-alpha line for ionized helium
T = 46,500 K, n_e = 3.0 x $10^{17}/cm^3$
Dashed line - dipole treatment
Solid line - full Coulomb
1000
500
100
50
10
5
1
.5
I(ω)
0
.04
.08
.12
.16
.20
.24
Δλ in Angströms

the value of R for small wavelengths, $\Delta\lambda < 3$ Å. This result may indicate that the broadening due to static electron fields is underestimated in these formulations.

In performing the microfield convolutions, better agreement with experimental data is obtained when low-frequency microfields are used for both the electron and ion microfields than when either high-frequency or Holtsmark microfields are employed. The low-frequency microfields account for electron and ion correlations. It is expected that the ion-ion interactions are fully shielded (in the Debye sense) by the electrons in the plasma whereas the electron-electron interaction will not be shielded to the same degree. Hence, the low-frequency convolution should form a lower bound and the Holtsmark convolution an upper bound for the value of R in the static wing limit.

In the vicinity of the electron plasma frequency, $\Delta\lambda < 2$ Å, inclusion of higher order terms in the time dependent perturbation expansion given in equation (4.12) is expected to improve the agreement between the static wing theory and the experimental data. These time dependent terms introduce electron dynamics into the wing formula.

As an alternative to using the time expansion, one could develop a theory that employs time dependent microfields[45] to take into account electron dynamics. However, such a procedure has been shown to be computationally difficult[45] since it is necessary to evaluate multidimensional integrals numerically. Hence, using the

perturbation in time developed in Chapter IV may result in a more tractable form for computing line profiles.

The asymptotic static wing formula obtained in the unified theory contains a Holtsmark microfield distribution function that attempts to include electron correlations through a spatial cut-off. To explore the validity of such a treatment, a convolution of Holtsmark microfields computed using a spatial cut-off similar to that used in the unified theory was performed. The results are almost identical to the convolution of two Holtsmark microfields without a cut-off. Hence, it is concluded that the convolution of a Holtsmark distribution with a cut-off Holtsmark distribution will be insensitive to the value of the cut-off.

(V.9) THE LYMAN-ALPHA PROFILE FOR IONIZED HELIUM

In order to illustrate the application of the present theory to another hydrogenic system, computations were performed for the Lyman-alpha transition in ionized helium at a temperature of 46,500° K and an electron density of $3.6 \times 10^{17}/cm^3$. The full Coulomb and dipole treatment results are compared in Figure 18. The qualitative features for the full Coulomb treatment are very similar to the Lyman-alpha profiles in hydrogen, that is, the shoulder is fairly pronounced and the agreement between the two theories good in the line wings. However, it is of interest to note that for this particular case, the shoulder is fairly pronounced in the dipole treatment also.

At the present time, highly accurate experimental data is not available for the Lyman-alpha transition in ionized helium.[46] The primary problem in obtaining accurate experimental data is the difficulty encountered in measuring ultraviolet radiation. In the case of the above transition, the wavelengths involved are less than 350 Å.

(V.10) COMMENTS

At the present time there are several treatments of the line broadening problem in plasmas. The differences in these treatments arise mainly from the different methods used in evaluating the electron collision term. Some of the methods used in describing the electron-atom interaction in the electron collision term are:

a) The interaction between the perturbing electron and radiating atom is treated as a dipole interaction and a quantum mechanical perturbation expansion is developed to second order in the coupling constant.[9,12,23]

b) The interaction is described by a dipole potential and the perturbation expansion is carried out to all orders in the coupling constant. Classical paths are used to describe the trajectories of the perturbing electrons.[2,43]

c) A complete multi-pole expansion is used for the interaction and a perturbation expansion is carried out to all orders in the coupling constant using classical paths to describe the electron trajectories.[41,42]

The work presented in this dissertation has introduced the following new features:

1) The interaction is treated by an exact Coulomb potential and a quantum mechanical second order perturbation expansion employed.

2) A quasi-static wing formula is developed that is based on a convolution of static electron and ion microfields.

3) The approach listed in (a) above is extended to include the effects of electron symmetry in an approximate manner.

The differences between the full Coulomb interaction treatment and the other treatments listed in items (a) through (c) above, indicate that in the line center higher order terms in the coupling constant perturbation expansion can become significant. Hence, it would be interesting to develop a theoretical treatment that uses a full Coulomb interaction and includes all orders in the coupling constant perturbation expansion.

Since electron symmetry effects are shown to have some effect on the profile, a more exact treatment of the effective distribution function for the electrons may be warranted. Such a treatment should take into account the fact that the radiating atom is initially in an excited state. It is expected that the probability of finding an electron a distance x from the atom will depend on the particular excited state of the atom. It may still be possible to take into account the effects of electron symmetry in an average way through an effective cut-off.

Another problem that should be considered in developing a static wing formula is the computation of a microfield for a two-component system in which the two species have charges of different sign. It is expected that the convolution used

in this presentation is adequate in the wings of the profile, $\Delta\lambda > 5.0$ Å. However, for smaller wavelength separations, a microfield distribution calculated with a more exact treatment of the electron-ion interaction may be required.

Yet another extension of the present work would be to reduce the higher order terms in the time dependent perturbation expansion, presented in Chapter IV, into a tractable form and to compute line profiles including these higher order terms. It is hoped that carrying out this procedure will lead to a wing profile that will overlap treatments of the line center.

In conclusion, there are still many unresolved questions regarding the line broadening problem. I hope that this work will add to the understanding of the line broadening phenomenon in plasmas.

APPENDICES

APPENDIX A

THE EFFECTIVE POTENTIAL V_s

In this appendix an effective potential including exchange is developed for a perturbing electron-atom system. The electron-proton potential is obtained from the radial distribution function $g_{ep}(\beta, r)$, defined by,

$$g_{ep}(\beta, r) = \exp(-\beta \bar{V}_{ep}) = \lambda^3 \sum_m \psi_m(r) \exp(-\beta E_m) \psi_m(r), \tag{A.1}$$

where $\beta = 1/k_B T$, $\bar{V}_{ep}$ is the effective potential or potential of mean force, $\lambda^2 = (2\pi\beta/\hbar^2\mu)$, where μ is the reduced mass. The effective interaction operator $\mathcal{H}(\omega)$ introduced in Chapter II represents a free electron scattering term. Hence, the summation in equation (A.1) will be restricted to the scattered states only. These states are described by Coulomb wave functions.[47,48] Thus, equation (A.1) becomes

$$g_{ep}(\beta, r) = \lambda^3 \frac{4\pi}{(2\pi)^3} \int_0^\infty \exp\left(-\frac{\beta \hbar^2 k^2}{2\mu}\right) \sum_{l=0}^\infty (2l+1) \left(F_l(\alpha, kr)\right)^2 k^2 \, dk$$

where $\alpha = \dfrac{\mu e^2}{\hbar^2 k a_0}$

$a_0 \equiv$ Bohr radius (A.2)

F_l is the Coulomb wave function.

The above expression has been computed by Barker.[24] The integration over k is truncated at a sufficiently high value to assure four place accuracy in determining $\overline{V}_{ep}$. The summation over ℓ is truncated when F_ℓ becomes less than 1.0×10^{-34}. For $\ell = 0$ the Coulomb functions are generated using methods derived by Frobert.[49] The higher order Coulomb wave functions are generated by formulae given in reference 47. As seen from equation A.1, the potential $\overline{V}_{ep}$ is the logarithm of the radial distribution function.

The effective interaction between electrons is obtained in a similar manner. However, for the spin = 1 case, the sum over ℓ is restricted to odd values of ℓ. All values of ℓ are allowed for the spin = 0 case. The effective electron-electron potential is obtained by

$$\overline{V}_{ee} = \ln\left((1/4)g_{\text{up-down}} + (3/4)g_{\text{up-up}}\right) \qquad \text{(A.3)}$$

where the subscripts indicate the spin orientation. The potential V_s defined in Chapter II is the sum of $\overline{V}_{ee}$ plus the electron-proton potential obtained from equation (A.2).

$$V_s = \overline{V}_{ee} + \ln(g_{ep}). \qquad \text{(A.4)}$$

Thus, ρ_e becomes

$$\begin{aligned} \rho_e &= \exp(-\overline{V}_{ae}) \\ &\simeq \exp(-\beta A_e)\exp(-V_s). \end{aligned} \qquad \text{(A.5)}$$

The effective density matrix given in equation (A.5) is used in evaluating $\mathcal{H}(\omega)$. For large values of x

(x greater than 50 Bohr radii), $\exp(-V_s)$ reduces to one as expected. A non linear least squares fit is performed on the function $\exp(-V_s)$ using exponential functions allowing one to perform the spatial integration occurring in $\mathcal{H}(\omega)$ analytically. Since the integration range is small, the numerical error introduced by using this procedure should be negligibly small. It is estimated that the error due to the numerical procedures used in evaluating $\mathcal{H}(\omega)$ is less than 1 percent.

APPENDIX B

PROPERTIES OF THE OPERATORS L_0 AND P

Five equations involving the operators L_0, P and L_1 are derived in this appendix. These relations are required in reducing the perturbation expansion for $\mathcal{P}(\omega)$ to a useful form.

1. Let A represent a general operator; then,

$$\langle PA \rangle = \langle A \rangle . \tag{B.1}$$

Proof of (B.1):

$$\langle PA \rangle = Tr_e \langle PA \rho_e \rangle$$

$$= Tr_e (\rho_e Tr_e A \rho_e) .$$

Since the term $Tr_e(A \rho_e)$ does not depend on the electron coordinates one has

$$\langle PA \rangle = Tr_e(A \rho_e) = 0 \qquad \text{Q.E.D.}$$

where the normalization condition $Tr_e \rho_e = 1$ has been explicitly used.

2. The commutator relationship, $[L_0, P]$, is examined next. In order to evaluate this commutator the matrix elements of L_0 and P are required. The system under consideration is a composite system consisting of electrons

and atoms. Let μ,ν represent atomic states and α,β represent electron states. The matrix elements of ρ_e are

$$\langle \mu\alpha | \rho_e | \nu\beta \rangle = \left(f_{\alpha\beta}\delta_{\alpha\beta} + (1-\delta_{\alpha\beta}) f_{\alpha\beta} \right) \delta_{\mu\nu} \qquad \text{(B.2)}$$

where $\delta_{\mu\nu}$ is the Kronecker delta and

$$f_{\alpha\beta} = \langle \alpha | \exp(-K_e/k_B T) \exp(-V_s/k_B T) | \beta \rangle. \qquad \text{(B.3)}$$

Note that the matrix elements of ρ_e are written in terms of a diagonal and non diagonal part.

Next consider the matrix elements of PA between composite states. One has

$$(PA)_{\mu\alpha\nu\beta} = \langle \mu\alpha | \rho_e T_{n_e}(A) | \nu\beta \rangle = \langle \mu\alpha | \rho_e \sum_{\alpha'} \langle \alpha' | A | \alpha' \rangle | \nu\beta \rangle. \qquad \text{(B.4)}$$

Using (B.3) one can show that

$$(PA)_{\mu\alpha\nu\beta} = \left(f_{\alpha\beta}\delta_{\alpha\beta} + (1-\delta_{\alpha\beta}) f_{\alpha\beta} \right) \sum_{\alpha'} A_{\mu\alpha',\nu\alpha'}. \qquad \text{(B.5)}$$

Consider next the matrix elements of L where L is the Liouville operator. The matrix elements of L are given by

$$L_{mm',m'n'} = H_{mm'}\delta_{mn'} - H^*_{nn'}\delta_{mn'}. \qquad \text{(B.6)}$$

Hence, for a composite atom-electron system

$$(L_0 A)_{\mu\alpha\nu\beta} = \sum_{\mu'\alpha'\nu'\beta'} L_{0\,\mu\alpha\nu\beta,\mu'\alpha'\nu'\beta'} A_{\mu'\alpha'\nu'\beta'}. \qquad \text{(B.7)}$$

Using equations (B.6) and (B.7) the matrix elements of the compound operator, (PL_0) can be determined. These are

$$(PL_0A)_{\mu\alpha\nu\beta} = \left(F_{\alpha\beta}\delta_{\alpha\beta} + (1-\delta_{\alpha\beta})F_{\alpha\beta}\right) \sum_{\substack{\alpha'' \\ \mu'\alpha'\nu'\beta'}} L_{0\,\mu\alpha''\nu\alpha'',\,\mu'\alpha'\nu'\beta'} A_{\mu'\alpha'\nu'\beta'}. \tag{B.8}$$

L_0 is defined by equation (2.30) to be

$$L_0 = (H_0 + H_2) \otimes I - I \otimes (H_0 + H_2)^*$$

where $H_0 = H_a + V_{ai}$.

Using equations (2.33), (2.34), (2.35) and (B.6), one has

$$\begin{aligned} L^a_{0\,\mu\alpha\nu\beta,\,\mu'\alpha'\nu'\beta'} &= \langle \mu\alpha | H_0 | \mu'\alpha' \rangle \delta_{\nu\nu'}\delta_{\beta\beta'} - \langle \nu\beta | H_0^* | \nu'\beta' \rangle \delta_{\mu\mu'}\delta_{\alpha\alpha'} \\ &= \left(\hbar\omega_{\mu\nu}\delta_{\mu\mu'}\delta_{\nu\nu'} + e\vec{E}_i \cdot \left(\vec{R}_{\mu\mu'}\delta_{\nu\nu'} - \vec{R}^*_{\nu\nu'}\delta_{\mu\mu'}\right)\right)\delta_{\alpha\alpha'}\delta_{\beta\beta'} \\ &\equiv \hbar\bar{\omega}_{\mu\nu} \end{aligned} \tag{B.9}$$

$$L^e_{0\,\mu\alpha\nu\beta,\,\mu'\alpha'\nu'\beta'} = \hbar\omega_{\alpha\beta}\,\delta_{\mu'\mu}\delta_{\nu\nu'}\delta_{\alpha\alpha'}\delta_{\beta\beta'} \tag{B.10}$$

where $\hbar\omega_{\mu\nu} = E_\mu - E_\nu$.

The results of equations (B.9) and (B.10) are substituted into equation (B.8). The sums over $\mu'\alpha'\nu'\beta'$ can be easily performed using properties of the delta functions. The results are

$$(PL_0A)_{\mu\alpha\nu\beta} = \left(F_{\alpha\beta}\delta_{\alpha\beta} + (1-\delta_{\alpha\beta})F_{\alpha\beta}\right)\hbar\bar{\omega}_{\mu\nu} \sum_{\alpha''} A_{\mu\alpha''\nu\alpha''}. \tag{B.11}$$

A similar procedure is followed to determine the matrix elements of (L_0PA).

$$(L_0PA)_{\mu\alpha\nu\beta} = \left(\hbar\bar{\omega}_{\mu\nu} F_{\alpha\beta}\delta_{\alpha\beta} + \hbar(\bar{\omega}_{\mu\nu} + \omega_{\alpha\beta})(1-\delta_{\alpha\beta})F_{\alpha\beta}\right)$$

$$\times \sum_{\alpha''} A_{\mu\alpha''\nu\alpha''}. \qquad \text{(B.12)}$$

Equations (B.11) and (B.12) are used to obtain the matrix elements for the commutator $[L_0,P]$:

$$(L_0PA)_{\mu\alpha\nu\beta} - (PL_0A)_{\mu\alpha\nu\beta} = \hbar\omega_{\alpha\beta}(1-\delta_{\alpha\beta})F_{\alpha\beta}\sum_{\alpha''} A_{\mu\alpha''\nu\alpha''}$$

$$= \hbar\omega_{\alpha\beta} F_{\alpha\beta_{\text{mom-DIAG.}}} \sum_{\alpha''} A_{\mu\alpha''\nu\alpha''}. \qquad \text{(B.13)}$$

If one assumes $F_{\alpha\beta}$ is diagonal, e.g., if one neglects the back reaction in the electron density matrix, then

$$[L_0,P] = 0. \qquad \text{(B.14)}$$

This is not a good approximation for strong collisions. Hence, care must be taken whenever (B.14) is used.

3. Using the commutivity of P and L_0 one can verify equations (2.39) and (2.40). One has

$$(1-P)\,L\,\rho_e = L_0(1-P)\,\rho_e + (1-P)\,L_1\,\rho_e$$

$$= (1-P)\,L_1\,\rho_e. \qquad \text{(B.15)}$$

Hence,

$$\langle A(1-P)L\rangle = \langle A(1-P)L_1\rangle.$$

Using (B.1) one can write

$$\langle L(1-P)\ A\rangle = \langle P\ L(1-P)\ A\rangle$$
$$= \langle P\ L_1(1-P)\ A\rangle + \langle L_0 P(1-P)\ A\rangle .$$

But $P(1-P) = P - P^2 = P - P = 0$; hence,

$$\langle L(1-P)\ A\rangle = \langle L_1(1-P)\ A\rangle . \qquad \text{(B.16)}$$

4. The next relationship to be proved is

$$\left[\hbar\omega - (1-P)L_0\right]^{-1} = \left[\hbar\omega - L_0\right]^{-1}(1-P). \qquad \text{(B.17)}$$

Expanding the left hand side in powers of L_0, one has

$$\left[\hbar\omega - (1-P)L_0\right]^{-1} = \frac{1}{\hbar\omega}\sum_{n=0}^{\infty}\left(\frac{(1-P)L_0}{\hbar\omega}\right)^n,$$

or, since $[L_0, P] = 0$,

$$\left[\hbar\omega - (1-P)L_0\right]^{-1} = \frac{1}{\hbar\omega}\sum_{n=0}^{\infty}\frac{L_0^n}{(\hbar\omega)^n}(1-P),$$

where the idempotent property of P has been used. Hence,

$$\left[\hbar\omega - (1-P)L_0\right]^{-1} = \left[\hbar\omega - L_0\right]^{-1}(1-P). \qquad \text{(B.18)}$$

5. In a similar manner as above the following identity can be proved:

$$\left[\hbar\omega - (1-P)L_0\right]^{-1} = (1-P)\left[\hbar\omega - L_0\right]^{-1}. \qquad \text{(B.19)}$$

APPENDIX C

A COMPUTATIONAL FORM FOR $\langle \mathcal{H}(\omega) \rangle_{\mu\nu,\mu'\nu'}$

(C.1) THE FULL COULOMB TREATMENT

A computational form for the operator $\langle \mathcal{H}(\omega) \rangle$ occurring in equation (2.54) is derived in this appendix. The derivation is carried out for both the dipole approximation and the full Coulomb interaction between the radiating atom and the perturbing electron.

In equation (2.54) the operator $\langle \mathcal{H}(\omega) \rangle_{\mu\nu,\mu'\nu'}$ is given in terms of four summations. The summands of the four terms are related to one another through permutation of the indices. Hence, it will be sufficient to consider only one of these terms in detail. In the derivation that follows, the third term in equation (2.54) will be considered and be referred to as $F(\omega)$. Using equation (2.49) for $\mathcal{K}_0(\omega)$ one has

$$F(\omega) = -i \sum_{\alpha\beta} \langle \nu\alpha | V^{*}_{\alpha\mu} | \nu'\beta \rangle \langle \mu\alpha | V_{\alpha\mu} | \mu'\beta \rangle f_{\beta\beta} \times \int \exp\left(i \left(\overline{\Delta\omega}_{\mu\nu'} - \omega_{\alpha\beta} \right) x \right) dx \qquad (C.1)$$

where in this appendix $\overline{\Delta\omega}_{\mu\nu'}$ is defined to be

$$\omega - \omega_{\mu\nu'} - \frac{e\mathcal{E}}{\hbar} \left(\vec{R}_{\mu\mu'} - \vec{R}^{*}_{\nu\nu'} \right).$$

The eigenvalues of the operator H_e when operating on the wave functions $\langle\alpha|$ and $\langle\beta|$ are $\hbar\omega_\alpha$ and $\hbar\omega_\beta$ respectively. With these eigenvalues the exponential, $\exp(-i\omega_{\alpha\beta}x)$, can be written in operator notation. Hence equation (C.1) becomes

$$F(\omega) = -i\int_0^\infty \exp(i\Delta\omega_{\mu\nu'}x)\sum_{\alpha\beta}^{I}\langle\alpha|V_{\mu\mu'}|\beta\rangle F_{\beta\beta}$$

$$\times\langle\beta|\exp(iH_e x/\hbar)V^*_{\nu\nu'}\exp(-ixH_e/\hbar)|\alpha\rangle dx \qquad (C.2)$$

where $V_{\mu\mu'}$ represents matrix elements of V_{ae} between the atomic states μ and μ'.

The inverse Fourier transform of function $F(\omega)$) has been treated in reference 23 using the dipole approximation for V_{ae} and an uncorrelated single electron distribution function defined as $1/V$, where V is the volume of the system. This derivation and that presented in reference 23 are essentially the same up to equation (A.19) in that reference. Using equation (A.19) in reference 23 and equation (C.2), one obtains

$$F(\omega) = \frac{\hbar}{k_B T}h^{-3N}\int\exp(i\omega s)\int\langle\mu|V_{ae}(x)|\mu'\rangle P(x)$$

$$\times\int\langle\nu|V^*_{ae}(y)|\nu'\rangle\int\exp(i\vec{g}\cdot(\vec{y}-\vec{x})/\hbar)$$

$$\times\exp(-g^2(s^2+is)/2mk_BT)\,d\vec{g}\,dy\,d\vec{x}\,ds \qquad (C.3)$$

where $a = \hbar\Delta\omega/k_BT$, $s = tk_BT/\hbar$, and q represents

momentum transfer for the perturbing electron.

The s integration can be performed using the following integrals:[47,50]

$$\int_0^\infty \cos(bs)\exp(-cs^2)\,ds = \frac{1}{2}\sqrt{\frac{\pi}{c}}\exp(-b^2/4c) \qquad (C.4)$$

$$\int_0^\infty \sin(bs)\exp(-cs^2) = \frac{1}{\sqrt{c}} D(b/2\sqrt{c}) \qquad (C.5)$$

where D(x) is Dawson's integral defined by[47]

$$D(x) = \exp(-x^2)\int_0^x \exp(x^2)\,dx.$$

The s integration yields a function of q:

$$\mathcal{J}(q) = \sqrt{\frac{\pi}{4}}\sqrt{\frac{2mk_BT}{q^2}}\exp(a/2)\exp\left(-\frac{a^2mk_BT}{2q^2} - \frac{q^2}{8mk_BT}\right)$$
$$+ i\sqrt{\frac{2mk_BT}{q^2}} D\left(a\left(\frac{2mk_BT}{q^2}\right)^{1/2}/2 - \left(\frac{q^2}{2mk_BT}\right)^{1/2}/2\right). \qquad (C.6)$$

Thus performing the time integration the expression for F(ω), equation (C.3), becomes

$$F(\omega) = \frac{\pi\hbar^{3N}}{k_BT}\int \mathcal{J}(q)\int \langle u|V_{ee}(r)|u'\rangle P(r)$$
$$\times \exp(-i\vec{q}\cdot\vec{R}/\hbar)\int \langle v|V_{ee}^*(y)|v'\rangle$$
$$\times \exp(i\vec{q}\cdot\vec{y}/\hbar)\,d\vec{y}\,d\vec{r}\,d\vec{q}. \qquad (C.7)$$

The $\vec{y}$ integration is performed next. The potential $V_{ae}(y)$ can be written as

$$V_{ae}(y) = \sum_j V_{ae}(y_j) \tag{C.8}$$

where j is the perturbing electron index. Furthermore, we may write

$$V_{ae}(y_j) = e^2 \left(\frac{1}{|\vec{y}_j - \vec{R}|} - \frac{1}{|\vec{y}_j|} \right)$$

where $\vec{R}$ and $\vec{y}_j$ are the position operators for the atomic and perturbing electron respectively, and the nucleus is assumed to be located at the origin. The integration over $\vec{y}_j$ is just the Fourier transform of the Coulomb potential which is

$$\int \exp(i \vec{p}_j \cdot \vec{y}_j / \hbar) \left(\frac{1}{|\vec{y}_j - \vec{R}|} - \frac{1}{|\vec{y}_j|} \right) d\vec{y}_j =$$

$$= \frac{4\pi \hbar^2}{p_j^2} \left(\exp(i \vec{p}_j \cdot \vec{R} / \hbar) - 1. \right). \tag{C.9}$$

For the total potential defined in equation (C.8) the $\vec{y}$ integration yields

$$\int V_{ae}(y) \exp(i \vec{p} \cdot \vec{y} / \hbar) \, d\vec{y} = \int \cdots \int \sum_{j=1}^{N} V_{ae}(\vec{y}_j) \exp(i \vec{p}_j \cdot \vec{y}_j / \hbar)$$

$$\times \prod_{i \neq j}^{N} \exp(i \vec{p}_i \cdot \vec{y}_i / \hbar) \, d\vec{y}_1 \cdots d\vec{y}_N$$

$$= \frac{\hbar^{3N} e^2}{\pi \hbar} \sum_{j=1}^{N} \frac{\exp(i \vec{p}_j \cdot \vec{R} / \hbar) - 1}{p_j^2} \prod_{i \neq j}^{N} \delta(p_i). \tag{C.10}$$

Inserting these results into the expression for $F(\omega)$, one finds

$$F(\omega)_{\mu\mu';\nu\nu'} = \frac{e^4}{2\pi^2 k_B T}\int d(g)\int\cdots\int \langle\mu|\sum_{k=1}^{N}\frac{1}{|\vec{r}_k-\vec{R}|}-\frac{1}{|\vec{r}_k|}|\mu'\rangle$$

$$\times \exp(-i\vec{g}_k\cdot\vec{r}_k/\hbar)\,P(r_1\cdots r_N)\prod_{l\neq k}^{N}\exp(-i\vec{g}_l\cdot\vec{r}_l/\hbar)$$

$$\times \langle\nu|\sum_{j=1}^{N}(\exp(-i\vec{g}_j\cdot\vec{R}/\hbar)-1)/g_j^2\,|\nu'\rangle$$

$$\times \prod_{i\neq j}^{N}\delta(g_i)\,d\vec{r}_1\cdots d\vec{r}_N\,d\vec{g}. \qquad \text{(C.11)}$$

There are two distinct terms in the above expression for $F(\omega)$, $j = k$ and $j \neq k$. The $j = k$ term, labeled F_0, is considered first. The subscripts are suppressed for compactness.

Since all the perturbers under consideration are identical, the summation over j can be replaced by N, the total number of electrons, times the $j = 1$ term:

$$F_0 = \frac{e^4 N}{2\pi^2 k_B T}\int d(g)\int\cdots\int \langle\mu|\frac{1}{|\vec{r}_1-\vec{R}|}-\frac{1}{|\vec{r}_1|}|\mu'\rangle$$

$$\times \exp(-i\vec{g}_1\cdot\vec{r}_1/\hbar)\,P(r_1\cdots r_N)\prod_{l\neq 1}^{N}\exp(-i\vec{g}_l\cdot\vec{r}_l/\hbar)$$

$$\times \langle\nu|(\exp(-i\vec{g}_1\cdot\vec{R}/\hbar)-1)/g_1^2\,|\nu'\rangle\prod_{i\neq 1}^{N}\delta(g_i)\,d\vec{r}_1\cdots d\vec{r}_N\,d\vec{g}. \qquad \text{(C.12)}$$

All the integrations over q_i except i = 1 can be readily performed using the properties of the Dirac delta function. Hence,

$$F_0 = \frac{e^4 N}{2\pi^2 k_B T} \int J(\vec{r}_1) \int d\vec{r}_1 \langle u | \frac{1}{|\vec{r}_1 - \vec{R}|} - \frac{1}{|\vec{r}_1|} | u' \rangle$$
$$\times \exp(-i\vec{r}_1 \cdot \vec{r}_1 / \hbar) \langle v | (\exp(-i\vec{r}_1 \cdot \vec{R}/\hbar) - 1)/r_1^2 | v' \rangle$$
$$\times d\vec{r}_1 \cdots d\vec{r}_N d\vec{r}. \qquad \text{(C.13)}$$

We define

$$\int d\vec{r}_2 \cdots d\vec{r}_N P(r_1 \cdots r_N) = \frac{1}{V} p(r_1) \qquad \text{(C.14)}$$

where $p(x_1)$ is a reduced distribution function and is interpreted as representing the probability of finding a perturbing electron at x_1 regardless of the location of the other N-1 electrons. An approximation for $p(x_1)$ that takes into account the effects of electron symmetry is developed in Appendix A.

The potential $(1/|\vec{r}_1 - \vec{R}| - 1/|\vec{r}_1|)$ occurring in equation (C.13) can be written in terms of an inverse Fourier transform

$$\frac{1}{|\vec{r}_1 - \vec{R}|} - \frac{1}{|\vec{r}_1|} = \frac{1}{2\pi^2 \hbar} \int \exp(i\vec{r}' \cdot \vec{r}_1 / \hbar)$$
$$\times (\exp(-i\vec{r}' \cdot \vec{R}/\hbar) - 1)/r'^2 \, d\vec{r}'. \qquad \text{(C.15)}$$

Using the definition of $p(x_1)$ in equation (C.14) and equation (C.15), F_0 becomes

$$F_0 = \frac{n_e e^4}{4\pi^4 k_B T \hbar} \int J(\vec{q}) \int \rho(\vec{r}) \int \exp(i\vec{q}'\cdot\vec{r}/\hbar)$$

$$\times \langle u|(\exp(-i\vec{q}'\cdot\vec{R}/\hbar)-1)/q'^2|u'\rangle \exp(-i\vec{q}\cdot\vec{r}/\hbar)$$

$$\times \langle v|(\exp(-i\vec{q}\cdot\vec{R}/\hbar)-1)/q^2|v'\rangle \, d\vec{q}' \, d\vec{r} \, d\vec{q} \qquad \text{(C.16)}$$

where subscripts on x and q have been suppressed for compactness in writing, and n_e is the electron density, N/V.

The atomic matrix elements of the operator (exp(iq·R/ħ)-1) are evaluated in Appendix D. Let

$$G_{vv'} \equiv \langle v|\exp(i\vec{q}\cdot\vec{R}/\hbar)-1|v'\rangle. \qquad \text{(C.17)}$$

In terms of $G_{vv'}$, F_0 becomes

$$F_0 = \frac{n_e e^4}{4\pi^4 k_B T \hbar} \int J(\vec{q}) \frac{G^*_{vv'}}{q^2} \int \rho(\vec{r}) \exp(-i\vec{q}\cdot\vec{r}/\hbar)$$

$$\times \int \exp(i\vec{q}'\cdot\vec{r}/\hbar) \frac{G^*_{uu'}}{q'^2} \, d\vec{q}' \, d\vec{r} \, d\vec{q}. \qquad \text{(C.18)}$$

The angular part of the $\vec{x}$ integration is performed next, choosing x_z along the $\vec{q}'$-$\vec{q}$ direction:

$$F_0 = \frac{n_e e^4}{4\pi^4 k_B T \hbar} \int J(\vec{q}) \frac{G^*_{vv'}}{q^2} \int \frac{G^*_{uu'}}{q'^2} \int_0^\infty r \, \rho(r)$$

$$\times \sin(r|\vec{q}-\vec{q}'|/\hbar)/(|\vec{q}-\vec{q}'|/\hbar) \, dr \, d\vec{q}' \, d\vec{q}. \qquad \text{(C.19)}$$

The angular integrations involving q' and q are performed next. The coordinate system for the q' integration is chosen so that q_z' lies along the q direction. After carrying out the angular integration in q', the angular integration in q is trivial. F_0 becomes

$$F_0 = \frac{16 m_e a^4 \hbar}{\pi k_B T} \int_0^\infty J(q) G^*_{VV'}/q \int_0^\infty G^*_{\mu\mu'}/q' \times \int_0^\infty p(x) \sin(qx/\hbar) \sin(q'x/\hbar)\, dx\, dq'\, dq. \tag{C.20}$$

For sufficiently large x, $x > x_m \approx 50$ Bohr radii, $p(x) \approx 1$. Thus it is convenient from a computational stand point to split the x integration up into two regions, $x < x_m$ and $x > x_m$, where $p \approx 1$ for $x > x_m$. Hence

$$\int_0^\infty p(x) \sin(qx/\hbar) \sin(q'x/\hbar)\, dx = m_e \int_0^\infty \sin(qx/\hbar) \sin(q'x/\hbar)\, dx + \int_0^{x_m} (p(x) - m_e) \sin(qx/\hbar) \sin(q'x/\hbar). \tag{C.21}$$

The first integral is carried out by writing the sine terms in exponential form and using the integral definitions of the Dirac delta functions:

$$\int_0^\infty p(r)\,\mathrm{SIN}(qr/\hbar)\,\mathrm{SIN}(q'r/\hbar) = -\frac{\hbar\pi M}{2}\left(\delta(q+q') - \delta(q-q')\right) + \int_0^{r_m} (p(r) - M_e)\,\mathrm{SIN}(qr/\hbar)\,\mathrm{SIN}(q'r/\hbar)\,dr. \tag{C.22}$$

By substituting equation (C.22) into equation (C.20) and performing the q' integration, one can show that

$$F_0 = \frac{8 M_e e^4 \hbar}{k_B T} \int_0^\infty J(q)\, G^*_{\nu\nu'}(q)\, G^*_{\mu\mu'}(q)/q^2 + \text{PTERM} \tag{C.23}$$

where PTERM is defined as

$$\text{PTERM} = \frac{16 M_e e^4 \hbar}{\pi k_B T} \int_0^\infty J(q)\,\frac{G^*_{\nu\nu}}{q} \int_0^\infty \frac{G^*_{\mu\mu'}}{q'} \times \int_0^{r_m} (p(r) - M_e)\,\mathrm{SIN}(q'r/\hbar)\,\mathrm{SIN}(qr/\hbar)\,dr\,dq'\,dq. \tag{C.24}$$

After performing a minor change in variables, the first term in expression (C.23) is evaluated numerically.

The second term, which contains p(x), has been examined by using a non linear least squares fit for p(x).

The x integration can then be performed analytically. The remaining two-dimensional q, q' integral contains oscillatory functions and is poorly behaved, hence it is very difficult to evaluate. However, in the dipole approximation the q' integration can be performed analytically. Thus, the detailed effect of using the effective distribution function is examined only in the dipole approximation. For the full Coulomb interaction treatment, only an order of magnitude estimate is obtained for the second term, and this by means of an effective cut-off (see Section V.5).

The term $j \neq k$, labeled F_c, occurring in equation (C.11) is evaluated next. Electron correlation effects will enter into the theory via this term.

Due to the identical nature of the perturbing electrons N(N-1) identical terms will result when the summations are carried out. Making the approximation $N(N-1) = N^2$ and setting $j = 1$, $k = 2$ one has

$$F_c = \frac{\varepsilon^4 N^2}{2\pi^2 \hbar_B T} \int J(\vec{q}) \int \cdots \int \langle \mu | \frac{1}{|\vec{r}_2 - \vec{R}|} - \frac{1}{|\vec{r}_2|} | \mu' \rangle$$

$$\times P(\vec{r}_1 \cdots \vec{r}_N) \exp(-i \vec{q} \cdot \vec{r}_1 / \hbar)$$

$$\times \langle \nu | \left(\exp(-i \vec{q}_1 \cdot \vec{R}/\hbar) - 1. \right) / q_1^2 | \nu' \rangle \, d\vec{r}_1 \cdots d\vec{r}_N \, d\vec{q} \, .$$

(C.25)

Defining $p(x_1, x_2)$ by

$$p(\vec{r}_1, \vec{r}_2) = V^2 \int \cdots \int P(\vec{r}_1 \cdots \vec{r}_N) \, d\vec{r}_3 \cdots d\vec{r}_N$$

(C.26)

and using the inverse transform of V_{ae} one can show that

$$F_c = \frac{e^4 M_e^2}{4\pi^2 k_B T \hbar} \iint v(q)\, G^*_{\nu\nu'}\, G^*_{\mu\mu'} / (q^2 q'^2)$$

$$\times \iint p(r_1, r_2)\, \exp(-i\vec{q}\cdot\vec{r}_1/\hbar)\, \exp(i\vec{q}'\cdot\vec{r}_2/\hbar)$$

$$\times d\vec{r}_1 d\vec{r}_2 dq' dq \qquad \text{(C.27)}$$

where $G^*_{\nu\nu'}$ and $G^*_{\mu\mu'}$ are defined in equation (C.17).

The angular integrations in $\vec{q}$ and $\vec{q}'$ are performed next. q_z and q_z' are taken to lie along the $\vec{x}_1$ and $\vec{x}_2$ directions respectively. One obtains

$$F_c = \frac{4e^4 M_e^2}{\pi^2 \hbar k_B T} \int_0^\infty \int_0^\infty v(q)\, G^*_{\nu\nu'}\, G^*_{\mu\mu'} \iint p(r_1 r_2)$$

$$\times \sin(q r_1/\hbar) \sin(q' r_2/\hbar) / (q r_1 q' r_2/\hbar^2)$$

$$\times d\vec{r}_1 d\vec{r}_2 dq' dq. \qquad \text{(C.28)}$$

If correlations between electrons are neglected, $p(x_1,x_2) \simeq 0$ and F_c is zero due to the angular integrations over x_1 and x_2.

In terms of the pair distribution function,[51] $p(x_1,x_2)$ may be written as

$$p(r_1, r_2) = 1 - \tilde{g}(y) = -\bar{g}_2(y) \qquad \text{(C.29)}$$

where $\tilde{g}_2(y) = -\frac{e^2}{k_B T y} \exp(-y/\lambda_D)$

$$y = |r_1 - r_2|$$

and

$$\lambda_D^2 = k_B T / 4\pi n_e e^2. \qquad \text{(C.30)}$$

The spatial integrations are carried out next. A transformation to relative coordinates is made and the definitions appearing in equation (C.30) are used to obtain,

$$\int\int (---)\, d\vec{r}_1\, d\vec{r}_2 = -\int\int \hat{g}_2(y) \times \frac{Si N(g|\vec{r}+\vec{y}|/\hbar)\; Si N(g'r/\hbar)}{(g|\vec{r}+\vec{y}|/\hbar)(g'r/\hbar)}\, d\vec{r}\, d\vec{y}. \qquad \text{(C.31)}$$

The angular integration in $\vec{y}$ yields a factor,

$$\frac{4\pi\, Si N(gr/\hbar)\, Si N(gy/\hbar)}{(g/\hbar)^2\, ry}. \qquad \text{(C.32)}$$

Substituting equation (C.32) into equation (C.31) and performing the angular integration in x yields,

$$\frac{-16\pi^2 e^2}{(g'/\hbar)(g/\hbar)^2 k_B T}\int_0^\infty dy\, exp(-y/\lambda_D)\, Si N(gy/\hbar) \times \int_0^\infty Si N(gr/\hbar)\, Si N(g'r/\hbar)\, dr \qquad \text{(C.33)}$$

which is further reduced by performing the x integration

$$-\frac{8\pi^3\hbar e^2}{(q'/\hbar)(q/\hbar)k_B T}\left(\frac{\lambda_D^2}{1+(\lambda_D q/\hbar)^2}\right)$$

$$\times\left(\delta(q-q')-\delta(q+q')\right),$$

(C.34)

where $\delta(x)$ is the Dirac delta function. When these results are inserted into F_c and the q' integration carried out one obtains

$$F_c = -\frac{8e^4 m_e}{k_B T}\int_0^\infty \frac{\mathcal{J}(q)\, G^*_{\nu\nu'}\, G^*_{\mu\mu'}}{(q/\hbar)^2\left(1+(\lambda_D q/\hbar)^2\right)}\, dq .$$

(C.35)

Combining equations (C.35) and (C.23) one obtains F for the case of full Coulomb interaction between the radiating atoms and perturbing electrons,

$$F = \frac{8 m_e e^4 \hbar^2}{k_B T}\int \mathcal{J}(q)\frac{G^*_{\nu\nu'}\, G^*_{\mu\mu'}}{q^2}$$

$$\times\left[1-\frac{1}{1+(\lambda_D q/\hbar)^2}\right] + \text{PTERM}, \qquad \text{(C.36)}$$

The above expression is evaluated by numerical techniques.

C.2 THE DIPOLE APPROXIMATION

If the dipole approximation is used, the potentials V(x) and V(y) in equation (C.7) are replaced by the dipole interaction between the atom and perturbing electron. Then,

$$F = \frac{\hbar_1 \hbar_1^{-3N} e^4}{k_B T} \int J(\xi) \int \sum_{i=1}^{N} \left(\vec{R}_{\mu\mu'} \cdot \vec{x}_i / x_i^3 \right) \exp\left(-i \vec{\xi}_i \cdot \vec{x}_i / \hbar_1\right)$$

$$\times P(x_1 \cdots x_N) \prod_{\ell \neq i}^{N} \exp\left(-i \vec{\xi}_\ell \cdot \vec{x}_\ell / \hbar_1\right)$$

$$\times \int \sum_{j=1}^{N} \left(\vec{R}_{\nu\nu'} \cdot \vec{y}_j / y_j^3 \right) \exp\left(i \vec{\xi}_j \cdot \vec{x}_j / \hbar_1\right)$$

$$\times \prod_{k \neq j}^{N} \exp\left(i \vec{\xi}_k \cdot \vec{y}_k / \hbar_1\right) d\vec{y}_1 \cdots d\vec{y}_N \, d\vec{x}_1 \cdots d\vec{x}_N \, d\vec{\xi}. \tag{C.37}$$

Equation (C.37) also yields two terms, i = j, and i ≠ j. The i = j term, labeled F_{DO} in the following derivation, is evaluated first. Following a procedure similar to that used in evaluating F_0 one obtains

$$F_{DO} = \frac{e^4 N_e}{8\pi^3 k_B T \hbar_1^2} \int J(\xi) \int p(x) \, \vec{R}_{\mu\mu'} \cdot \vec{x} / x^3$$

$$\times \exp\left(-i \vec{\xi} \cdot \vec{x} / \hbar_1\right) \int \vec{R}_{\nu\nu'} \cdot \vec{y} / y^3 \exp\left(i \vec{\xi} \cdot \vec{y} / \hbar_1\right) d\vec{y} \, d\vec{x} \, d\vec{\xi}. \tag{C.38}$$

The y integration is performed using the coordinate system illustrated below.

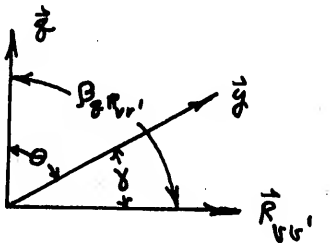

The results of this integration are

$$F_{DO} = \frac{i e^4 R_{vv'}}{2\pi^2 k_B T t_1} \int J(z) \int d\vec{\nu} \, p(\nu) \vec{R}_{\mu\mu'} \cdot \vec{\nu} / \nu^3$$

$$\times \exp(-i \vec{z} \cdot \vec{\nu} / t_1) \cos(\beta_z R_{vv'}) / z \, d\vec{\nu} \, d\vec{z} \, .$$

(C.39)

The $\vec{x}$ integration can be performed by a similar procedure yielding the following expression for F_{DO}:

$$F_{DO} = \frac{2 e^4 m_e \vec{R}_{\mu\mu'} \cdot \vec{R}_{vv'}}{\pi k_B T t_1} \int J(z) \cos(\beta_z R_{vv'})$$

$$\times \cos(\beta_z R_{\mu\mu'}) / z \int p(\nu) \left(\sin(z\nu/t_1) / (z\nu/t_1) \right.$$

$$\left. - \cos(z\nu/t_1) / (z\nu/t_1) \right) d\nu \, d\vec{z} \, .$$

(C.40)

The angular part of the $\vec{q}$ integration is performed using the coordinate system illustrated below.

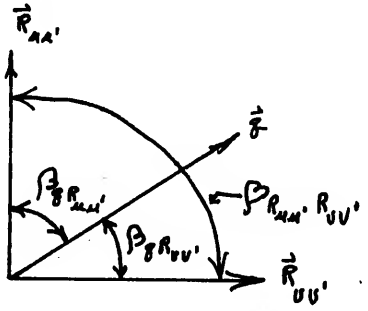

This integration yields

$$F_{Do} = \frac{8e^4 n_e \vec{R}_{uu'} \cdot \vec{R}_{vv'}}{3k_B T \hbar} \int J(q) q \int T^2(x) \times \left(\mathrm{SIN}(8x/\hbar)/(8x/\hbar) - \cos(8x/\hbar)/(8x/\hbar) \right) dx\, dq .$$

(C.41)

A similar procedure is followed for the i ≠ j term. The details are rather lengthy but straightforward and will be omitted. The resulting expression for the correlation term (see Section C.1), F_{DC}, is

$$F_{DC} = \frac{8e^4 n_e \vec{R}_{uu'} \cdot \vec{R}_{vv'}}{3k_B T} \int \frac{J(q)}{(1 + (\lambda_D q/\hbar)^2)} dq .$$

(C.42)

Combining equations (C.42) and (C.41) one has, in the dipole approximation,

$$F_D = \frac{8e^4 m_e \vec{R}_{\mu\mu'} \cdot \vec{R}_{\nu\nu'}}{3k_B T} \int d(q) \left[\int p(x) (q/\hbar) \right.$$

$$\times \left(\sin(qx/\hbar)/(qx/\hbar) - \cos(qx/\hbar)/(qx/\hbar) \right) dx$$

$$\left. - 1./(1 + (\lambda_D q/\hbar)^2 \chi \right] dx\, dq . \qquad \text{(C.43)}$$

If one follows the commonly accepted procedure of setting p(x) equal to unity and using a strong collision cut-off, x_o, the expression for F_{DO} becomes

$$F_{Do} = \frac{8e^4 m_e \vec{R}_{\mu\mu'} \cdot \vec{R}_{\nu\nu'}}{3k_B T} \int_0^\infty d(q) \sin(q x_o/\hbar)/(q x_o/\hbar)$$

(C.44)

$$F_D = \frac{8e^4 m_e \vec{R}_{\mu\mu'} \cdot \vec{R}_{\nu\nu'}}{3k_B T} \int d(q) \left[\sin(q x_o/\hbar)/(q x_o/\hbar) \right.$$

$$\left. - 1./(1. + (\lambda_D q/\hbar)^2) \right] dq .$$

(C.45)

Computer programs have been written for the various approximate forms of F given in equations (C.36), (C.43) and (C.45).

APPENDIX D

MATRIX ELEMENTS OF EXP(i $\vec{k}\cdot\vec{r}$) - 1

The atomic matrix elements of the operator exp(i $\vec{k}\cdot\vec{r}$)-1, required in the evaluation of $\langle \mathcal{H}(\omega) \rangle_{nss',n's'}$, are evaluated in this appendix.

The parabolic wave functions for a hydrogen atom are given by[38]

$$\Psi_{n,s,m}(\mu,\lambda,\phi) = \left[\frac{s!\,(n-s-|m|-1)!}{(na_0)^3\, n\pi\, ((s+|m|)!\,(n-s-1)!)^3} \right]^{1/2}$$

$$\times \exp(im\phi)\, (\sqrt{\lambda\mu}/na_0)^{|m|} \exp(-(\lambda+\mu)/2na_0)$$

$$\times L_s^{m}(\lambda/na_0)\, L_{n-s-|m|-1}^{m}(\mu/na_0) \qquad \text{(D.1)}$$

where a_0 is the Bohr radius, L_q^p are the associated Laguerre polynomials,[47] and, in this Appendix, n, s, m are the parabolic quantum numbers.

The transformation equations between the parabolic and spherical coordinate systems are,

$$x = \sqrt{\lambda\mu}\,\cos(\phi) \tag{D.2a}$$

$$y = \sqrt{\lambda\mu}\,\sin(\phi) \tag{D.2b}$$

$$z = (\lambda-\mu)/2. \tag{D.2c}$$

$$r = (\lambda+\mu)/2 \tag{D.2d}$$

$$d\tau = ((\lambda+\mu)/4)\,d\lambda\,d\mu\,d\phi\,. \tag{D.2e}$$

If a coordinate system is chosen so that the z component of $\vec{r}$ lies along the $\vec{k}$ direction,

$$\exp(i\vec{k}\cdot\vec{r}) \rightarrow \exp(ikz) \rightarrow \exp(ik(\lambda-\mu)/2). \tag{D.3}$$

In the following derivation μ and ν will be used to represent the atomic states. Using this notation and the above expression for $\exp(i\vec{k}\cdot\vec{r})$ one has

$$\langle\mu|\exp(i\vec{k}\cdot\vec{r})|\nu\rangle = C(n_\mu, s_\mu, m_\mu, n_\nu, s_\nu, m_\nu)$$

$$\times \frac{1}{\pi n_\mu^3 n_\nu^3 a_0^6} \int_0^{2\pi} \exp(i(m_\nu - m_\mu)\phi)\,d\phi \int_0^\infty d\lambda \int_0^\infty d\mu$$

$$\times (\sqrt{\lambda\mu}/n_\mu a_0)^{|m_\mu|} (\sqrt{\lambda\mu}/n_\nu a_0)^{|m_\nu|} \exp(ik(\lambda-\mu)/2)$$

$$\times ((\lambda+\mu)/4) \exp\left(-\frac{\lambda+\mu}{2a_0}\left(\frac{1}{n_\mu}+\frac{1}{n_\nu}\right)\right) L_{s_\mu}^{|m_\mu|}(\lambda/n_\mu a_0)$$

$$\times L_{n_\mu - s_\mu - |m_\mu| - 1}^{|m_\mu|}(\mu/n_\mu a_0)\; L_{s_\nu}^{|m_\nu|}(\lambda/n_\nu a_0)\; L_{n_\nu - s_\nu - |m_\nu| - 1}^{|m_\nu|}(\mu/n_\nu a_0)$$

(D.4)

where

$$C(n_\mu, s_\mu, m_\mu, n_\nu, s_\nu, m_\nu) = \left[\frac{s_\mu!\,(n_\mu - s_\mu - |m_\mu| - 1)!}{((s_\mu + |m_\mu|)!\,(n_\mu - s_\mu - 1)!)^3} \right.$$

$$\left. \times \frac{s_\nu!\,(n_\nu - s_\nu - |m_\nu| - 1)!}{((s_\mu + |m_\mu|)!\,(n_\mu - s_\mu - 1)!)^3} \right]^{1/2} \frac{1}{n_\mu\, n_\nu} \,. \tag{D.5}$$

The integration over ϕ yields a factor $2\pi\,\delta_{m_\mu m_\nu}$ where δ_{ij} is the Kronecker delta. The remaining integrations depend only on the absolute value of m. Therefore, for convenience |m| will be denoted as m where m is assumed positive.

A transform of variables is performed in equation (D.4):

$$\eta = (n_\mu + n_\nu)\,u / (2a_0\, n_\mu\, n_\nu) \tag{D.6a}$$

$$v = (n_\mu + n_\nu)\,\lambda / (2a_0\, n_\mu\, n_\nu). \tag{D.6b}$$

Then

$$\langle \mu | \exp(i\vec{k}\cdot\vec{r}) | \nu \rangle = C(n_\mu, s_\mu, m_\mu, n_\nu, s_\nu, m_\nu) \left((n_\mu + n_\nu)/4\right)$$

$$\times (\Omega_\mu \Omega_\nu)^{m+2} \int_0^\infty \int_0^\infty \exp(ib(v-\eta))\,(v\eta)^m\,(v+\eta)\exp(-(v+\eta))$$

$$\times L_{s_\mu}^m(\Omega_\nu v)\; L_{n_\mu}^m(\Omega_\nu \eta)\; L_{s_\nu}^m(\Omega_\mu v)\; L_{n_\nu}^m(\Omega_\mu \eta)\; dv\, d\eta \tag{D.7}$$

where

$$b = \frac{k a_0 n_u n_v}{n_u + n_v}$$

$$\Omega_u = 2n_u/(n_u + n_v)$$

$$\Omega_v = 2n_v/(n_u + n_v)$$

$$k_u = n_u - s_u - m - 1$$

$$k_v = n_v - s_v - m - 1.$$

(D.8)

In the no-quenching approximation one requires matrix elements for which $n_u = n_v = n$, where n is the principal quantum number of the initial state. In this case $\Omega_u = \Omega_v = 1$, and $b = ka_0 n/2$. Hence,

$$\langle u | \exp(i\vec{k}\cdot\vec{r}) | v \rangle = D(n, m, s_u, s_v) \int\int V^m \times \exp(ibV) \exp(-V) L^m_{s_u}(V) L^m_{s_v}(V) \eta^m \exp(-ib\eta) \times (V+\eta) L^m_{k_u}(\eta) L^m_{k_v}(\eta) \, d\eta \, dV$$

(D.9)

where

$$D(m,m',S_u,S_v) = C(m,S_u,m',m,S_v,m')\,m/2 .$$

Equation (D.9) can be written in terms of the following integral

$$h(I,M,J,K) = \int \exp(i^0 b x)\, x^I \exp(-x) \times L_J^M(x)\, L_K^M(x)\, dx \qquad \text{(D.10)}$$

resulting in the following expression,

$$\langle u | \exp(i\vec{k}\cdot\vec{r}) | v \rangle = D(m,m',S_u,S_v) \times \left[h(m+1,m,S_u,S_v)\, h^*(m,m',S_u,k_v) + h(m,m',S_u,S_v)\, h^*(m+1,m',k_u,k_v) \right]. \qquad \text{(D.11)}$$

The integral h(i,m,j,k) can be reduced to a closed form that can be easily programmed for machine computation. First note that the generating function for the associated Laguerre polynomials is[38]

$$L_J^M(x) = \frac{\Gamma(M+J+1)\, e^x}{\Gamma(J+1)\, x^M} \left[\frac{d^J}{dx^J} \left(x^{J+M} e^{-x} \right) \right].$$

Carrying out the indicated derivatives in the above expression yields the following summation:

$$L_J^M(x) = (M+J)! \sum_{l=0}^{J} (-x)^l \binom{J+M}{J-l} \frac{1}{l!}$$

(D.12)

where $\binom{p}{q}$ is the generalized binomial coefficient defined by

$$\binom{p}{q} = \frac{p!}{q!(p-q)!} .$$

Inserting the above results into equation (D.10) leads to

$$h(I,M,J,K) = \sum_{l=0}^{J} (-1)^l \binom{J+M}{J-l} \frac{(J+M)!}{l!} \sum_{r=0}^{K} (-1)^r$$

$$\times \binom{K+M}{K-r} \frac{(K+M)!}{r!} \int_0^\infty x^{r+l+I} \exp(-x)$$

$$\times \exp(ibx).$$

(D.13)

The x integration can be performed using the integral derived from formulae appearing in reference 50.

$$\int_0^\infty x^M \exp(-x) \exp(ibx) = \frac{M!(1+ib)^{M+1}}{(1+b^2)^{M+1}} .$$

(D.14)

One finally arrives at the following closed expression for h(i,m,j,k).

$$h(I,M,J,K) = (J+M)!\,(K+M)!\left(\frac{1+ib}{1+b^2}\right)^{I+1}\sum_{l=0}^{J}(-1)^l$$

$$\times\binom{J+M}{J-l}\frac{1}{l!}\sum_{x=0}^{K}(-1)^x\binom{K+M}{K-x}\frac{1}{x!}$$

$$\times(I+l+x)!\,(1+ib)^{l+x}/(1+b^2)^{l+x}. \qquad \text{(B.15)}$$

A computer program has been written to evaluate the above expression; because it is diagonal in the magnetic quantum number, m, the matrix $\exp(i\vec{k}\cdot\vec{r})-1$, will at most be of order n.

APPENDIX E

USEFUL MATRIX RELATIONSHIPS

Two matrix relationships useful in line shape computations are derived in this appendix.

A complex matrix, M, can be written as, $M = A + iB$, where A and B are real matrices. Its inverse is written as, $M^{-1} = C + iD$. Expressions for C and D can be derived in terms of A and B and their inverses. By definition,

$$(A + iB)\ (C + iD) = 1$$

where 1 is the identity matrix. The above expression yields two matrix equations when multiplied out

$$AC - BD = 1$$

$$BC - AD = 0.$$

Solve for C and D.

$$C = (A + BA^{-1}B)^{-1}$$

$$D = -(B + AB^{-1}A)^{-1}.$$

Assume that A can be written as

$$A = A' + \alpha E$$

where E is diagonal and α is a scalar parameter. Then,

$$(B + AB^{-1}A) = (B + (A' + AE)B^{-1}(A' + AE))$$

$$= B + A'B^{-1}A' + \alpha(AEB^{-1}A' + A'B^{-1}AE) -$$

$$+ \alpha^2 AEB^{-1}AE$$

$$= B1 + \alpha B2 + \alpha^2 B3$$

where the definitions of B1 and B3 follow from the derivation.

When the above relationships are applied to the line shape problem, many of the matrix products can be performed outside of the ion-field integration routine, thus saving a considerable amount of computer time.

APPENDIX F

DIPOLE MATRIX ELEMENTS IN THE PARABOLIC REPRESENTATION

The dipole matrix elements of the atomic dipole operator are evaluated directly in the parabolic representation in this appendix. The derivation is partially based on material presented in Chapter II of reference 18.

The z component of the dipole operator is considered first. In the parabolic coordinate system one has

$$z = (\lambda - \mu)/2$$

where λ and μ are the parabolic coordinates as defined in Appendix D. Following a similar procedure as that used to compute the matrix elements of $\exp(ib(V - \eta))$ in Appendix D, one can derive the following expression for the matrix elements of z:

$$\langle \mu | z | \nu \rangle = D(m, m, S_\mu, S_\nu)\, a_0 \int_0^\infty dV \int_0^\infty d\eta\; V^m \eta^m e^{-V-\eta}$$

$$\times (V^2 - \eta^2)\, L^m_{S_\mu}(V)\, L^m_{S_\nu}(V)\, L^m_{\eta_\mu}(\eta)\, L^m_{\eta_\nu}(\eta)\, \delta_{m_\mu, m_\nu}$$

where the terms involved in this expression are defined in Appendix D.

Defining the following integral

$$I_{II}(m,\epsilon,\delta,a,b) = \int e^{-x} x^{m+\epsilon} L_I^{m}(ax)\; L_J^{m+\delta}(bx)\, dx$$

one can write

$$\langle \mu | z | \nu \rangle = a_0\, D(n,m,S_\mu,S_\nu)\Big\{ I_{S_\mu S_\nu}(m,2,0,1,1) \times I_{R_\mu R_\nu}(m,0,0,1,1) - I_{S_\mu S_\nu}(m,0,0,1,1)\, I_{R_\mu R_\nu}(m,2,0,1,1)\Big\}\delta_{m_\mu m_\nu}.$$

The matrix elements of x and y components can be obtained in terms of an operator, $\Gamma_\pm$, defined as

$$\Gamma_\pm \equiv X \pm iY = \sqrt{\mu\lambda}\, e^{\pm i\phi}.$$

After performing the ϕ integration (see equation D.9), one obtains:

$$\langle \mu | \Gamma_\pm | \nu \rangle = \delta_{m_\mu, m_\nu \pm 1}\, D'(n,S_\mu,m_\mu,S_\nu,m_\nu) \times \Big\{ I_{S_\mu S_\nu}(m_\mu,\epsilon+1,\delta,1,1)\, I_{R_\mu R_\nu}(m_\mu,\epsilon,\delta,1,1) + I_{S_\mu S_\nu}(m_\mu,\epsilon,\delta,1,1)\, I_{R_\mu R_\nu}(m_\mu,\epsilon+1,\delta,1,1)\Big\}$$

where

$$\delta = |m_\nu| - |m_\mu|$$

$$\epsilon = (\delta+1)/2$$

and

$$D'(n, S_{\mu}, m_{\mu}, S_{\nu}, m_{\nu}) = \frac{a_0}{2}\left[\frac{S_{\mu}!\,(n-S_{\mu}-|m_{\mu}|-1)!\;S_{\nu}!\,(n-S_{\nu}-|m_{\nu}|-1)!}{(S_{\mu}+|m_{\mu}|)!\,(n_{\mu}-S_{\mu}-1)!\,(n_{\nu}+S_{\nu})!\,(n_{\nu}-S_{\nu}-1)!)^3}\right]^{1/2}.$$

The integral I is evaluated in reference 18.

Using the above results, one arrives at the following matrix elements for the Lyman-alpha transitions in hydrogen:

$$(x) = a_0 \begin{pmatrix} 0 & C & 0 & 0 & C \\ C & 0 & -1.5 & -1.5 & 0 \\ 0 & -1.5 & 0 & 0 & -1.5 \\ 0 & -1.5 & 0 & 0 & -1.5 \\ C & 0 & -1.5 & -1.5 & 0 \end{pmatrix} \qquad (F.1)$$

$$(y) = a_0 \begin{pmatrix} 0 & C & 0 & 0 & C \\ -C & 0 & 1.5 & 1.5 & 0 \\ 0 & -1.5 & 0 & 0 & 1.5 \\ 0 & -1.5 & 0 & 0 & 1.5 \\ -C & 0 & -1.5 & -1.5 & 0 \end{pmatrix} \qquad (F.2)$$

$$(z) = a_0 \begin{pmatrix} 0 & 0 & C & -C & 0 \\ 0 & 0 & 0 & 0 & 0 \\ C & 0 & -3 & 0 & 0 \\ -C & 0 & 0 & 3 & 0 \\ 0 & 0 & 0 & 0 & 0 \end{pmatrix} \qquad (F.3)$$

where a_0 is the Bohr radius, c = .5267482 and the state labels are

$1 \equiv |100\rangle$

$2 \equiv |20\text{-}1\rangle$

$3 \equiv |210\rangle$

$4 \equiv |200\rangle$

$5 \equiv |200\rangle$.

For the Lyman-alpha transitions the above matrix elements could have been obtained directly from the wave functions without developing a general expression for the matrix elements. However, such a procedure would be unduly complicated for the higher transitions.

To obtain the matrix elements for helium ion transitions, one replaces the Bohr radius by $a_o/2$.

BIBLIOGRAPHY

1. H. R. Griem, Plasma Spectroscopy (McGraw-Hill Book Co., New York, 1964).

2. E. W. Smith, C. R. Vidal, and J. Cooper, J. Res. Nat. Bur. Stand. 73A, 389 (1969).

3. M. Baranger, Atomic and Molecular Processes, D. R. Bates, Ed. (Academic Press, Inc., New York, 1962).

4. R. Zwanzig, Lectures in Theoretical Physics, W. E. Downs and J. Down, Eds. (Interscience Publishers, Inc., New York, 1961); J. Chem. Phys. 33, 1338 (1960); Phys. Rev. 124, 938 (1961); Physica 30, 1109 (1964).

5. R. Kubo, Lectures in Theoretical Physics, W. E. Downs and J. Down, Eds. (Interscience Publishers, Inc., New York, 1959).

6. R. C. Elton and H. R. Griem, Phys. Rev. 135, A1550 (1964).

7. G. Boldt and W. S. Cooper, Z. Naturforsch 19A, 968 (1964).

8. H. Bremermann, Distributions, Complex Variables, and Fourier Transforms (Addison-Wesley Publishing Co., Inc., Reading, Massachusetts, 1965).

9. E. W. Smith, Dissertation, University of Florida (1966).

10. L. Galatry, Phys. Rev. 122, 1218 (1961).

11. E. W. Smith, J. Cooper, W. R. Chappell, and T. Dillon, to be published.

12. E. W. Smith and C. F. Hooper, Jr., Phys. Rev. 157, 126 (1967).

13. E. W. Smith, J. Cooper, and C. R. Vidal, Phys. Rev. 185, 140 (1969).

14. C. F. Hooper, Jr., Phys. Rev. 165, 215 (1968); Phys. Rev. 169, 193 (1968).

15. C. F. Hooper, Jr., Phys. Rev. 149, 77 (1966).

16. A. C. Kolb and H. R. Griem, Phys. Rev. 111, 514 (1958).

17. H. R. Griem, A. C. Kolb, and K. Y. Shen, Phys. Rev. 116, 4 (1959).

18. P. Kepple, Report #831, University of Maryland (1969).

19. H. A. Lorentz, Proc. Acad. Sci. Amsterdam 8, 591 (1906).

20. V. Weisskopf, Z. Physics 75, 287 (1932).

21. M. Lewis, Phys. Rev. 121, 501 (1961).

22. H. R. Griem, Phys. Rev. 140, A1140 (1965).

23. E. W. Smith, Phys. Rev. 166, 102 (1968).

24. A. A. Barker, Aust. J. Phys. 21, 121 (1968).

25. F. W. Sears, Thermodynamics, the Kinetic Theory of Gases, and Statistical Mechanics (Addison-Wesley Publishing Co., Inc., Reading, Massachusetts, 1964).

26. U. Fano, Phys. Rev. 131, 259 (1963); Rev. Mod. Phys. 29, 74 (1957); Lectures on the Many-Body Problem, E. R. Caianiello, Ed. (Academic Press, Inc., New York, 1964).

27. N. Davidson, Statistical Mechanics (McGraw-Hill Book Co., Inc., New York, 1962).

28. K. Huang, Statistical Mechanics (John Wiley and Sons, Inc., New York, 1965).

29. A. A. Barker, J. Chem. Phys. 55, 1751 (1971).

30. A. Ohno, Linear Stark Broadening by Charged Particles (Quantum Chemistry Group, Uppsala U., Uppsala, Sweden, 1963), Preprint No. 109.

31. B. Mozer, Dissertation, Carnegie Institute of Technology (1960).

32. E. Merzbacher, Quantum Mechanics (John Wiley and Sons, Inc., New York, 1960).

33. S. S. Schweber, An Introduction to Relativistic Quantum Field Theory (Harper and Row, Publishers, Inc., New York, 1961).

34. E. W. Smith, Private Communication, Fall 1971..

35. E. W. Smith, Phys. Rev. Letters 18, 990 (1967).

36. J. T. O'Brien, Dissertation, University of Florida (1970).

37. L. A. Jones, J. R. Grieg, T. Oda, and H. R. Griem, Phys. Rev. 4, 833 (1971).

38. P. M. Morse and H. Feshback, Methods of Theoretical Physics (McGraw-Hill Book Co., Inc., New York, 1953).

39. J. W. Dufty, Phys. Rev. 187, 305 (1969).

40. R. M. Wilcox, J. Math. Phys. 8, 962 (1967).

41. M. Bacon, F. K. Shen and J. Cooper, Phys. Rev. 188, 50 (1969).

42. M. E. Bacon and D. F. Edwards, Colorado State University, Physics Department Technical Report No. TR-68-1 (unpublished), 1967.

43. J. T. Godfrey, C. R. Vidal, E. W. Smith and J. Cooper, Monograph No. 121, (Nat. Bur. of Stand., Washington, D. C. 1971).

44. M. Baranger and B. Mozer, Phys. Rev. 115, 521 (1959).

45. L. J. Roszman, Dissertation, University of Florida (1971).

46. J. R. Grieg, H. R. Griem, L. A. Jones, and T. Oda, Phys. Rev. Letters 24, 3 (1970); Phys. Rev. A4, 833 (1971).

47. M. Abramowitz and I. A. Stegun, Handbook of Mathematical Functions (U. S. Government Printing Office, Washington, D. C., 1964).

48. N. F. Mott and H. S. W. Massey, The Theory of Atomic Collisions (Oxford Univ. Press, London and New York, 1949).

49. C. A. Frobert, Rev. Mod. Phys. 27, 399 (1955).

50. S. M. Selby and B. Girling, Standard Mathematical Tables (The Chemical Rubber Co., Cleveland, Ohio, 1965).

51. T. L. Hill, Statistical Mechanics (McGraw-Hill Book Co., Inc., New York, 1960).

BIOGRAPHICAL SKETCH

Joseph Edward Whalen was born July 7, 1944, in Boston, Massachusetts. In June, 1962, he was graduated first in his class from Bellingham High School, Bellingham, Massachusetts. In June, 1966, he received the degree of Bachelor of Science with a major in physics from Worcester Polytechnic Institute in Worcester, Massachusetts. He entered the Graduate School of the University of Florida in September, 1966. He worked as a graduate teaching assistant in the Department of Physics and Astronomy until January, 1971. In January, 1971, he took on the duties of Scientific Programmer for the Department of Physics and Astronomy at the University of Florida, a post which he has held up to the present time. Throughout his enrollment at the University of Florida he has pursued his work toward the degree of Doctor of Philosophy.

Joseph Edward Whalen is married to the former Judith Anne Campbell and is the father of two children. He is a talented commercial and jazz pianist and has led and participated in many musical groups since his early high school days. He is a member of Sigma Xi and the American Physical Society.

I certify that I have read this study and that in my opinion it conforms to acceptable standards of scholarly presentation and is fully adequate, in scope and quality, as a dissertation for the degree of Doctor of Philosophy.

C. F. Hooper, Jr., Chairman
Associate Professor of Physics

I certify that I have read this study and that in my opinion it conforms to acceptable standards of scholarly presentation and is fully adequate, in scope and quality, as a dissertation for the degree of Doctor of Philosophy.

R. C. Isler
Associate Professor of Physics

I certify that I have read this study and that in my opinion it conforms to acceptable standards of scholarly presentation and is fully adequate, in scope and quality, as a dissertation for the degree of Doctor of Philosophy.

B. S. Thomas
Assistant Professor of Physics

I certify that I have read this study and that in my opinion it conforms to acceptable standards of scholarly presentation and is fully adequate, in scope and quality, as a dissertation for the degree of Doctor of Philosophy.

J. W. Dufty
Assistant Professor of Physics

I certify that I have read this study and that in my opinion it conforms to acceptable standards of scholarly presentation and is fully adequate, in scope and quality, as a dissertation for the degree of Doctor of Philosophy.

C. P. Luehr

C. P. Luehr
Assistant Professor of Mathematics

This dissertation was submitted to the Department of Physics and Astronomy in the College of Arts and Sciences and to the Graduate Council, and was accepted as partial fulfillment of the requirements for the degree of Doctor of Philosophy.

June, 1972

A. G. Smith

Dean, Graduate School